UNIVERSITÀ DEGLI STUDI DI SALERNO

DIPARTIMENTO DI SCIENZE FARMACEUTICHE

Dottorato di Ricerca in Scienze Farmaceutiche

XXIII CICLO (IX-CICLO NS)

2007-2010

DESIGN, SYNTHESIS AND PHARMACOLOGICAL STUDIES OF STRUCTURAL ANALOGUES MODELED ON BIOACTIVE NATURAL PRODUCTS

Tutor
Prof. Ines Bruno

PhD Student
Rosa De Simone

Coordinator
Prof. Nunziatina De Tommasi

To my grandparents:
Virgilio and Giustina

Preface

In November 2007, I started PhD three years course in Pharmaceutical Sciences at the Department of Pharmaceutical Sciences of University of Salerno under supervision of Prof. Ines Bruno.

My PhD project was focused on design and synthesis of molecules potentially able to inhibit the microsomal prostaglandin E_2 synthase (mPGES-1), a crucial enzyme involved in the last step of the arachidonic acid cascade. Specifically, as first task of my research I developed a small collection of molecules potentially able to inhibit the expression of the target enzyme, whereas in the second part I focused the attention on the realization of molecules potentially able to directly inhibit the activity of mPGES-1. The entire research work was carried out under the direct supervision of Prof. Ines Bruno.

The collections mentioned above were designed taking advantages of professor Giuseppe Bifulco's experience in molecular modeling-based approaches. Finally, to assess the bioactivity of the synthesized compounds, I joined forces of professors Miguel Paya and Oliver Werz from the University of Valencia and Tuebingen, respectively, that were involved in the biological assays.

List of publications related to the scientific activity performed during the three years PhD course in Pharmaceutical Sciences:

Papers:

- **De Simone, R.**; Andres, R. M.; Aquino, M.; Bruno, I.; Guerrero, M. D.; Terencio, M. C.; Paya, M.; Riccio, R. "Toward the discovery of new agents able to inhibit the expression of microsomal prostaglandin E_2 synthase-1 enzyme as promising tools in drug development". *Chem Biol Drug Des* **2010**, *76*, 17-24.

- **De Simone R.**; Chini M. G.; Bruno I.; Riccio R.; Muller D.; Werz O.; Bifulco G. "Structure-based discovery of inhibitors of microsomal prostaglandin E_2 synthase (mPGES)-1, 5-lipoxygenase (5-LO) and 5-lipoxygenase-activating protein (FLAP): promising hits for the development of new anti-inflammatory agents". *J Med Chem.* Accepted.

- **De Simone, R.**; Bruno, I.; Werz O.; Muller D.; Riccio, R. "Development of a third generation of petrosaspongiolide M (PM) analogues as interesting inhibitors of microsomal prostaglandin E_2 synthase 1 (mPGES-1) expression". *Manuscript in preparation*.

- **De Simone, R.**; Bruno, I.; Muller D.; Werz O.; Bifulco G.; Riccio, R. "Design and synthesis of a second generation of triazole derivatives as potential inhibitors of microsomal prostaglandin E_2 synthase 1 (mPGES-1)". *Manuscript in preparation*.

Table of Contents

Microsomal prostaglandin E_2 synthase-1 (mPGES-1) is the enzyme responsible for the conversion of the cyclooxygenase (COX)-derived prostaglandins (PG)H_2 into PGE_2. This enzyme is deeply involved in different pathologies; in fact it is over-expressed in several inflammatory disorders as well as in some human tumours. Hence, the inhibition of mPGES-1 has been proposed as a promising approach for the development of safer drugs in inflammatory disorders, devoid of classical NSAID side effects. Indeed, this enzyme is responsible for the biosynthesis of inducible PGE_2 as a response to inflammatory stimuli whereas it doesn't affect constitutive PGE_2 involved in crucial physiological functions. Today two are the main approaches employed in the inhibition of mPGES-1 activity. The first consists in the negative modulation of its expression, while the second one concerns the direct and selective inhibition of the enzyme.

In order to identify novel molecules able to block mPGES-1, in the first part of this project we focused our attention on the design and synthesis of molecules able to inhibit the expression of our target enzyme. Specifically, as first task we decided to undertake the structural optimization of a γ-hydroxybutenolide related to petrosaspongiolide M (PM) **5**, compound **6**, that showed to be a potent negative modulator of mPGES-1 expression (IC_{50} = 1.80 μM). In the course of our investigation we identified two new hits that revealed an increased activity compared to the parent molecule **6**, compounds **30** (IC_{50} = 0.79 μM) and **31e** (IC_{50} = 0.85 μM). Encouraged by these results, in order to amplify the chemical diversity of the γ-hydroxybutenolide scaffold and identify new lead structures able to inhibit mPGES-1 expression, we decided to develop a new collection of PM-derivatives featuring amido-aromatic portions linked to the γ-hydroxybutenolide scaffold. These compounds are currently under biological investigations whose outcomes could suggest new guidelines useful in the discovery of more effective agents.

As second task, we concentrated our efforts on the development of molecules able to directly interfere with mPGES-1. Owing to the lack of its crystallographic structure in protein data bank (PDB), we decided to choose, as model for our investigations, microsomal glutathione transferase 1 (MGST-1), an enzyme belonging to membrane associated proteins in eicosanoid and gluthatione metabolism (MAPEG) family and showing a high homology sequence with our selected target. On the basis of virtual screening outcomes, we designed and synthesized a collection of potential mPGES-1 inhibitors based on 1,4-disubstituted triazole moiety, a scaffold extensively employed in drug discovery that can be obtained through click chemistry approach, a powerful tool for the rapid exploration of the chemical universe based on practical and reliable chemical reactions. The biological evaluation of these compounds allowed us to individuate three new potential anti-inflammatory agents: (I) compound **54** displaying selectivity for mPGES-1 with an IC_{50} value of 3.2 μM, (II) compound **70** that dually inhibits 5-lipoxygenase (5-LO) and mPGES-1 and (III) compound **57** acting as 5-lipoxygenase-activating protein (FLAP) inhibitor (IC_{50} = 0.4 μM).

On the basis of these results, as last task of this project, we directed our attention on the new hit **54**, emerged as a selective inhibitor of mPGES-1. In more details, on the basis of the suggestions coming from both the biological screening and the 3D model of interaction with MGST-1, aiming at improving its biological activity, we decided to rely on some well-reasoned structural changes of the basic molecule in order to enhance the binding affinity for the target enzyme. In this perspective, a new collection of triazole derivatives has been efficiently synthesized and their biological profile is currently under investigation.

Introduction

The improvement of the social-environmental conditions, medical care and quality of life, registered around the 1970s in all industrialized countries, caused a general enhancement of population health status and a consequent reduction of 1–2% per year of mortality and of the overall morbidity in individuals over 80 years old. Numerous epidemiological and clinical studies demonstrated that most of the disorders afflicting aged population, such as prostate and breast cancers, Alzheimer's disease and heart diseases, including atherosclerosis and clogged arteries, have their base in inflammation. Therefore it can be well understood the growing need of anti-inflammatory drugs devoid of the severe side effects connected with the chronic use of the commercially available anti-inflammatory drugs. Aspirin is the most used non steroidal anti-inflammatory drugs (NSAIDs) in the world for the treatment of several kinds of inflammatory diseases, but it is increasingly used for prophylaxis of vascular events, too. It is calculated that the percentage of people 65 years old or older, using NSAIDs at least once a week, has been reported to be as high as 70%, half of which takes at least seven doses a week.[1] Unfortunately, an important factor limits the use of this class of molecules: their gastrointestinal and renal toxicity.[2] To give an idea of the gravity of the NSAIDs side-effects, we can consider that a single dose of aspirin leads to gross gastric injury as subepithelial hemorrhages within 15–30 minutes from the ingestion.[3;4] After aspirin administration for 24 hours at dose of 650 mg four times a day, gastric erosions usually develop.[3;5] In theory people taking aspirin develop gastric lesions in the first days of use. [2;3] However, subepithelial hemorrhages and erosions do not cause major gastro-intestinal bleeding or lead to other complications such as perforation or obstruction, that may develop within one week of regular NSAIDs administer. In fact, it is demonstrated that the incidence of gastroduodenal ulcers reaches 25%–30% at three months and 45% at six months of continued administrations of this class of drugs.[6] All the side effects described are supposed to be

connected to the general suppression of constitutively formed prostanoids such as cyclooxygenase (COX)-1-derived cytoprotective prostaglandin (PG) E_2 and prostacyclin (PGI_2) in gastroduodenal epithelium. Indeed, even if PGE_2 are the most prominent prostanoid in inflammation, fever and pain, they are also endowed with physiological functions in gastrointestinal tract, kidney and nervous systems.[7]

A solution of these problems seemed to derive at the end of '90 from the discovery of molecules able to selectively inhibit COX-2, the so called "coxibs". This class of compounds able to selectively inhibit only PGE_2 produced by inflammatory stimuli, showed an improved gastrointestinal tolerance. Unfortunately, subsequent clinical studies revealed significant increased risk for cardiovascular events such as myocardial infarction, stroke, systemic and pulmonary hypertension, congestive heart failure and sudden cardiac death,[8] apparently due to an imbalance of anti-thrombotic and vasodilatory PGI_2 on one hand and pro-thrombotic thromboxane (Tx)A_2 on the other hand. Therefore as inflammatory chronic pathologies, such as rheumatoid arthritis, require long-term drug application, side-effects represent a serious problem for therapy. This is the reason why, in recent years, there is an urgent need of efficient anti-inflammatory drugs that can be safely used in chronic inflammatory conditions.

One of the most employed approach in pharmaceutical research today is the target-based drug discovery. It consists in the preliminary identification of the biological target involved in the pathology of interest and in the identification of agents able to selectively modulate the activity of this target. To satisfy these requirements several new technologies have been developed in order to both identify the protein and the potential ligands interfering with the macromolecule. Specifically, for example gene expression profiling can be employed to clarify the role played by a certain protein in the development and progression of a specific pathology.[9] On the other hand, in order to discovery

molecules able to interact with this target, it is particularly useful to evaluate large libraries of compounds. At this regard extremely useful technologies, including combinatorial chemistry and high throughput screening (HTS) approaches, give us the possibility to increase the number of compounds to be tested and, consequently, the probability to identify active compounds.[10] Moreover, aimed at increasing discovery productivity in terms of time efficiency and cost reduction, virtual screening[11] and structure-based drug design[12] offer us the possibility to reduce the members of compounds need to be evaluated narrowing down the investigations to those compounds that, at least in theory, showed the higher binding affinity. Finally, a new approach, that has been successfully applied in drug discovery, is fragment-based drug design which allows the screening of smaller numbers of molecular fragments to identify low-molecular weight compounds that weakly bind the target macromolecule. Knowledge of how the fragments bind to the protein of interest allows to develop high affinity compounds by linking low affinity fragments together.[13]

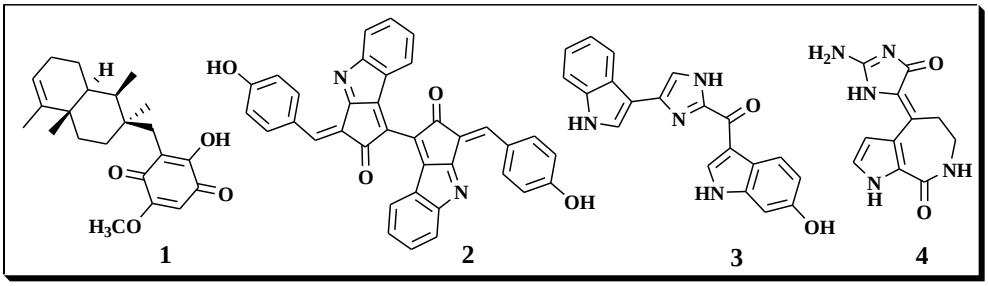

Chart 1. *Chemical structures of bolinaquinone **1**, scytonemin **2**, topsentin **3** and debromohymenialdisine **4**.*

Another more conventional approach in drug discovery starts from the consideration that the source of structurally unique molecules necessary for the drug discovery, is mainly accumulated in living organisms from terrestrial and marine environment. Hence the identification of new lead compounds within natural products appeared particularly promising also in the field of anti-inflammatory agents. In fact a considerable number of natural molecules

have recently been discovered to display a remarkable anti-inflammatory activity.[14] Compounds such as bolinachinone **1**,[15] scytonemin **2**[16] and the topsentins (e.g. **3**)[17] (Chart 1) have been extensively studied and represent interesting lead compounds for the development of promising anti-inflammatory drugs, while debromohymenialdisine **4** (Chart 1) have been taken into account for the treatment of rheumatoid arthritis and osteoarthritis.[18]

In particular a family of marine sesterterpenes containing a γ-hydroxybutenolide moiety and showing a potent anti-inflammatory activity attracted our attention. Specifically, among this group of interesting sponge metabolites, petrosaspongiolide M (PM) **5** (Chart 2) emerged as a very promising molecule able to irreversibly inhibit phospholipase (PL) A_2, the key enzyme involved in the inflammatory response.[19;20] Through *de novo* design approaches and molecular modeling studies, focused collection of PM derivatives have been designed and synthesized by our research group with the aim of shedding more lights on the molecular mechanism of action and discovering new promising drug candidates. In the course of this project we identified several significant PLA_2 inhibitors but the most relevant result was the discovery of 4-benzo[b]thiophen-2-yl-3-bromo-5-hydroxy-5H-furan-2-one **6** (Chart 2) emerged as a potent selective inhibitor of microsomal prostaglandin E_2 synthase-1 (mPGES-1) expression,[21;22] a very promising target-enzyme involved in the last step of arachidonic acid cascade. On the basis of these premises we decided to embark in a new project focused on this relevant target. Indeed, mPGES-1 has recently been recognized as a very promising therapeutic target owing to its involvement in COX-2-dependent PGE_2 biosynthesis induced during inflammation.[23] Thereby, a selective inhibitor of this enzyme isoform has been supposed to block PGE_2 generation connected to pathologies and to avoid the severe side-effects of the

commercially available anti-inflammatory drugs due to the massive suppression of physiological relevant prostanoids.

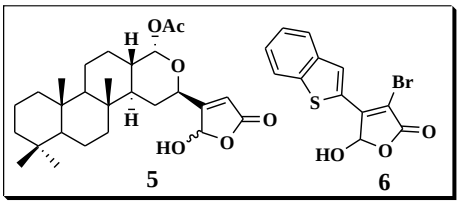

Chart 2. *Chemical structures of petrosaspongiolide M (PM)* ***5*** *and its simplified derivative* ***6****.*

~Chapter 1~

Inflammation:
Mechanisms, Actors and Mediators

Inflammation is defined as the response to injuries of vascularized tissues to deliver blood cells and fluid at the side of damage. Three are the main problems caused by injuries: some vessels are severed, some tissue is destroyed and the door is open to invaders such as bacteria, viruses, fungi, worms and other parasites. The first problem, the bleeding, is critical but instantly solved by the local mechanism of hemostasis. The loss of the tissue, less urgent, will be compensated in a few days or weeks by regeneration, while local scavenger cells clear up the debris. The last problem, the infection, is critical also because the local defense is not adequate. In fact, the local antibacterial natural guard, present in the tissue, amounts to a few sleepy macrophages scattered among the fibroblasts that are not enough to ward off sudden bacterial attacks. However, the problem is solved thanks to defensive forces in the blood, where they circulate in inactive form and are activated in case of injury. Two are the main materials supplied by the inflammatory response: leukocytes, some of which are specialized for fighting bacteria, and plasma, which brings the defensive proteins. Plasma, indeed, contains opsonins, proteins that coat foreign materials and make them easier to be phagocytized. Moreover, there is a source of about twenty proteins, known as complement, which can be locally assembled to build a bacterial-performing machine, and antibodies that are able to recognize and bind the surface of bacteria or other unknown parasites. As a consequence of the arrival of cells and fluid to the place of injury, the inflamed part swells. In addition, as the local blood vessels dilate in order to speed up the delivery, the inflamed part becomes hot and red. On the basis of these considerations, we can confirm that four are cardinal signs of inflammation: redness and swelling with heat and pain (*rubor et tumor cum calore et dolore*). What is really interesting is that cells and fluid have to be extravasated without interrupting the blood flow. If we consider that extravasing blood cells are larger than red cells, we can understand that the organism needs of inflammation mediators able to create

the condition necessary for the travel of these important defenders to the site of injury. So, some mediators will instruct the endothelium to become leady and others will tell the leukocytes to stop and emigrate. What is nice is that the injured tissue itself produces the earliest mediators to appear on the scene of injury: the defense reaction is triggered by the product of the aggression. The mixture of leukocytes and plasma accumulated in the injured tissue is called exudates, while exudate in presence of cells, which are firstly leukocytes that phagocytized bacteria, is known as pus. It is easy to understand that inflammation lasts as long as required to eliminate the cause and to repair the damage. Obviously, with time, inflammation chances its characteristics. Specifically, vascular dilatation tends to subside and the redness correspondingly abates; moreover, the amount of fluid and the swelling decrease. Finally the cell population changes to a predominance of mononuclear cells.[24]

On the basis of the time course, inflammations are classified in acute and chronic. Specifically, inflammation is defined acute if the event comes sharply, in hours or days, to a climax, while it is called chronic if the event persists for weeks, months or years.

If we want to summarize the inflammatory response, we can consider it a cast of ten cells that are normally quiescent and become activated in the inflammatory focus. Every cell has subtype and can produce inflammatory mediators. Specifically, for example, while neutrophils are bacteria-killing machines, eosinophils are specific against worms. Moreover, macrophages are delegated to phagocytose cellular debris and pathogens and to stimulate lymphocytes and other immune cells responding to them.

1.1. Inflammatory mediators

When leucocytes reach the site of injury thanks to the increased vessels permeability, they release different mediators able to control accumulation and

activation of others cells. Inflammatory mediators are small soluble molecules divided into two groups: external and endogenous mediators. The first ones are bacterial products and toxins, such as endotoxins and lipo-polysaccharides (LPS) produced by Gram negative bacteria. They cause the activation of the complement system and the consequent production of C_3 and C_5 anaphylatoxins that are responsible for vasodilatation and enhanced vascular permeability. Moreover they can induce the activation of the Hageman factor involved in fibrin formation and coagulation. Differently from external mediators, the endogenous ones, such as histamine and platelet activating factor (PAF), are produced by immune system itself. As part of an immune response to foreign pathogens, histamine is produced by basophils and mast cells found in nearby connective tissues. Histamine increases the permeability of the capillaries to white blood cells and other proteins, in order to allow them to engage foreign invaders in the infected tissues. On the contrary PAF is produced in response to specific stimuli by a variety of cell types, including neutrophils, basophils, platelets and endothelial cells. It is a potent phospholipid activator and mediator of the inflammatory function of leukocytes and is responsible for the formation of exudate.

Extremely important mediators in inflammatory events are eicosanoids, molecules derived from phospholipids, obtained thanks to the oxidation of long-chain polyunsaturated fatty acids. Coming from the autacoids family, eicosanoids derive from the arachidonic acid (Figure 1), a carboxylic acid with a 20-carbon chain and four *cis* double bonds, released from membrane phospholipids by different isoforms of PL enzyme (PLA_2 and PLC). As described in Figure 1, arachidonic acid can be processed along two pathways: the COX pathway which leads to PGs, prostacyclins and Tx[25] and lipoxygenase (LO) pathway which produces the leucotrienes.[26] Each type of cell, appropriately stimulated by injury or other mediators, generates its own

particular choose of eicosanoids. For example, endothelium responds to stimulation by producing prostacyclins, whereas plateles go the way of Tx.

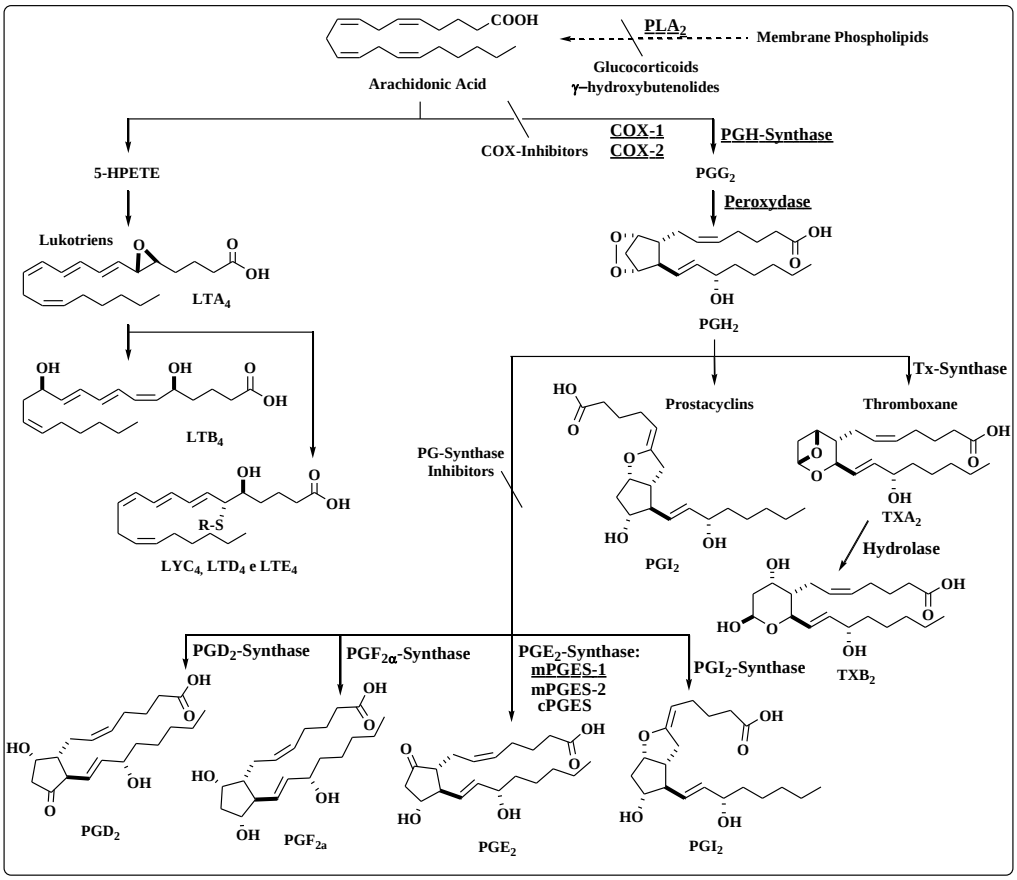

Figure 1. *Arachidonic acid cascade: the pathway connected with inflammatory stimuli is underlined.*

In more details, 5-LO converts arachidonic acid into 5-hydroperoxyeicosatetraenoic acid (5-HPETE), which spontaneously turns in 5-hydroxyeicosatetraenoic acid (5-HETE). Successively, 5-LO itself converts 5-HETE into leukotriene (LT) A_4, an unstable epoxide. In cells equipped with LTA_4 hydrolase, such as neutrophils and monocytes, LTA_4 is converted in the dihydroxy acid LTB_4, which is a powerful chemo-attractant for neutrophils. On the other hand, in cells where LTC_4 synthase is expressed, such as mast cells and eosinophils, LTA_4 is conjugated with the tripeptide glutathione

(GSH) forming the first of the cysteinyl-LTs, LTC_4. Outside the cells, LTC_4 can be converted by ubiquitous enzymes to form successively LTD_4 and LTE_4. The cysteinyl-LTs C_4, D_4 and E_4 are responsible for contraction of bronchial and vascular smooth muscles and of the increased permeability of small blood vessels. Moreover, they are able to enhance secretion of mucus in the airway and gut and to recruit leukocytes to sites of inflammation.

LTs are involved in asthmatic and allergic reactions and act to sustain inflammatory reactions causing or potentiating airflow obstruction, increasing secretion of mucus, mucosal accumulation, broncho-constriction and infiltration of inflammatory cells in the airway wall.

PGs, synthesized as response to inflammatory stimuli, are lipidic compounds produced by different cells. For example, whereas mastocytes biosynthesize PGD_2, macrophages and monocytes produce preferentially PGE_2 and PGF_2. The main PGs involved in inflammation are PGE_2, produced by stimulated macrophages, and PGI_2, also called prostacyclins, produced by vascular tissues. Their principal effect is vasodilatation, but they can also increase the exudation of fluid and supply leukocytes by increasing flow through vessels that are already leaky, without affecting permeability or causing diapedesis. PGs contribute to all the four cardinal signs of inflammation listed by Cornelius Celsus and previously discussed: *rubor*, *tumor*, *calor* and *dolor*. Overall, the main role of PGs in inflammation is to guarantee an ample supply of blood despite local controlling factors.[24]

As shown in Figure 1, a common precursor of PGs and prostacyclins is PGH_2. In fact, the opportune Tx or PG synthase converts it to Tx or to the other PGs, involved in the arachidonic cascade, respectively. Consequently, because of the main actors of inflammation are PGE_2, drugs able to inhibit their production are particularly efficient in the treatment of inflammatory diseases.

The anti-inflammatory drugs commercially available are classified in steroidal (SAIDs) and non-steroidal (NSAIDs) on the basis of their chemical structures

and targets. Specifically SAIDs act on PLA_2, whereas NSAIDs act as inhibitors of the COX enzyme.

1.2. Anti-inflammatory targets

1.2.1. Phospholipase A_2 (PLA_2)

PL is the enzyme hydrolyzing membrane phospholipids into fatty acids and other lypophilic substances. On the basis of the catalyzed reactions, PLs are classified in four classes: A, B, C and D (Figure 2). Specifically, the class of PLA is involved in the cleavage of acyl chains and contains PLA_2, that is responsible for the releasing of the arachidonic acid, and PLA_1, which removes the 1-acyl group. On the other hand, PLB, known as lypophospholipase, acts on both the acyl chains, while PLC is involved in signal transduction because it cleaves phosphate group and releases diacylglycerol and a phosphate-containing head group. Finally, PLD cleaves phosphate group and release phosphatidic acid and alcohol.

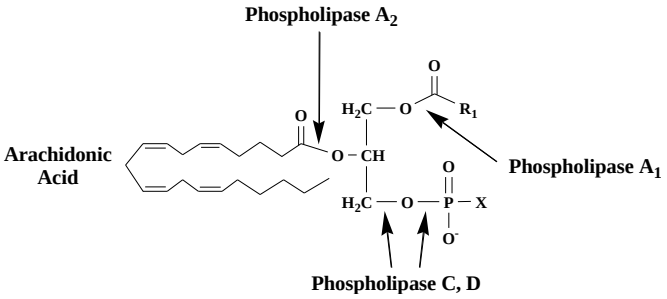

Figure 2. *Hydrolisis of phosphatidilinositole by PLs.*

On the basis of this short description, we can easily deduce that the isoform involved in inflammation is PLA_2. Therefore, it can be considered an interesting target for the development of anti-inflammatory drugs as it begins the arachidonic acid cascade. Molecules able to act indirectly on PLA_2 are NSAIDs, the well known and potent glucocorticoids such us beclometasone,

budesonide and mometasone.[27] They interfere with lipocortin-1 (annexin-1) synthesis, which is responsible for the suppression of PLA_2 expression.

A wide range of molecules of natural origin have been discovered to be able to irreversibly inhibit this enzyme. Particularly interesting in this field is the family of marine sesterterpenes containing a γ-hydroxybutenolide moiety, such us manoalide, cacospongionolides and petrosaspongiolides, that have been the object of extensive investigations by our research group with the aim of identifying the mechanism of interaction at molecular level.[28]

In addition to the production of eicosanoids, PLA_2-catalyzed membrane phospholipids hydrolysis is also the initiating step in the generation of PAF, a potent inflammatory agent. Thus, inhibition of PLA_2 activity should be, in theory, a really effective anti-inflammatory approach. However, PLA_2 have been proved to determine the massive suppression of prostanoids and LTs production, including those constitutively expressed and involved in crucial physiological functions.

1.2.2. Cyclooxygenase (COX)

COX is the enzyme responsible for the formation of prostanoids, including PGs, prostacyclins and Tx. This biosynthesis takes place on the two active sites: the cyclooxygenase and the peroxidase. Specifically, the first one is responsible for the conversion of arachidonic acid in the hydroperoxy endoperoxide PGG_2, whereas peroxidase site is involved in the reduction of PGG_2 to PGH_2 (Figure 1).

Today three different isoforms of COX are known: COX-1, COX-2 and COX-3, a variant of COX-1. Whereas COX-1 is considered a constitutive enzyme, COX-2 is an inducible enzyme, becoming abundant in activated macrophages and other cells in the sites of inflammation. COX-1 and COX-2 are characterized by 65% aminoacid sequence homology and near-identical

catalytic sites. The most significant difference between the two isoenzymes is the substitution of Ile at position 523 in COX-1 with Val in COX-2.[29]

The first molecule able to non-selectively inhibit COX is acetylsalicylic acid that, in 1899, was marked and commercialized as Aspirin. After about six decades new NSADs were employed in treatment of inflammatory diseases with aspirin-like actions. It is worth to note that aspirin-like drugs were initially developed without a rationale mechanistic support, as their mechanism of action was not discovered until 1971. Indeed, they revealed hard gastrointestinal and renal side-effects due to the non-selective inhibition of all PGE_2, including those constitutively expressed and involved in gastric mucosa and kidney protection.[30]

The discovery of COX-2 isoform and the elucidation of its 3D structure, in 1999, allowed the design and synthesis of selective COX-2 inhibitors, the well known "coxibs" such as celecoxib and rofecoxib.[6] At the beginning they were considered the solution to all the problems connected with the use of the conventional anti-inflammatory drugs, because of the selective suppression of prostanoids induced by inflammatory stimuli in the gastro-intestinal mucosa and platelets.[6;29] Unfortunately, it was early demonstrated that long term treatment with coxibs led to increased risks for heart attack, thrombosis and stroke, probably due to an unbalance between anti-thrombotic agents, such as prostacyclins, and pro-thrombotic molecules, like Tx.[8]

The failure of this class of anti-inflammatory drove the scientific community to search novel and safer anti-inflammatory targets. Indeed, recently, researchers focused their attention on a new class of interesting enzymes involved in the last step of arachidonic acid cascade: the prostaglandin E_2 synthase (PGES).

1.3. Prostaglandin E_2 Synthase (PGES)

PGES is the enzyme involved in the terminal step of the biosynthesis of PGE_2 (Figure 1). Specifically, it is responsible for the isomerization of the COX-derived peroxide PGH_2 in PGE_2.[31] Three isoforms of this enzyme have been identified and cloned: cytosolic PGES (cPGES),[32] membrane PGES-1 (mPGES-1) and membrane PGES-2 (mPGES-2).[33] Both cPGES and mPGES-2 are constitutively expressed in various cells and contribute to the basal PGE_2 synthesis with the difference that while mPGES-2 is functionally coupled with the activity of COX-1 and COX-2,[32;34] cPGES is functionally coupled with COX-1.[33] On the contrary, mPGES-1 is the predominant isoform involved in COX-2-mediated PGE_2 production[35] and represents the only isoform mainly induced by various inflammatory stimuli.[36] This feature makes mPGES-1 an extremely interesting target because its inhibition is connected to the suppression of inducible PGE_2 responsible for inflammatory pathologies that should reduce the typical side effects of the anti-inflammatory drugs commercially available.

1.3.1. Microsomal prostaglandin E_2 synthase (mPGES-1)

Human mPGES-1 is a membrane protein of 16 KDa and represents the first isoform of PGES identified and cloned by Jakobsson *et al*. in 1999.[37] It is a member of the membrane associated proteins involved in eicosanoid and glutathione metabolism (MAPEG) family, which also contains LTC_4 synthase, 5-lipoxygenase-activating protein (FLAP) and three GSH transferases/peroxidases, namely microsomal glutathione transferases (MGST) 1-3.[38]

mPGES-1 is a homotrimer[39;40] with each monomer consisting of four transmembrane helices (TM1-4) and a large cytoplasmatic loop between TM1 and TM2. The three TM2s of each trimer form an inner core with a funnel-shaped opening towards the cytoplasmatic side. GSH, bound in a U-shaped

conformation, is located at the interface between subunits in the protein trimer being exposed to the lipid bilayer.[40] GSH is an essential cofactor for catalytic turnover.[37] In fact, it seems that it is responsible for a catalytic mechanism in which its thiolic function attacks the peroxide of PGH_2.[41;42] Structure comparisons between LTC_4 synthase and mPGES-1 suggest that mPGES-1 has to undergo conformational changes from a closed to an open conformation before PGH_2 can access the active site.[40;43;44]

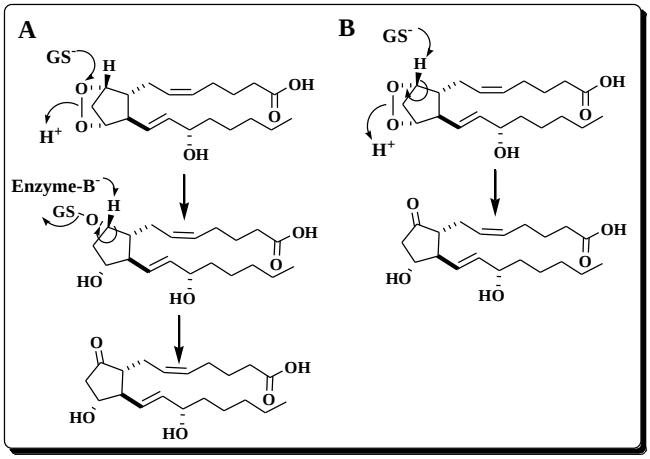

Figure 3. *Molecular mechanisms proposed for GSH-dependent conversion of PGH_2 to PGE_2.*

Concerning the molecular mechanism of GSH-dependent conversion of PGH_2 to PGE_2, two mechanisms have been proposed, both provide a nucleophilic attack by the thiolate anion of GSH (GS^-). Specifically, the first mechanism proposed consists in a GSH-assisted hydride shift with the formation of the instable intermediate, thiohemiketal. Successively, the nucleophilic thiolate anion attacks the peroxide oxygen on C-9 and brings to the adduct between GSH (or enzyme cystein thiol) and PGH_2. The following enzyme-assisted deprotonation of C-9 furnishes PGE_2 and thiolate anion GS^-. Then another GS^- (or enzyme cysteine thiolate) in solution acts as base in the second step (Figure 3A). The second proposed mechanism proceeds concerted. In more details,

glutathione or enzyme cysteine thiolate removes the proton on C-9 of PGH_2 that isomerizes into PGE_2 (Figure 3B).[35]

1.3.2. Pathologies where mPGES-1 is involved

Recent studies demonstrated that mPGES-1 is over-expressed and plays a pivotal role in diseases related to inflammation and tumorigenesis.[45-47] Nevertheless it is constitutively expressed at low level in few tissues in mice and rats, such us seminal vesicles,[37] ovary,[48] kidney,[49] male reproductive organs,[50] placenta,[51] lung, spleen and gastric mucosa[30] where its physiological functions are not well understood.

The over-expression of mPGES-1, along with COX-2, seems to be stimulated by several pro-inflammatory stimuli and mediators such us interleukin-1β (IL-1β), tumor necrosis factor-α (TNF-α) and LPS, in different cells and tissues. In addition, in humans, it is up-regulated in arthritic synovial tissues,[52] in the cartilage and chondrocytes of osteoarthritic patients[53-55] and in inflamed intestinal mucosa of patients with inflammatory bowel diseases.[56] Moreover, mPGES-1 seems to be responsible not only for atherosclerotic carotid plaques,[57] but it is expressed in Alzheimer disease tissues[58] and heart tissue after acute myocardial infarction;[32] it is also abundant in liver tissue from patients with hepatitis and muscle biopsies from people with polymyositis or dermatomyositis.[59] Closely related to the inflammatory diseases, mPGES-1 is recently emerged to be involved in the pathogenesis of different form of cancers and in induction of angiogenesis.[60] Specifically, several clinical studies have shown increased levels of mPGES-1 in various human cancers, including colon,[61] lung,[62] stomach,[63] pancreas,[64] cervix,[65] prostate,[66] papillary thyroid carcinoma,[67] head and neck squamaous carcinoma[68] and brain tumors.[69;70] Moreover, the elevated levels of mPGES-1 and mPGES-2 correlate with a worse prognosis in late stages of colorectal cancer,[71] suggesting that the PGE_2 synthase may play a key role in cancer progression.

Finally, mPGES-1-derived PGE_2, in cooperation with vascular endothelial cell growth factor (VEGF), seem to play a critical role in the development of inflammatory granulation and angiogenesis. Indeed, mPGES-1 deficiency has been well documented to be associated with reduced induction of VEGF in the granulation tissue.[72] On the basis of all these considerations mPGES-1 inhibition could be considered a valid strategy not only for the treatments of inflammatory diseases but also in chemotherapeutical field.

1.3.3. mPGES-1 as pharmacological target

As discussed before, elevated levels of mPGES-1 are often observed in connection with COX-2 over-expression.[35;73] Nevertheless, it has recently emerged that mPGES-1 can also be functionally activated in the absence of induced COX-2 levels,[74] providing evidence that these two enzymes can be independently regulated. This could corroborate that mPGES-1 is outlined as a promising drug target for inflammatory diseases because its inhibition leads to the reduction of inducible PGE_2 by mechanisms that circumvent the toxicity associated with inhibition of COX-1 and COX-2 activity. Actually, this last issue is still debating because in some cell type a redirection of prostanoid synthesis to other prostanoid synthases has been observed after mPGES-1 inhibition.[30;75-77] Hence, the therapeutic efficiency and safety of drugs targeting mPGES-1 remains to be further investigated; thus selective mPGES-1 inhibitors are strongly required to fully clarify some crucial mechanicistic details.

Recently increasing evidences outline the possibility of a dual inhibition of mPGES-1 and 5-LO as a more effective approach in inflammatory diseases. This strategy rely on the consideration that suppression of both LTs and PGs synthetic pathways might be of advantage in terms of effectiveness and relief from side effects.[78] In fact, LTs are involved in gastric epithelial injury and atherogenesis and were suggested to contribute to the gastrointestinal and

cardiovascular side-effects of traditional NSAIDs and coxibs, respectively.[79] In any case, even this topic, that is whether dual inhibition of mPGES-1 and 5-LO is of therapeutic value, needs to be further investigated.

On the basis of these considerations, in the last years the interest for mPGES-1 as therapeutic target is still increasing. Despite many efforts have been profuse in this area, only a few small molecules have been discovered to target this enzyme. In theory to affect mPGES-1 levels two different approaches can be used: an inhibition of mPGES-1 expression or a selective inhibition of mPGES-1 activity. The first strategy consists in the identification of molecules potentially able to negatively modulate the expression level of the gene responsible for mPGES-1 biosynthesis. The second approach consists in the discovery of molecules that could directly and selectively inhibit the activity of the enzyme.

1.3.4. mPGES-1 inhibitors

1.3.4.1. Inhibitors of mPGES-1 expression

As mentioned before, an interesting approach to affect mPGES-1 activity consists in the modulation of the enzyme expression. So far the only molecules that have been shown to inhibit mPGES-1 expression are **6** and resveratrol **7**.

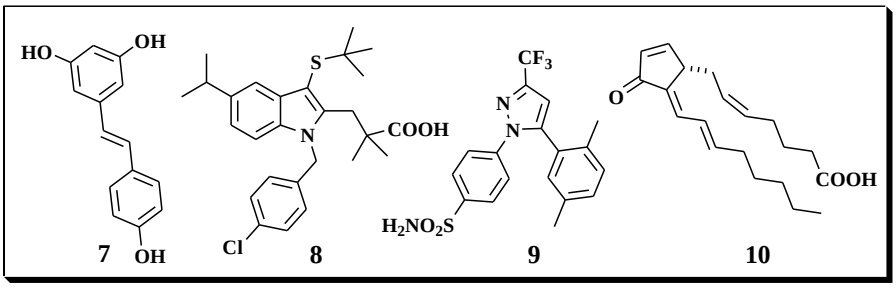

Chart 3. *Inhibitors of mPGES-1 expression.*

In more details, compound **6** is a γ-hydroxybutenolide-derivative identified by our research group, that potently inhibits PGE_2 formation (IC_{50} = 1.8 μM) in

LPS-stimulated RAW264.7 cells through a selective inhibition of mPGES-1 expression (IC_{50} < 1 μM). The molecular mechanism of **6** remain to be fully elucidates.[22]

The polyphenolic antioxidant resveratrol **7** (Chart 3) was found to suppress cellular PGE_2 formation (IC_{50} = 2.5-30 μM) by modulation of multiple events in PGE_2 biosynthesis.[80] Indeed, in addition to its anti-oxidative effects and ability to inhibit the COX-1 peroxidase reaction (IC_{50} = 0.1-1 μM),[81] compound **7** selectively blocks the induction of mPGES-1, without any effect on COX-1 or COX-2, in LPS-stimulated rat microglial cells (IC_{50} = 10-25 μM).[82]

Finally, particularly noteworthy are MK-886 **8**,[83] dimethylcelecoxib **9**[84] and 15-deoxy-$\Delta^{12,14}$-PGJ_2 **10**[85] (Chart 3) that combine direct mPGES-1 inhibition with repression of mPGES-1 induction.

1.3.4.2. Small molecules as inhibitors of mPGES-1 activity

The alternative approach to inhibit the activity of mPGES-1 consists in the discovery of potential ligands able to directly interact with the enzyme blocking its activity. In the last years we assisted to a considerable increase of publications and patent applications concerning this field. Based on the data reported in literature we can found non selective and selective inhibitors of mPGES-1.

1.3.4.2.1. Non-selective inhibitors of mPGES-1

On the basis of the chemical features, non-selective enzyme inhibitors can be divided in two groups. In the first group we found NSAIDs and Coxibs while endogenous fatty acids and lipid mediators belong to the second one.

Among the NSAIDs and Coxibs (Chart4) it is worth to note some COX-2-selective drugs possessing carboxylic or sulfonylamide groups, such us celecoxib **11** (IC_{50} = 22 μM), lumiracoxib **12** (IC_{50} = 33 μM), valdecoxib **13**

(IC_{50} = 75 µM)[84] and NS-398 **14** (IC_{50} = 20 µM),[74] that have been identified as mPGES-1 inhibitors in cell-free assays, even if at a concentration substantially higher than those needed for COX-2 inhibition. In addition, the Coxibs derivative dimethylcelecoxib **9** does not inhibit COX-2,[86] whereas inhibits mPGES-1 (IC_{50} = 16 µM) better than celecoxib **11**,[84] probably *via* an allosteric mechanism, as PGE_2 formation is only partially inhibited even at higher concentration (1 mM). Finally, among the traditional NSAIDs, only the active metabolite of the prodrug sulindac, the sulindac sulfide **15** (IC_{50} = 80 µM), has a weak inhibitory effect on the target enzyme.[74]

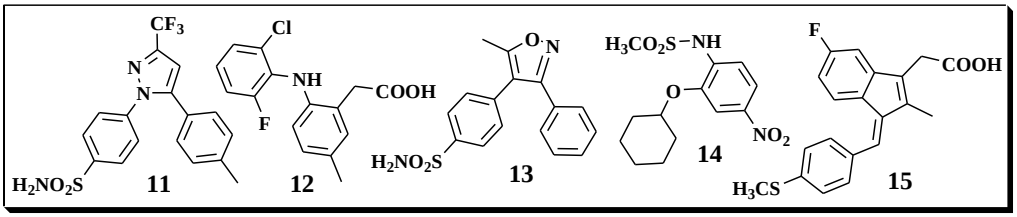

Chart 4. *Non-selective mPGES-1 inhibitors: NSAIDs and Coxibs.*

Among the unsaturated and non-unsaturated fatty acids the molecules that showed the most potent inhibitory activity are arachidonic acid, eicosapentaenoic acid and docosahexaenoic acid (IC_{50} = 0.3 µM, each),[87] along with palmitic acid (IC_{50} = 2 µM), 6-heptenoic acid (IC_{50} = 30 µM) and 15-deoxy-$\Delta^{12,14}$-PGJ_2 (IC_{50} = 0.3 µM).[87] Finally, also LTC_4 moderately inhibits mPGES-1 (IC_{50} = 5 µM),[74] probably thanks to a competition with GSH,[88] necessary for mPGES-1 activity.

1.3.4.2.2. Selective inhibitors of mPGES-1

On the basis of chemical features, selective mPGES-1 inhibitors can be classified in derivatives of MK-886, azaphenathrenone and oxicam (Chart 5).

MK-886 **8** was originally described as potent inhibitor of FLAP (IC_{50} = 2,5 µM) and later revealed an interesting inhibitory activity on mPGES-1 (IC_{50} = 2,4 µM). Starting from this lead structure, several potential inhibitors of

mPGES-1 were developed and some of them revealed IC_{50} values in the nanomolar range (**16** IC_{50} = 7 nM and **17** IC_{50} = 3 nM).[89]

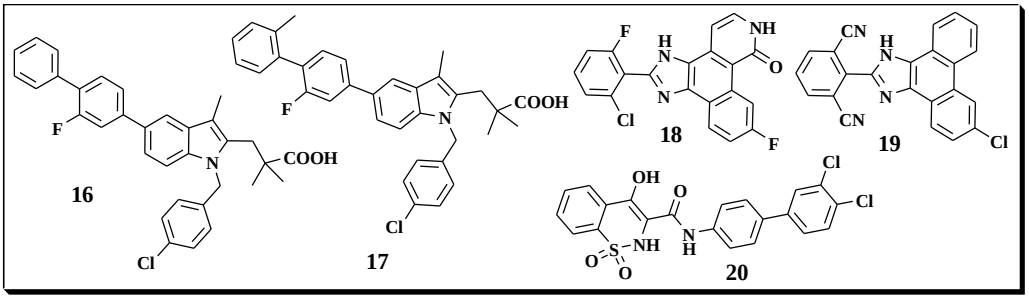

Chart 5. *Selective inhibitors of mPGES-1.*

Furthermore, the JAK kinase inhibitor azaphenanthrenone **18**[90] was discovered to be able to inhibit both cell-free mPGES-1 activity (IC_{50} = 0.14 μM) and PGE_2 formation in IL-1β-stimulated A549 cells (IC_{50} = 1.6 μM, 50% FCS) and was used as new lead compound.[91] Its structural optimization led to the discovery of several analogues, whose activity was not particularly interesting, and of MF63 **19** that revealed a potent inhibitory activity on mPGES-1 (IC_{50} = 1 nM).[91]

Finally, also the oxicam template has emerged as an interesting lead compound for the synthesis of potent and selective mPGES-1 inhibitors. Specifically, compound **20** showed to selectively inhibit mPGES-1 in nanomolar range in human fetal fibroblast cell assay.[92]

1.3.4.3. Dual inhibitors of mPGES-1 and 5-LO

As mentioned before, suppression of both LTs and PGs biosynthetic pathways might be more advantageous than single interference with prostaglandins formation, in terms of anti-inflammatory effectiveness and of reduced incidence of gastrointestinal and cardiovascular side-effects showed by the traditional NSAIDs and coxibs, respectively.[78] This assumption paved the way for the development of a new class of molecules able to inhibit both mPGES-1 and 5-LO. Within this class we can include MK-886 **8** and related

derivatives,[89] pirinixic acid analogues[93] and acylphloroglucinols[94] (Chart 6).

MK-886 **8** and its derivatives seem to interfere with cellular PGE_2 biosynthesis also through other mechanisms different from a direct inhibition of mPGES-1. For example, they were proved to interfere with several members of the MAPEG family (FLAP, mPGES-1, and LTC_4 synthase)[95;96] that might result from a conserved amino acid motif within this family,[97] in the MK-886 binding pocket of FLAP.[98] Furthermore, licofelone **21**, currently undergoing phase III trials for osteoarthritis, showed potent anti-inflammatory properties in clinical and pre-clinical studies lacking gastrointestinal toxicity.[99] This activity has been related to the simultaneous inhibition of COX-1,[100] mPGES-1[101] and 5-LO.[102]

The dual mPGES-1 and 5-LO pirinixin acid derivatives inhibitors were synthesized starting from the PPARγ agonist WY-14,643. The structural optimization of this lead compound led to the discovery of the potent carboxylic acid **22** which represents the most potent dual inhibitor within this series (mPGES-1: IC_{50} = 1.3 µM; 5-LO: IC_{50} = 2 µM).[93]

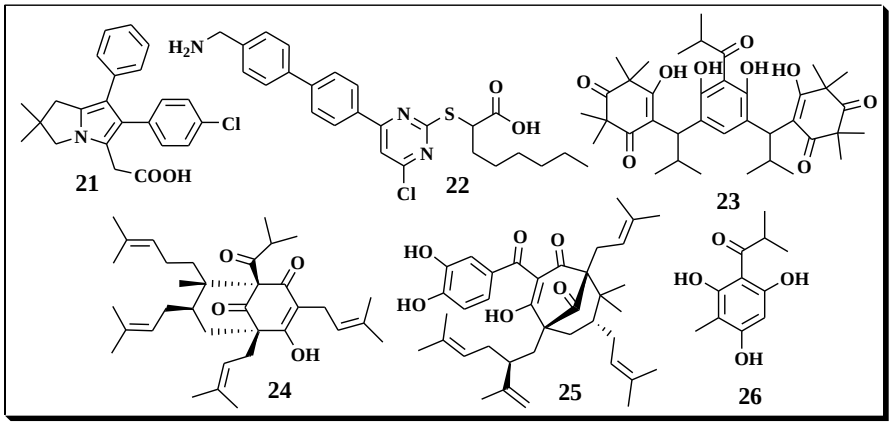

Chart 6. *Dual inhibitors of mPGES-1 and 5-LO.*

Finally among the acylphloroglucinols noteworthy are myrtucommulone **23** (mPGES-1: IC_{50} = 1.0 µM; 5-LO: IC_{50} < 30µM) from myrtle, hyperforin **24**

(mPGES-1: IC_{50} = 1.2 μM; 5-LO: IC_{50} = 0.09 μM) from St. John's wort and garcinol **25** (mPGES-1: IC_{50} = 0.3-1.2 μM; 5-LO: IC_{50} = 0.1 μM).[94] Their activity seems to be connected with the presence of acylphloroglucinol core **26** which itself is hardly active (IC_{50} > 30 μM).[94;103]

1.4. Aim of the project

On the basis of the considerations that mPGES-1 inhibitors could represent a new frontier in the field of anti-inflammatory drugs, the scientific community focused the attention on this attractive target with the aim of developing molecules able to act either directly on the enzyme or to affect its expression.

Although some structurally different compounds able to potently inhibit mPGES-1 have been developed, the discovery of new and more effective mPGES-1 inhibitors are strongly required in order to confirm the real efficiency and safety of these molecules in humans.

On the basis of these considerations, the first aim of this project was directed to the identification of new small molecules modeled on the natural marine compound PM **5**, able to negatively modulate the expression of mPGES-1. In more details, starting from a previous project developed by our research group that provided the identification of compound **6** as a very interesting mPGES-1 negative modulator, we tried to optimize its activity performing some well reasoned chemical modification on the lead scaffold. As second, we focused our attention on the development of new synthetic simplified derivatives of PM **5** in order to amplify the chemical diversity of the parent γ-hydroxybutenolide scaffold, in the attempt to identify new compounds able to inhibit the expression of the enzyme. As last step of this project, we considered the possibility to discover potential binders of the target enzyme able to selectively block its activity. In this frame we took advantages of molecular modeling studies in order to develop small molecules bearing the

triazole nucleus that, on the basis of a preliminary virtual screening showed a significant binding affinity for mPGES-1 enzyme.

1.5. Methodologies employed

Before starting the discussion concerning the results obtained, in our opinion it is appropriate to do first a brief introduction on the methodologies utilized to realize the project. Actually, to synthesize the three above mentioned small libraries, we took advantages on some advanced strategy of organic synthesis like Suzuki coupling, Huisgen's 1,3-dipolar cycloaddition and photooxydation reactions that have been properly optimized to provide the desired compounds in good yields. To gain safe predictions of the effectiveness of our molecules, we exploited molecular docking calculation and a *de novo* design approach as Ludi. Finally, to speed up the reactions and increase products yield, we employed microwaves technology.

1.5.1. Molecular docking

Molecular docking is the computational process of searching for a ligand that is able to fit both geometrically and energetically the binding site of a target protein. It is frequently used to predict the affinity and activity of potential binders for a protein; hence it plays a crucial role in rational drug design. The recent improvement of molecular docking finds its driving force not only in the drastic growth of computer availability and power, that characterize the last decades, but also in the ease of access to small molecules and proteins databases.[104-107]

The application of computational methods to study the formation of intermolecular complexes has been the subject of intensive research during the last years. It is widely accepted that drug activity is the result of the molecular binding of a small molecule, called ligand, to the pocket of another, generally a protein, known as receptor. In their binding conformations, the ligand and

receptor exhibit geometric and chemical complementarities, both of which are essential for successful drug activity.

Since the rapid generation of lead compounds represents the main requirement in the development of bioactive compounds, accurate automated procedures would be extremely useful in the drug discovery field. In this frame, ligand–protein docking is a powerful method able to predict the predominant binding modes between a ligand and the 3D structure of a given protein and can help synthetists to focus their efforts toward the most promising compounds. Hence, molecular docking can be used to perform a preliminary virtual screening on large libraries of compounds, ranking the results and proposing a possible binding mode between the ligand and the own target. This can be helpful also in structural optimization process to provide preliminary guiding lines in structure–activity studies.

Among the softwares available for docking calculation, one of the most used is AutoDock. This program was originally developed in 1990 by D. S. Goodsell[108] to perform automated docking of ligands on their macromolecular target. Since then its application in medicinal chemistry became ever increasing.

1.5.2. De novo design

A different approach to rationally individuate potential ligands for a defined target is the relatively new software Ludi, introduced in 1990 by Accelrys Inc. in collaboration with Prof. H. J. Böhm. It works positioning small molecules into clefts of protein structures, commonly the active site of an enzyme, in such a way that hydrogen bonds can be formed with the enzyme and hydrophobic pockets are filled with hydrophobic groups. The program acts in three steps (Figure 4). As first it calculates interaction sites, which are discrete positions in space suitable to form hydrogen bonds or to fill a hydrophobic pocket. The sites of interaction are derived from distributions of non-bonded

contacts generated by a search through the Cambridge Structural Database. The second step consists in the fit of molecular fragments onto the interaction sites. The final step is represented by the connection of some or all of the fitted fragments to a single molecule using bridge fragments.[109] To guarantee the synthetic accessibility of the selected molecules, Ludi is equipped with Ludi/CAP, a library of compounds based on two databases: Chemical Available for Purchase (CAP), which is a database of the commercially available compounds and CAPScreening, a database of molecules available in specific libraries.

Obviously the generated compounds do not have the same potency but everyone has an own score. On the basis of the score value it is extremely useful to screen the results and identify the most promising compounds that will be synthesized.

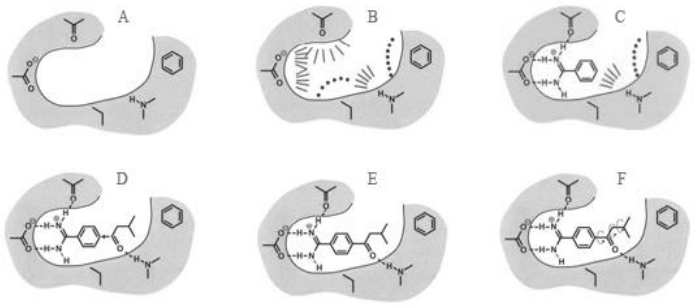

Figure 4. *Scheme of software Ludi operations.*

Ludi has been largely used in drug discovery and in particular I took advantages of its use to generate a focused collection of PM **5** simplified analogues in order both to amplify the chemical diversity and to simplify the synthetic procedures.

1.5.3. Suzuki cross-coupling reaction

The Suzuki cross coupling reaction was first reported by A. Suzuki and his group in 1979.[110] It is a versatile methodology to generate carbon-carbon

bonds and it is widely used to synthesize poly-olefins, styrenes and substituted biphenyls. It is extremely useful in preparative organic chemistry not only for the synthesis of natural or synthetic products, but also to prepare new materials.

Basically Suzuki coupling takes place among an aryl- or vinyl-boronic acid acting as nucleophile with an aryl-, vinyl- or an alkyl-halide and is catalyzed by Ni(0) and Pd(0). As reported in Figure 5, by analogy to the other organo-catalytic cross coupling reactions, the mechanism of the catalytic cycle of Suzuki coupling reaction involves three basic steps: 1) oxidative addition, 2) transmetallation and 3) reductive elimination.[111]

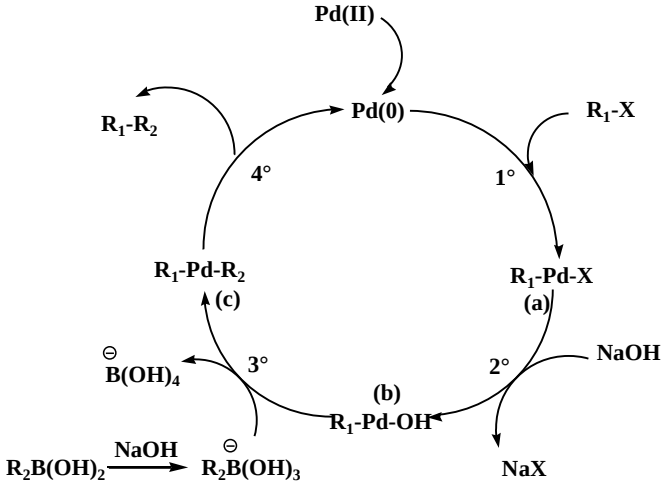

Figure 5. *Catalytic cycle of Pd(0) in Suzuki cross-coupling reaction.*

The reaction is initiated by oxidative addition of the appropriate halides (1-alkenyl, 1-alkynyl, allyl, benzyl or aryl halides) to a Pd(0) species affording a stable trans-δ-palladium(0) complex (a). The reaction proceeds with complete retention of configuration for alkenyl halides and with inversion for allylic and benzylic halides. Oxidative addition is often the rate-determining step in a catalytic cycle; hence it is fundamental that the substrate is sufficiently reactive for the oxidative addition. In more details, the relative reactivity of the

substrate decreases in the order of I > OTf > Br >> C1. Moreover, the aryl and 1-alkenyl halides, activated by the proximity of electron-withdrawing groups, are more reactive to the oxidative addition than those with donating groups. Afterwards, halogen linked on a organo-palladium (II) halide is readily displaced by the base anion to provide the reactive R_1-Pd-OH complex (b).[112] Because of the low nucleophilicity of organic group on boron atom, the cross coupling reaction requires the presence of a suitable base that coordinates the organic group on boron atom and enhances its nucleophilicity. Indeed the quaternization of the boron with negatively charged base makes easier the transmetallation of activated organic group to the Pd(II) complex with the consequent formation of trans R_1-Pd-R_2 (trans-c).[113]

Reductive elimination of organic partners from (b) reproduces the palladium(0) complex and affords the desired cross coupling product. The reaction takes place directly from cis-c intermediate, obtained from the isomerization to the corresponding trans-c complex. The order of reactivity is diaryl->(alky1)aryl->dipropyl->diethyl->dimethylpalladium(II), suggesting participation of the π-orbital of aryl group during the bond formation.

As the reaction is greatly affected by the experimental conditions, its success depends on the right choice of catalyst, base and solvents. In more details, a very wide range of palladium(0) catalysts or precursors can be used for cross-coupling reaction. $Pd(PPh_3)_4$ is the most commonly used, but $PdCl_2(PPh_3)_2$ and $Pd(OAc)_2$ plus PPh_3 or other phosphine ligands are also efficient since they are stable to air and readily reduced to the active Pd(0) complexes with organometallics or phosphines used for the cross-coupling. Palladium complexes that contain fewer than four phosphine ligands or bulky phosphines such as tris(2,4,6-trimethoxyphenyl)phosphine are, in general, highly reactive for the oxidative addition because of the ready formation of coordinate unsaturated palladium species. Among the available bases, particularly efficient are sodium or potassium carbonate, phosphate, hydroxide, fluoride

and alkoxide. The bases can be used as aqueous solution, or as suspension in dioxane and N,N- dimethylformamide (DMF).[110]

1.5.4. 1,3-dipolar cycloaddition among terminal alkyne and azide

Huisgen's 1,3-dipolar cycloaddition[114] among terminal alkynes and azide, are exergonic fusion processes that join two unsaturated reactants and provide fast access to an enormous variety of five-membered hetero-cycles. These process belong to click chemistry reactions which represent a revolution in the organic synthesis in response to the requests of drug discovery. Actually a click reaction is a process furnishing consistently high yields of products in brief time and in a few steps, starting from a wide variety of reactants. Moreover, it is easy to perform, insensitive to oxygen or water and it uses only readily available reagents, generally down market. Finally, work-up of the reactions and isolation of the products are simple and furnish pure products that do not need of any further chromatographic purification. Concerning lead discovery, this strategy gives the possibility to rapidly explore the chemical universe, whereas for lead optimization, it enables rapid structure-activity-relationship (SAR) profiling, through generation of libraries of analogues. In summary, click chemistry has proven to be a powerful tool in biomedical research. Obviously, click chemistry does not replace existing methods for drug discovery, but rather, it completes and extends them offering possibility to simplify the synthetic protocol and to provide the means for faster lead discovery and optimization. Indeed, it works well in conjunction with structure based design and combinatorial chemistry techniques and, through the choice of appropriate building blocks, can provide derivatives or mimics of 'traditional' pharmacophores, drugs and natural products.[115]

The Huisgen's 1,3-dipolar cycloaddition between terminal alkyne and azide represents the first example of a click reaction.[114] At the beginning, different problems limited the employing of this reaction in the organic synthesis. First

of all, differently from the most energetic species known, azides and alkynes are among the least reactive functional groups in organic chemistry. This stability is responsible for the slow nature of the cycloaddition reaction and the inertness of these functional groups towards biological molecules and towards the reaction conditions inside living systems. Moreover there was the problem concerning the regioselectivity: alkynes and azides react to furnish a mixture of 1,4 and 1,5 triazoles. The discovery of the possibility to accelerate the azide–alkyne coupling under Cu(I) catalysis[116;117] and the beneficial effects of water, connected with the complete and selectivity conversion to the 1,4-disubstituted 1,2,3-triazole[116] gave us the possibility to invest this reaction of the title of 'a perfect' reaction. Given this new process and the ready availability of the starting materials, highly diverse, large libraries become available quickly. Moreover, there are no protecting groups and purification is unnecessary. In addition, this process is really interesting in drug discovery, not only because of its reliability as a linking reaction, but also for the favorable physicochemical properties of triazoles obtained. Indeed, it works as rigid linking units that places the carbon atoms, attached to the 1,4-positions of the 1,2,3-triazole ring, at a distance of 5.0 Å, versus 3.8 Å of C-α distance in amides. Nevertheless, differently from amides, triazoles cannot be cleaved hydrolytically or otherwise and unlike benzenoids and related aromatic heterocycles, they are almost impossible to oxidize or reduce. Finally, they possess a large dipole moment and nitrogen atoms able to function as weak hydrogen bond acceptors.

Concerning with the mechanistic details of reaction, it has been proposed that the catalytic cycle begins with the formation of the Cu(I) acetylide (I) which reacts with the azide to give the six membered Cu-containing intermediate (III). Then, this last arranges to a thermally and hydrolytically stable triazole that lose the Cu(I) and furnish the desired 1,4-disubstituted 1,2,3-triazole (Figure 6).[116]

Triazole ring has already been employed to identify new lead compounds able to act on different targets. As supposed, biological studies showed that this scaffold is really interesting and could be employed to develop molecules useful for the treatment of different pathologies. Indeed, it has recently emerged that molecules with the triazole scaffold are active not only for the treatment of type II diabetes mellitus,[118;119] as antitumor,[120] antiviral,[121] antibacterial and antifungal[122] but also as inhibitors of mPGES-1 enzyme, as it will be reported in Chapter 4.

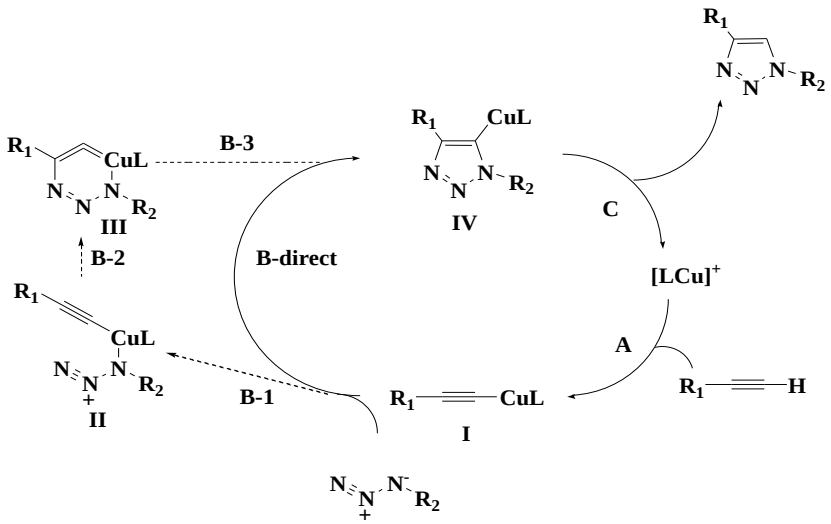

Figure 6. *Catalytic cycle of Cu(I) in 1,3-dipolar cycloaddition.*

1.5.5. Photooxydation

Photooxydation is a reaction in which the substrate gives an initial oxygenated adduct that consists of a combination among a substrate and oxygen in absence or in presence of a sensitizer absorbing a fundamental component for the reaction, light. This kind of reaction is able to furnish a considerable number of interesting intermediates. Indeed, the photooxygenation of heterocycles leads to a variety of products and serves as an important tool in the synthesis of a lot of natural products or compounds of special interest, such us the butenolides.

Before starting the description of the photooxydation mechanism, it could be useful to briefly explain the proprieties of oxygen in the singlet state and how it interferes with organic molecules.

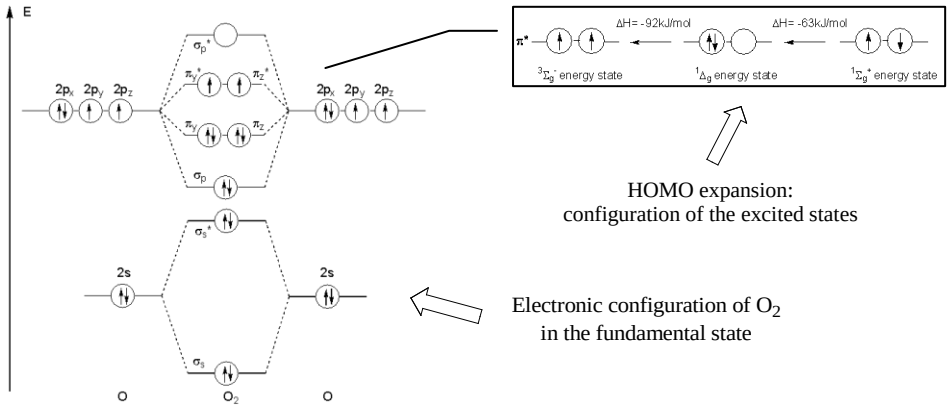

Figure 7. *Electronic configuration of oxygen.*

Singlet oxygen ($^1O_2$) is the common name of metastable state of molecular oxygen (O_2) with energy higher than fundamental state, known as triplet. In accordance with the theory of molecular orbital, the lowest energetic level (triplet, $^3\Sigma_g^-$) has two unpaired electrons localized in the two HOMO orbitals.

The arrangement of the electronic spin in these two degenerate orbitals generates two possible excited states (Figure 7). The first one (singlet, $^1\Delta_g$), 23 Kcal higher than the fundamental state, has two paired electrons in the same orbital whereas the second one, the more energetic state of singlet ($^1\Sigma_g^+$), has two electrons with opposite spin, coupled, in two different orbitals. On the basis of these considerations, as there are no unpaired electrons in both the electronic excited states, none of the excited states of the oxygen acts as radical but they just exploit the oxidant potential of oxygen.

But how can we create the singlet oxygen? It is necessary the presence of the photosensitiser, a gated light-absorbing substance able to transfer the absorbed energy to the oxygen that in this way became excited. Specifically, an electromagnetic irradiation excites the photosensitiser to the singlet state

(Figure 8a). At this point, the absorbed energy may be released through two different processes: the unexcited dye is restored by emission of a photon as fluorescence (Figure 8b) or the electronic system of the photosensitiser changes in favor of the triplet state (Figure 8c).

a)	$\mathbf{S + h\nu \longrightarrow {}^1S^{\bullet}}$	Excitation of photosensitiser to singlet state
b)	$\mathbf{{}^1S^{\bullet} \longrightarrow S + h\nu_F}$	Fluorescence
c)	$\mathbf{{}^1S^{\bullet} \longrightarrow {}^3S^{\bullet}}$	Change of photosensitiser in triplet state

Figure 8. *Mechanism of generation of $^1O_2$ by photosensitiser (S).*

At this point, the role of the photosensitiser is fundamental to determine the type of mechanism of photooxygenation (Figure 9). According to Gollnick classification,[123] in the Type I the substrate is activated by the sensitizer triplet. This last can abstract a hydrogen from a substrate leading to the radical $R^{\bullet}$ which then reacts with the ground state oxygen molecule to furnish $RO_2^{\bullet}$. On the other hand, the energy of the triplet sensitizer can be transferred to the ground state oxygen molecule to produce singlet oxygen $^1O_2$ which, after reaction with R, gives RO_2 (reaction of Type II).[124] It is also possible that an electron transfer occurs between the excited sensitizer and the substrate with formation of a radical cation $R^{\bullet+}$ that can react with $^3O_2$ or superoxide anion $O_2^{\bullet-}$ to furnish $RO_2^{\bullet+}$ or RO_2, respectively (Type III).

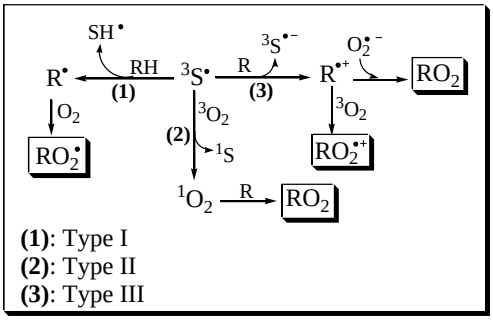

Figure 9. *Mechanisms of photooxydation.*

The diverse ways of oxygenation often lead to the same products or may be in competition. However a suitable choice of the reaction conditions may address the reaction to one type. Hence, for example, halogenated or deuterated solvents, low temperatures, continuous flow of oxygen, halogen lamps and dyes may favour reactions of Type II. UV light, high energy sensitizers (9,10-dicyanoanthracene, ketones), polar solvents, oxygen saturated solutions may favour the other two ways.

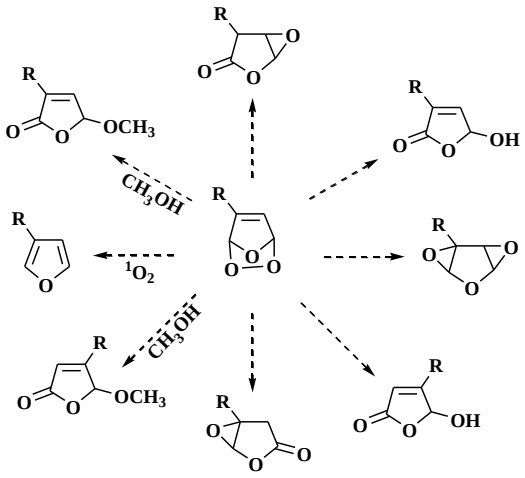

Figure 10. *Derivatives of furan obtained through photooxydation.*

The oxygenation of Type II by singlet oxygen is largely used, whenever possible, because of the high selectivity of this species and the mild reaction conditions. Indeed, the use of halogen lamps prevents the possibility of the decomposition of the peroxidic or hydroperoxidic products which may occur with UV lamps. Moreover, due to the high number of the dye-sensitizers available, such as rose bengal and blu methylene, the reaction can be carried out in a variety of organic solvents, from apolar to polar, including water. Specifically, the reactions of Type II, involving excited state ($^1\Delta_g$), is employed above all in the Schenck's and Dies-Alder reactions and has been applied to the most studied heterocycles as furans, thiophenes, pyrroles, oxazoles, imidazoles, indoles and nitrogen-containing six-membered systems.

One of the most useful eterocycle for the synthesis of natural derivatives is furan. Indeed, it is known to provide a lot of products including 1,3-diepoxides, epoxy lactones and hydroxybutenolides (Figure 10). Some of these products are formed by thermal decomposition of the unstable endoperoxides. For example, the formation of a 3-alkyl-4-hydroxybutenolide requires the regiospecific removal of the hydrogen at C-1 position on the endoperoxide that can be accomplished by treatment of the endoperoxide with a hindered base at low temperature in order to favour base-catalyzed decomposition rather than thermal decomposition (Figure 11).

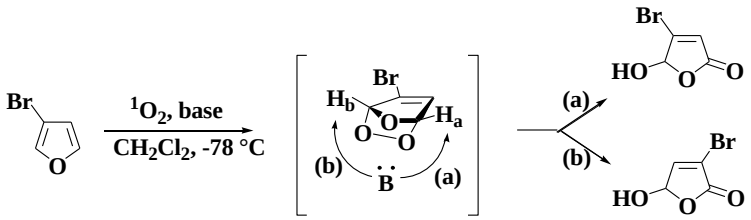

Figure 11. *Regioselective photooxydation of furan.*

This reaction has been widely studied by our research group. In the course of our investigations, we observed the formation of a complex mixture of by-products in absence of relatively strong bases. On the contrary, at -78°C in dichloromethane (DCM), strong and particularly bulky bases, especially phosphazene, lead to the preferential formation of precursor 3-bromobutenolides (ratio 8:2) whereas the bulky and strong base 1,8-diazabicyclo[5.4.0]undec-7-ene (DBU), able to remove the most acid H_b, furnishes the only 4-bromobutenolide (Figure 11).[125]

Photooxydation of furan in presence of singlet oxygen probably represents the most important reaction of this group. Indeed, it is largely employed to synthesize the γ-hydroxybutenolide ring that characterizes several natural products active as antinflammatory agents, like manoalide, cacospongionolides and petrosaspongiolides.[125]

1.5.6. CEM discover

Microwaves represent today a valid methodology to speed up a lot of the reactions widely used. Indeed, microwave-assisted organic synthesis is characterized by the spectacular accelerations produced in a lot of reactions as a consequence of the heating rate, which cannot be reproduced by classical heating. Thanks to this peculiarity, even reactions that do not occur by conventional heating can be performed using microwaves. This effect is exploited in a lot of fields, such as in the preparation of isotopically labelled drugs that have a short half-life,[126] high throughput chemistry like combinatorial chemistry and parallel synthesis[127] and catalysis where, the short reaction times, preserve the catalyst from decomposition and increase the catalyst efficiency.[128] In a few words, higher yields, milder reaction conditions and shorter reaction times that characterize microwaves synthesis give organic chemists more time to expand their scientific creativity, test new theories and develop new processes.

The development of microwaves technology was stimulated by World War II, when the magnetron was designed to generate fixed microwaves frequency for radar devices. Further investigation showed that microwaves could increase the internal temperature of foods much more than a conventional oven. This discovery led to the introduction of the first commercial microwaves oven for home use in 1954. Afterwards, in 1980s microwaves irradiation was investigated also in organic chemistry, but the common oven appeared not appropriate for the laboratory usage. Indeed, acids and solvents corroded the interior, there were no safety controls and temperature or pressure monitoring and the cavities were not able to sustain possible explosions. Hence, later microwave ovens specific for laboratories were designed and now multi-mode systems, featuring corrosion-resistant stainless steel cavities with reinforced doors, temperatures and pressures monitoring and automatic safety control, are commercially available.

But what are microwaves? A microwave is an electromagnetic radiation with frequencies ranging from 300 to about 300.000 MHz. In microwaves irradiation the transmission and absorption of energy is different from conventional thermal heating since microwaves transfer energy directly to the reactive species. But the innovation of microwave technology concerns with the kind of energy involved. Indeed, energy in microwaves photons is 0.037 Kcal/mol, really low relative to the energy required to cleave molecular bonds (80-120 Kcal/mole); thus microwaves will not affect the structure of organic molecules and the effect of microwaves absorption is purely kinetic. In this way, while traditional heating needs hours and brings to a lot of by-products, microwaves technologies allow a rapid rise in temperature and furnish quite pure products. One of the most important aspects of the microwaves is the rate at which it heats. Microwaves transfer energy at 10^{-9} seconds while the kinetic molecular relaxation from this energy is about 10^{-5} seconds. This means that energy transfers faster than the molecules can relax. As a consequence, temperature instantaneously increases together with collisions which are responsible for reduction of reaction time and by-products. What is important is that microwaves interact directly with the object being heated exploiting the ability of some compounds (liquids or solids) to transform electromagnetic energy into heat. Two are the fundamental mechanisms for transferring energy from microwaves to the substance being heated: dipole rotation and ionic condition. Specifically, dipole rotation is an interaction by which polar molecules try to align themselves with the rapidly changing electric fields of the microwaves. The rotational motion of the molecules trying to orient themselves with the field results in a transfer of energy. On the other hand, ionic conduction depends on free ions or ionic species present in the substances being heated. Indeed, as the molecules try to orient themselves to the rapidly changing field, the electric field generates ionic motion which is responsible for the instantaneous superheating. On the basis of these

considerations, it is clear that that microwave irradiation is a selective way of heating that generates rapid intense heating of polar substances whereas apolar substances do not absorb the radiation and are not heated. These thermal effects are a consequence of the inverted heat transfer, the non-homogeneity of the microwave field within the sample (hot spots) and the selective absorption of the radiation by polar compounds even in presence of apolar ones. In this way, it is possible to modify the selectivity of a given reaction or to avoid decomposition of thermally unstable compounds. These effects can be efficiently used to improve processes, modify selectivity or even to perform reactions that do not occur under classical conditions.

Today microwaves are employed to speed up a plethora of different reactions and to increase the yields of the target product. For example, the use of microwaves technology have been described in medicinal and combinatorial chemistry,[127] in cycloaddition reactions[129] and in the synthesis of radioisotopes,[126] polymers,[130] fullerene,[131] carbohydrates[132] and heterocyclic chemistry.[133] Furthermore microwaves reactions use less solvent than conventional reaction and, in some cases, offers the possibility to conduct solvent-free reactions. This is an interesting feature that allows the use of microwaves technology also in the green chemistry[134] accelerating reactions and avoiding decomposition of thermally unstable compounds.[135]

Among the instruments available, in our synthesis we took advantages on Discover® system, commercialized in the last years by CEM Corporation. This instrument is cheap and easy to use, so that it is employed in academies and industries. It is characterized by a single-mode cavity where homogeneous and intense reproducible energy is produced. In addition, it offers the possibility to conduct reaction both in normal glassware (until 125 mL) at atmospheric pressure and in pressurized conditions using specific vials (until 80 mL) resistant at 300 psi.

Results and Discussion

~Chapter 2~

Structural Optimization Process of Compound 6, the Promising Inhibitor of mPGES-1 Expression

---

De Simone, R.; Andres, R. M.; Aquino, M.; Bruno, I.; Guerrero, M. D.; Terencio, M. C.; Paya, M.; Riccio, R. Toward the discovery of new agents able to inhibit the expression of microsomal prostaglandin E_2 synthase-1 enzyme as promising tools in drug development. *Chem Biol Drug Des* **2010**, *76*, 17-24.

In order to identify small molecules able to inhibit the expression of mPGES-1, as first step of this project, we decided to focus our attention on compound **6**, which has been proved to be a potent and selective modulator of mPGES-1 expression.[21;22] This compound is a simplified derivative of PM **5** (Chart 2), a natural marine product able to potently inhibit the human synovial PLA_2 type IIA, the enzyme responsible for triggering the arachidonic acid cascade.[14] This interesting hit has been synthesized in the frame of our previous project involved in the generation of PM-derivatives as potential inhibitors of PLA_2; unfortunately the new molecules synthesized by our research group did not show a relevant activity toward this target, but an in-depth pharmacological study allowed us to identify compound **6** as a very promising negative modulator of mPGES-1 expression (IC_{50} = 1.80 μM). This result can be considered of great interest in consideration that so far only few molecules are known to be endowed with this activity.[82]

On the basis of these premises, in order to improve the pharmacological activity of this γ-hydroxybutenolide derivative, we decided to rely on some well-reasoned structural changes of the basic molecule (Chart 7). For this purpose, we decided to explore the structure-activity profile of a collection of analogues closely related with compound **6**. In more details, considering that this last consists of a 3-bromo-4-substituted hydroxybutenolide, as first we decided to replace the benzothiophene appendage with bioisosteric moieties, such as indole and benzofurane units (**27a** and **27b**); as result, we observed a clear loss of activity, especially for benzofurane derivative (Table 1). Afterwards, we decided to synthesize compounds **27c-d**, bearing on C-4 position of the 3-bromo γ-hydroxybutenolide scaffold an appendage that could mimic the same structural moiety present in resveratrol **7**, which has recently emerged as a potent modulator of mPGES-1 expression.[82] Unfortunately, none of these last molecules showed any increase of the activity with respect to the lead compound **6**. Hence, we decided to investigate the role played by

the bromine atom. For this purpose we examined the effects of two arrays of regioisomeric debrominated γ-hydroxybutenolides **28e-i** and **29e-i** respectively, previously synthesized by us, in the frame of a project focused on a synthetic implementation task and re-synthesized for the present purpose.

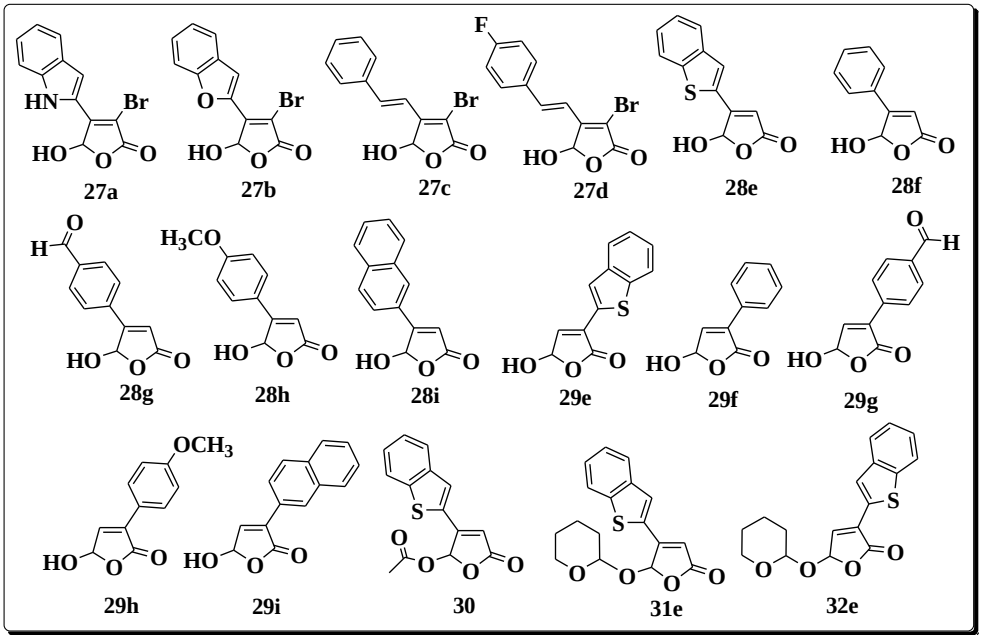

Chart 7. *Collection of compound **6**-derivatives.*

In the case of **28e**, the debrominated **6**, we observed a moderate increase of the activity (IC_{50} = 1.25 μM). On the contrary, the other 4-substituted butenolides **28f-i**, except **28g**, were found completely inactive. On the basis of these results, we can conclude that the elimination of bromine atom from the C-3 position of the lead compound **6** represents the only structural change proved to be effective for the activity. In line with these findings, the other array of regioisomeric compounds **29e-i**, all presenting substitutions on C-3 position of the scaffold, did not give satisfactory results.

Finally, to verify if the masked aldehyde was crucial for the activity, as it was proved to be for the inhibition mechanism of the other known natural butenolides,[28;136;137] we decided to perform on the most active derivative so

far obtained, compound **28e**, a protection of OH either with acetyl **30** or tetrahydropyran (THP) group **31e**. Compounds **30** and **31e** at last displayed a higher potency in inhibiting the expression of mPGES-1 (IC_{50} = 0.79 μM and IC_{50} = 0.85 μM respectively), in comparison with the reference compound **6**. This can be considered a really interesting result in view of discovery of new active molecules able to negatively affect mPGES-1 expression which can provide new tools for further mechanicistic investigation.

2.1. Chemistry

Concerning with the synthesis of this new series of molecules, the crucial step that allowed us to obtain compounds **27a-d** was a Suzuki coupling between the metoxy-ethoxy-methyl (MEM)-protected-mucobromic acid **34** and the appropriate boronic acid **a-d** (Scheme 1).

The first problem we had to solve, in order to apply this procedure, was the instability of the butenolide ring, observed also by Zhang,[138] in the basic condition required by Suzuki coupling. The decomposition of the scaffold is connected with the equilibrium that characterizes the butenolide moiety in solution: with the increase of pH the opening of the five-membered ring with the final formation of degradation products can be observed.[139]

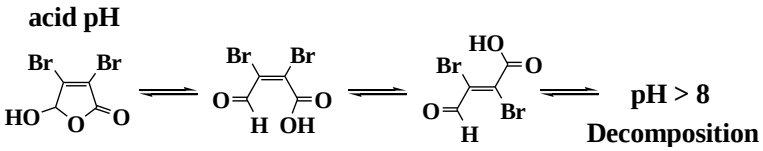

Figure 12. *Decomposition of butenolide ring with pH increasing.*

In more details, as depicted in Figure 12, in acid solution the cyclic structure is predominant, nevertheless with the pH increasing, the open form becomes more stable and, turning into its stereoisomer, it definitely evolves in by-products. This process can be avoided blocking the hemiacetal function. The choice of the protecting group has to be accurately done as this must be stable

in the alkaline conditions, required by Suzuki coupling, and easy to remove at the end of the reaction without affecting the other groups present on the main scaffold. Among the large number of known OH-protective groups, our choice fell on MEM for several considerations:[140] it is sufficiently stable in non-extreme alkaline solution and easy to remove in acid conditions. As next step we connected the MEM-protected-γ-hydroxybutenolide scaffold **34** with the suitable boronic acids **a-d**,[140] using the Suzuki coupling reaction,[110] previously optimized by us.[141] This reaction was performed through the microwaves heating strategy,[142] which allowed us to obtain the desired compounds **35a-d** in good yields, with low formation of by-products, mainly consisting of bis-coupling and homo-coupling adducts. Finally, the cleavage of MEM-protecting group with a solution of trifluoroacetic acid (TFA) 95%, triisopropylsilane (TIS) 2.5% and water 2.5% afforded the desired compounds **27a-d**.

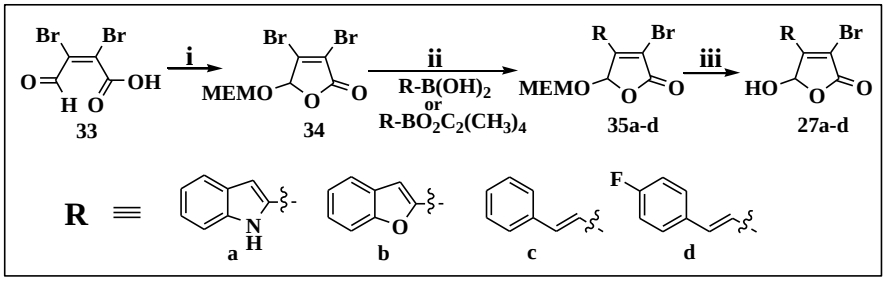

[a]Reagents and conditions: (i) MEM-Cl, DIPEA, CH_2Cl_2, r.t., 4h; (ii) Pd(dppf)Cl_2, TBAB, CsF, THF/H_2O 1:1, MW, 120°C, 3-6 min; (iii) TFA (95%), TIS (2.5%), H_2O (2.5%), r.t., 2h.

Scheme 1. *Synthetic protocol to generate derivatives **27a-d**.*

The two regioisomeric debrominate arrays **28e-i** and **29e-i** were obtained using the optimized protocol of photooxidation reaction performed on 3-bromofuran **36** in presence of a suitable base.[125] Specifically, to obtain the 3-bromobutenolide derivatives **28e-i** we performed the oxidation in presence of phosphazene that led to the preferential formation of 3-bromobutenolide (ratio

8:2). On the contrary, to obtain the regioisomer 4-bromobutenolide derivatives **29e-i**, we performed the photooxydation with DBU (Figure 11).[125]

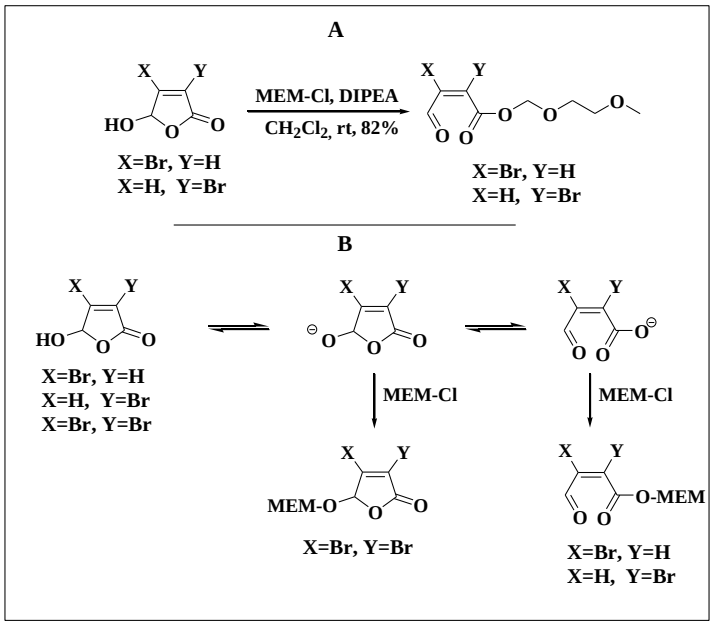

Figure 13. *Protective reaction of 3- and 4-bromo-5-hydroxy-5H-furan-2-one with methoxy-ethoxy-methyl-ether (MEM).*

Also in this case, to connect the aromatic appendages on the scaffold, we decided to perform a Suzuki coupling. As previously described for the brominated derivatives, even in this case the γ-hydroxybutenolide ring needed to be protected to avoid its decomposition in the basic conditions necessary for the Suzuki coupling. In more details, to protect the OH-emiacetalic, differently from the bromide-derivatives, we selected THP. This choice was in accordance with our previous findings and could avoid the risk of obtaining mainly MEM-ester byproducts instead of the desired MEM-protected monobrominated γ-hydroxybutenolides (Figure 13).[125]

Afterwards, a Suzuki coupling between the THP-γ-hydroxybutenolides **38** and **40** and the appropriate boronic acids **e-i** afforded the desired products **31e-i** and **32e-i** whereas their deprotection with a solution of TFA/TIS/H_2O

95:2.5:2.5 gave us the analogues **28e-i** and **29e-i**. Finally, the acetylation of compound **28e** afforded the desired compound **30** (Scheme 2).

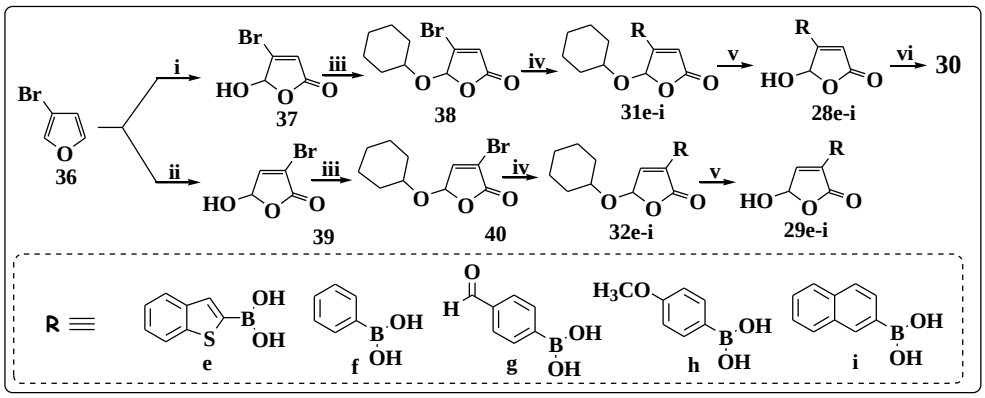

[a]Reagents and conditions: (i) P_1-octyl-phosphazene, rose bengal, $^1O_2$, CH_2Cl_2, -78°C. (ii) DBU, rose bengal, $^1O_2$, CH_2Cl_2, -78°C. (iii) p-tolensulfonic acid, DHP, CH_2Cl_2, r.t., 4h; (iv) Pd(dppf)Cl_2, TBAB, CsF, THF/H_2O 1:1, MW, 120°C, 3-6 min; (v) TFA (95%), TIS (2.5%), H_2O (2.5%), rt, 2h; (vi) $(CH_3CO)_2O$, DIPEA, DMF, r.t., 2h.

Scheme 2. *Synthetic protocol to generate derivatives* ***28e-i***, ***29e-i***, ***30***, ***31e*** *and* ***32e***.

Concerning with the protocol of Suzuki coupling we took advantages of the procedure previously optimized that suggested the use of Pd(dppf)Cl_2 as best catalyst. Indeed, Pd(II)-complex is considered a suitable precursor of Pd(0) as it is stable in presence of air and can be easily reduced *in situ* by the organometals and phosphine used for the cross coupling. Also crucial is the choice of the base because of the high instability of butenolide ring in extremely alkaline solutions.[138] In this frame the best results were obtained using CsF. Finally, concerning the solvents our choice fell on the mixture water/tetrahydrofuran (H_2O/THF) 1:1 because THF is partially mixable with water and is very useful in reactions among reactants with different polarity.

2.2. Bioactivity

In collaboration with Professor Miguel Paya of the University of Valencia (Spain), we evaluated the inhibitory activity of our compounds on mPGES-1 expression. For this purpose, their effect on PGE_2 production on mouse

macrophage cell line RAW264.7 stimulated with LPS was preliminary determined (Table 1).

Compound 10 µM	Percentage Inhibition	IC_{50} (µM)	Percentage Toxicity
27a	81.6 ± 4.7**	4.20	< 5.0
27b	46.7 ± 6.1**	n.d.	< 5.0
27c	45.1 ± 9.7**	n.d.	< 5.0
27d	46.5 ± 11.1**	n.d.	< 5.0
31e	100.0 ± 0.0**	0.85	28.9 ± 3.0**
32e	85.1 ± 3.5**	3.40	< 5.0
28e	87.1 ± 3.9**	1.25	< 5.0
28f	< 20.0	n.d.	< 5.0
28g	76.0 ± 5.7**	3.17	< 5.0
28h	< 20.0	n.d.	< 5.0
28i	< 20.0	n.d.	< 5.0
29e	65.9 ± 8.1**	4.46	< 5.0
29f	< 20.0	n.d.	< 5.0
29g	n.d.	n.d.	89.9 ± 0.2**
29h	< 20.0	n.d.	< 5.0
29i	< 20.0	n.d.	< 5.0
30	100.0 ± 0.0**	0.79	< 5.0
6	72.2 ± 5.7**	1.80	< 5.0

Results show means ± S.E.M (n=6). Statistical significances: ** p<0.01, with respect to the LPS-stimulated control group. PGE_2 (non-stimulated cells = 0.6 ± 0.2 ng/mL; LPS-stimulated cells = 16.0 ± 1.6 ng/mL). n.d.= not determined.

Table 1. *Inhibitory activity and cytotoxic effect of the γ-hydroxybutenolide derivatives **27a-d**, **28e-i**, **29e-i** **30**, **31e** and **32e** at 10 µM on the production of PGE_2 in LPS-stimulated RAW 264.7 cells.*

Specifically, after 18 h stimulation, compounds **6**, **27a**, **31e**, **32e**, **28e**, **29e**, and **30** were able to inhibit PGE_2 production with a percentage of inhibition higher than 50% at 10 µM, showing IC_{50} values in the micromolar range. In more details, only compounds **30**, **31e**, and **28e** exerted an inhibitory potency higher than the leader compound **6**. This profile is especially relevant for compounds **30** and **31e**, the two protected derivatives of the debrominated **6**. On the other hand, all the derivatives except **28g**, which was discarded, were devoid of

significant cytotoxic effects on RAW264.7 at concentrations higher than 10 µM, as assessed by the mitochondrial-dependent reduction of 3-(4,5-dimethylthiazol-2-yl)-2,5-diphenyltetrazolium bromide (MTT) to formazan (Table 1). The only exception was compound **31e** that showed a slight cytotoxic effect which disappeared at lower concentrations.

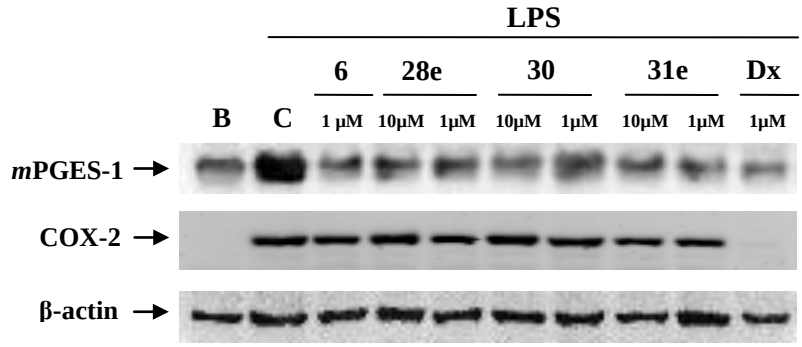

Figure 14. *Effect of derivatives **6**, **28e**, **30**, **31e** on mPGES-1 and COX-2 expression in LPS-stimulated RAW 264.7 cells. The Figure is representative of two similar experiments. B: normal cells. C: LPS-stimulated cells. Dx. dexamethasone.*

Finally, to confirm that analogues **30**, **31e**, **28e** and the leader compound **6** were able to inhibit selectively the mPGES-1 enzyme expression without any effect on COX-2, a western blot analysis for mPGES-1 and COX-2 proteins using 18 h LPS-stimulated RAW 264.7 cells was performed (Figure 14). The results clearly showed that the test compounds inhibit selectively mPGES-1 expression, without any effect on COX-2, whereas dexamethasone, the reference compound, as expected, reduced the expression of both inducible proteins.

-Chapter 3-

Design and Synthesis of New PM-Analogues

The intriguing biological results shown by synthetic analogues of the natural compound PM **5**,[21;22;141;143] encouraged us to continue our studies on this promising marine metabolite. Specifically, in this project as second step we decided to undertake the synthesis of a new generation of PM-derivatives bearing, on the γ-hydroxybutenolide ring, various molecular decorations in order to amplify the chemical space under investigation useful for the discovery of new agents with higher potency (Chart 8). Also in this case we decided to rely on the molecular structures suggested by Ludi.

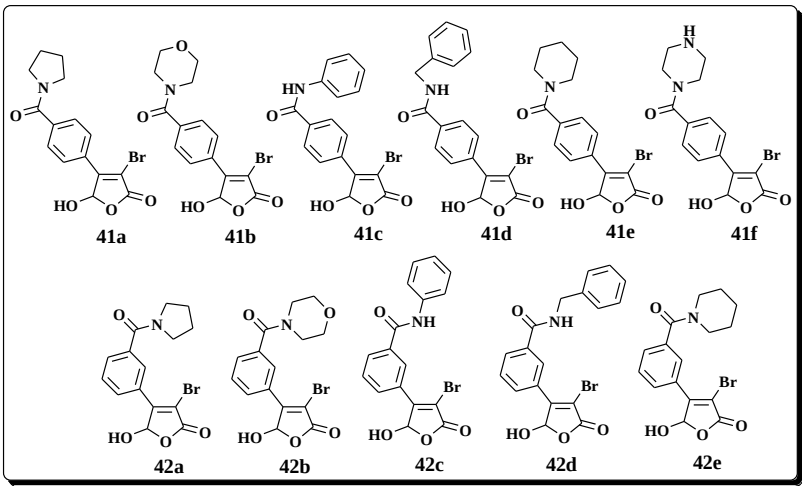

Chart 8. *Collection of new PM-derivatives.*

As described in Chapter 1, Ludi is a computational method which has been proven to be fairly predictive of the affinity properties of potential ligands. It was set in order to construct new promising binders for PLA_2, starting from PM **5** and replacing the sesterterpene moiety of the natural product, with suitable molecular fragments. Four classes of PM-analogues have been selected by the software; three of them have already been synthesized in our research group. Biological tests performed on these collections allowed us to individuate weak inhibitors of PLA_2 and compounds **6** as potent negative modulator of mPGES-1 expression as already reported.[21;22;141;143] Hence, encouraged by these results, we decided to complete the synthesis of PM-

derivatives, suggested by Ludi, characterized by amido-aromatic appendages on the 3-bromo γ-hydroxybutenolide moiety. Indeed, the presence of the brominate γ-hydroxybutenolide, accepted by Ludi, was selected as scaffold in order to simplify the synthetic approach.

3.1. Chemistry

As above reported, in order to simplify some crucial structural features of PM **5** and consequently the synthetic strategy, we decided to use the 3-bromo butenolide scaffold, which allowed us to select the commercially available mucobromic acid **33** as starting material. Concerning the decorations on C-4 position of the parent molecule, it was replaced by several molecular fragments selected from the database connected to the Ludi software. From a structural point of view, the new generation of compounds, possessing more complex ammido-aromatic fragments linked to the hydroxybutenolide scaffold, required elaborate synthetic procedures (Scheme 4).

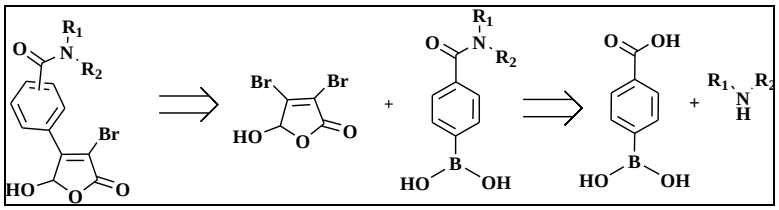

Scheme 3. *Retro-synthetic approach for the synthesis of the new PM-derivatives* ***41a-f*** *and* ***41a-e****.*

On the basis of the retro-synthetic analysis (Scheme 3), we decided to construct the amido-aromatic appendages through a reaction of ammidation starting from the appropriate ammines **a-f** and carboxylic acids **43** and **44**. As next step, these advanced intermediates should be linked to the MEM-protected mucobromic acid **34** through a Suzuki reaction. Thus, a final deprotection step could afford the desired products (Chart 8). In any case to drive successfully the synthetic strategy each step required to be accurately set.

In more detail, in order to reduce the polarity of the ammido-aromatic intermediates and make easier the purification step on silica columns, as first we converted the boronic acids **43** and **44** in the corresponding pinacol esters **45** and **46**. These last were subjected to amidation reaction with the appropriate ammine **a-f**, using the same protocol applied in peptide synthesis. In our specific case, we used triethylamine (TEA) as base, N-hydroxybenzotriazole (HOBt) and N,N'-dicyclohexylcarbodiimide (DIC) as carboxylic acid activators and DMF as solvent.

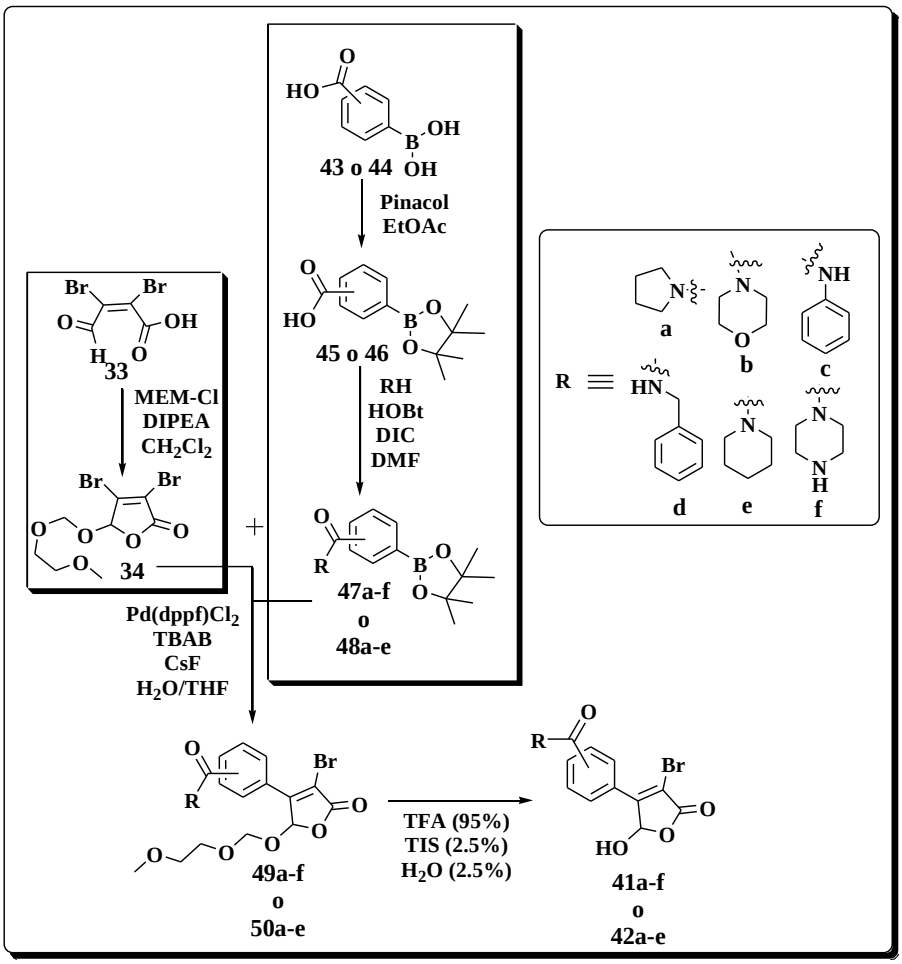

Scheme 4. *Synthetic protocol to generate derivatives **41a-f** and **42a-e**.*

After purification on silica gel, the synthetic scheme implied a Suzuki coupling between these advanced intermediates and the MEM-protected 3-bromo-γ-hydroxybutenolide scaffold **34** that afforded the protected adducts **49a-f** and **50a-e** (Scheme 4). Indeed, as for the synthesis of **6**-analogues, also in this case, it was necessary to protect the mucobromic acid **33** as MEM-derivative because of the instability of this ring in basic environment, as already explained in Chapter 2. We followed the previously optimized experimental conditions and, in order to speed up the reaction, we took advantages on microwave heating.

The last step, consisting in the removal of the protecting MEM group, using a solution of TFA/TIS/H_2O 95:2.5:2.5, afforded our products in good yield together with lower amounts of bis-substituted adducts as major by-products.

The new collection of PM-analogues (Chart 8) obtained is currently under biological studies in the laboratories of Professor Oliver Werz (Germany). The results of this investigation could help us to individuate new potential inhibitors of mPGES-1 expression and to trace the guidelines for further structural optimization of the active compounds.

~Chapter 4~

Design and Synthesis of Potential Selective mPGES-1 Inhibitors

---

De Simone R.; Chini M. G.; Bruno I.; Riccio R.; Muller D.; Werz O.; Bifulco G. Structure-based discovery of inhibitors of microsomal prostaglandin E_2 synthase (mPGES)-1, 5-lipoxygenase (5-LO) and 5-lipoxygenase-activating protein (FLAP): promising hits for the development of new anti-inflammatory agents. *J Med Chem.* Accepted.

Taking into account the interest shown by scientific community on mPGES-1 enzyme as promising anti-inflammatory target, we decided to direct our research towards the identification of new molecular platforms able to directly interact with this target. For this aim, as last step of this project, we focused the attention on the design and synthesis of molecules potentially able to selectively block the activity of mPGES-1. To rapidly direct the synthesis of the most promising new inhibitors, we took advantages of *in silico* screening. Specifically, we designed twenty-six new triazole-based compounds (Chart 9) in accordance with the pocket binding requirements of the human mPGES-1 enzyme. The choice of this scaffold was due to the possibility of applying 'click chemistry' reaction that are known to enable rapid generation of molecular collections in a few steps starting from a wide variety of reactants. That is perfect for medicinal chemistry project. According with ligand efficiency values (Figure 15), coming from docking calculations, we performed the synthesis of fifteen compounds that, at least in theory, showed to be more efficient in inhibiting mPGES-1. As expected by molecular docking data, the biological evaluation of these selected compounds disclosed a new interesting mPGES-1 inhibitor along with two relevant hits, **70** and **57**, that shown to be able to interact with two extremely important enzymes involved in the arachidonic acid cascade: 5-LO and FLAP respectively. In more details, compound **54** displayed selectivity for mPGES-1 with an IC_{50} value of 3.2 μM, while compound 5**7** apparently acts as FLAP inhibitor (IC_{50} = 0.41 μM). Finally, compound **70** showed a dual inhibitory activity on 5-LO and mPGES-1 (5-LO: IC_{50} = 0.8 μM; mPGES-1: IC_{50} = 11.7 μM) that could be a really promising strategy to improve the anti-inflammatory activity and, in the same time, to reduce the possible side effects that could arise from the inhibition of mPGES-1 and the redirection of PGH_2 to the other prostanoid synthases.[78]

4.1. Molecular docking studies

The first problem we had to face at the beginning of the design phase was the lack, in Protein Data Bank (PDB), of the crystallographic structure of the target enzyme in the bioactive conformation. Indeed, even if Jegerschöld *et al.* have recently elucidated the electron crystallographic structure of closed conformation of mPGES-1,[40] it has been demonstrated that the open form of the protein represents the productive enzyme. Consequently the absence of 3D X-ray crystal structure of open mPGES-1 conformation with a substrate or an inhibitor bound has represented the major difficulty for the rational design of new specific inhibitors, making the classical receptor-based approach quite challenging. That has stimulated many efforts for identifying the key characteristics of mPGES-1 inhibitors, based on quantum mechanic (QM) calculations,[144] SAR[92;145] and 3D-quantitative structure activity (QSAR) analysis,[146;147] multistep ligand-based strategy,[148] HTS screening,[91] molecular modeling and dynamics simulation[149] and site-direct mutagenesis studies. As reported by Mancini *et al.*[46] these efforts have led to the identification of several classes of mPGES-1 inhibitors: fatty acids and PGH_2 analogues,[87] MK-886 and indole analogues,[89] phenantrene imidazoles,[91] nonacidic agents and other inhibitors.[148] Considering as starting point the ring size of fatty acids and PGH_2 analogues, the well known peculiarity of indole based agents, such as the simultaneous contributions to the inhibitory activity on mPGES-1 of hydrophobic and electrostatic effects, we designed new triazole nucleus templates as potential scaffold for anti-inflammatory drugs. We designed a small set of compounds (Chart 9), decorating a di-substituted triazole ring, taking into account both the synthetic accessibility and the compatibility of substituents in positions 1 and 4 of the scaffold with the binding requirements of the pocket situated in the region at the interface of the two mPGES-1 subunits. Specifically, we gradually increased length, size,

hydro- and lipophilicity of R_1 and R_2 to optimize their chemo-physical properties.

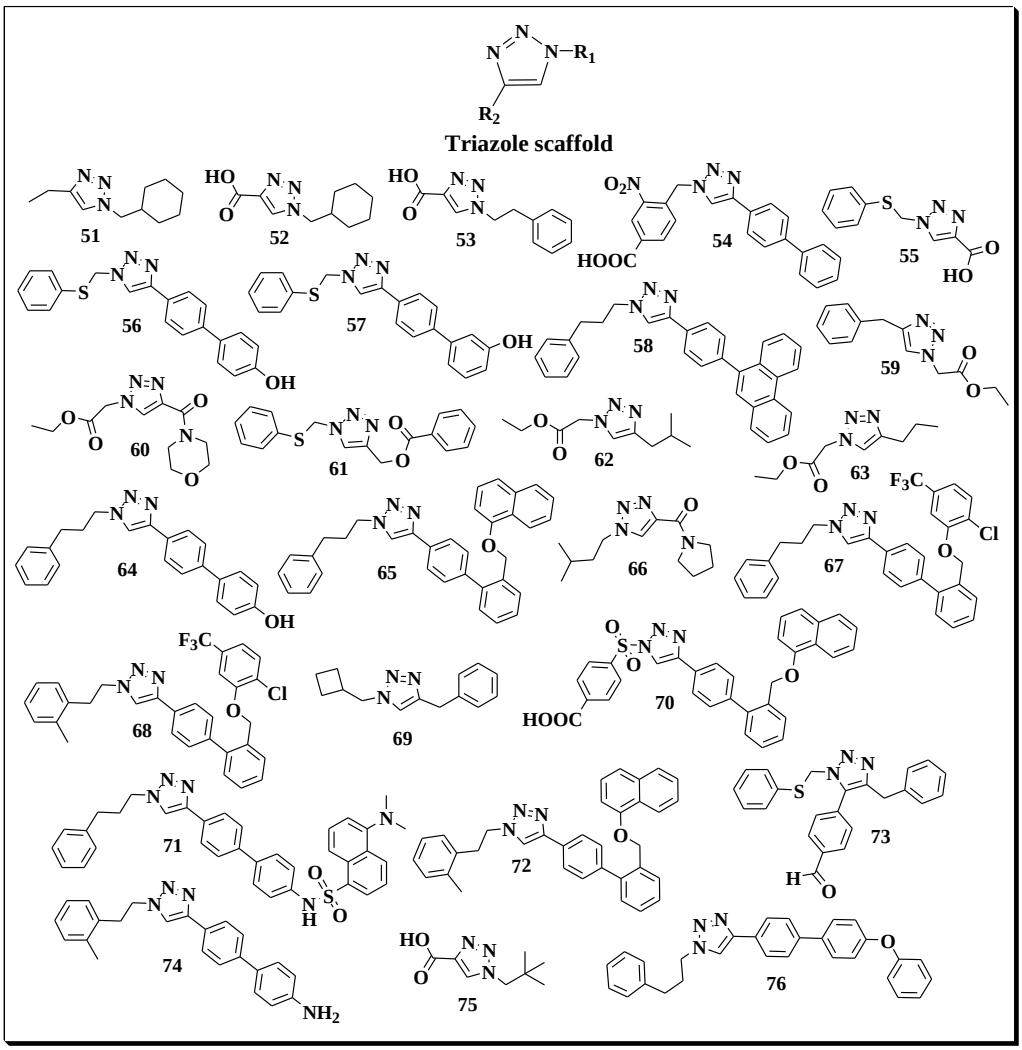

Chart 9. *Chemical structures of compounds **51-76** utilized for molecular docking studies.*

In order to identify the key structural features necessary for mPGES-1 inhibition, we performed an *in silico* screening by molecular docking using AutoDock 3.0.5 software[108] of a small set of molecules. Because of the impossibility to employ the crystallographic structure of mPGES-1, for our docking calculation we used the MGST-1 structure solved by Hebert *et al.* in 2006.[150] Indeed, like our target, it is an omotrimer, belonging to MAPEG

family, with the transmembrane hydrophobic portion, furthermore it has GSH as co-factor and showed the 38% of homology sequence with mPGES-1.[39] Recently the structure-based drug design targeting mPGES-1 has been facilitated by work of Hamza *et al.*[149] that have described the PGH_2 binding to the mPGES-1-GSH complex. In more details, as also demonstrated by site direct mutagenesis, the natural ligand, at the interface of each mPGES-1 monomer, establishes a strong salt bridge between its carboxylate group and the highly conserved Arg110 in the MAPEG family, and interacts with Arg70, Asn74, Arg73, Glu77, Tyr117, Leu121, Arg122, Arg126, Thr129, Arg110, His72, Lys26, Leu69 and Ile125. Taking into account the considerations above, we referred to the sequence alignment of these two MAPEG super family members for the rationalization of the small molecules binding mode (Table 2).[149]

mPGES-1	**MGST-1**
Arg110	Arg113
Arg70	Arg73
Asn74	Asn77
Tyr117	Tyr120
Leu121	Leu124
Arg126	Arg129
His72	His75
Lys26	Lys25
Glu66	Glu69
His113	His116
Arg73	Leu76
Arg122	Pro125
Thr129	Ala132
Leu69	Arg72
Ile125	Asn128
Thr78	Asn81
Tyr130	Phe133

Table 2. *List of the corresponding amino acids present both in mPGES-1 and MGST-1 catalytic sites.*

To individuate the compounds that, at least in theory, could have the most favorable binding energy with the target, we took into account the theoretical

affinities of the designed compounds **51-76** calculated by docking (Figure 15), reported as the most favorable MGST-1 free binding energy and ligand efficiency[151-153] (binding energy for heavy atom molecular ΔG/NHA).

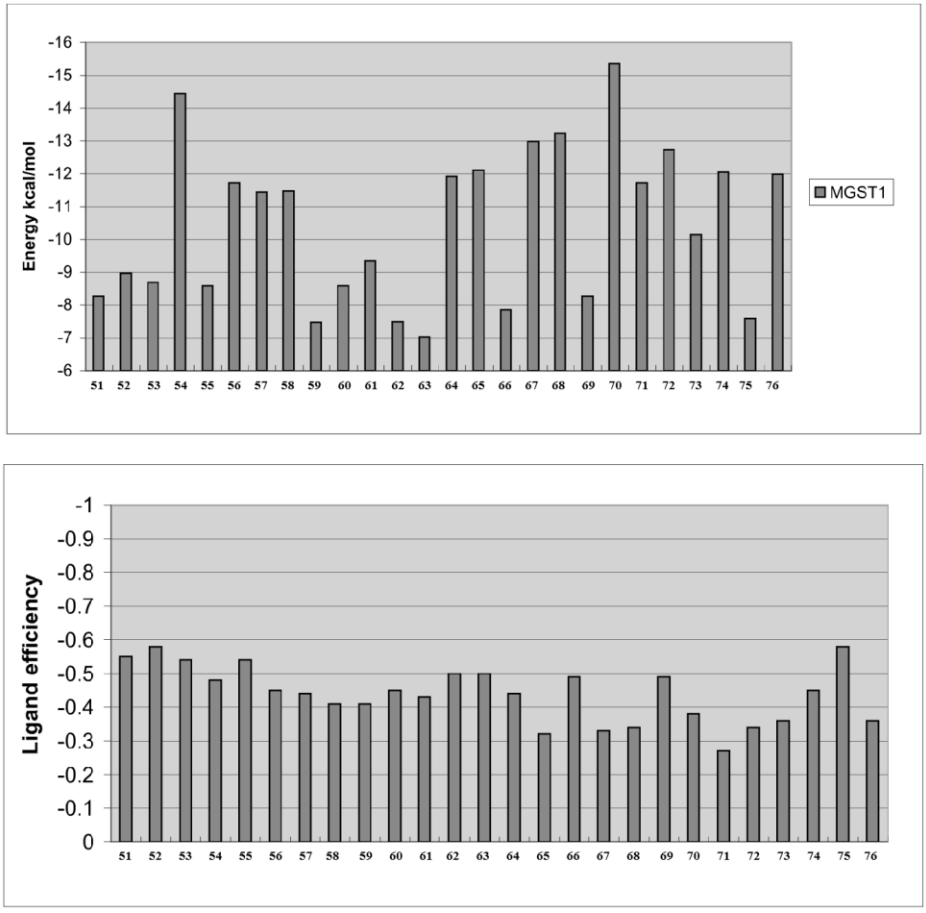

Figure 15. *Calculated affinities and ligand efficiency of compounds **51-76** with MGST-1.*

The above *in silico* results suggested the synthesis of compounds **54**, **56-58**, **61**, **64-65**, **67-68**, **70-74** and **76**, all showing the lowest free energy of binding and the best ligand efficiency ($E_{binding}$ lower than of 9 kcal/mol and ΔG/NHA deeper than -0.24 kcal/mol·NHA) as starting point for obtaining preliminary experimental results.

Particularly interesting were the *in silico* screening data concerning two compounds, **54** and **70** (Figure 16), which emerged as promising mPGES-1 inhibitors and trace the features of new potential anti-inflammatory drugs.

More specifically, both compounds disclosed a similar binding mode at the interface of the target monomer. Our proposed poses are in agreement with the model reported by Hamza *et al.*[23] In fact, the compounds make interactions with residues considered critical for PGH_2 binding, such as the hydrogen bonds with the carboxylic group in **54** and **70** with the highly conserved Arg113 in MGST-1 ($Arg110_{mPGES-1}$), guaranteeing, at least in theory, the enzyme binding specificity, as well as van der Waals and other interactions with residues of active site - the cation-π interaction with Lys67, Arg72 and Arg196 for **54** and with Lys67 and Arg196 for **70**.

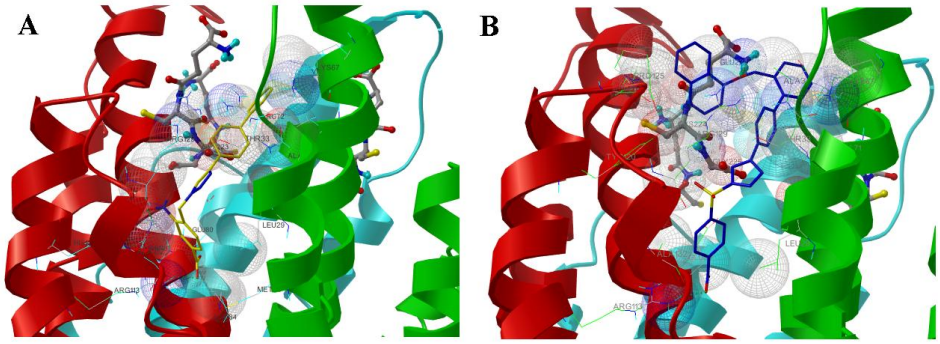

Figure 16. *3D model of interactions of compounds **54** (A) and **70** (B) with the MGST-1 binding site.*

4.2. Chemistry

Concerning the synthesis of the fifteen compounds traced by virtual screening calculations, the retro-synthetic analysis suggested us to obtain the triazole ring through a 1,3 dipolar cycloaddition reaction among appropriate terminal alkynes and azides. Finally, to obtain the desired compounds, the triazole adduct had to be subjected to a Suzuki coupling reaction (Scheme 5).

Specifically, for the synthesis of compounds **54**, **56**-**58**, **61**, **64**-**65**, **67**-**68**, **70**-**72**, **74** and **76** we utilized the synthetic procedure outlined in Scheme 6.

Except for **61**, we took advantages of 1,3-dipolar cycloaddition reaction (click reaction) among appropriate terminal alkynes and azides to generate the triazole intermediates **80-81**, **85-87** and **89** that were successively subjected to the Suzuki cross-coupling reaction with the appropriate commercially available boronic acids **a-i**.

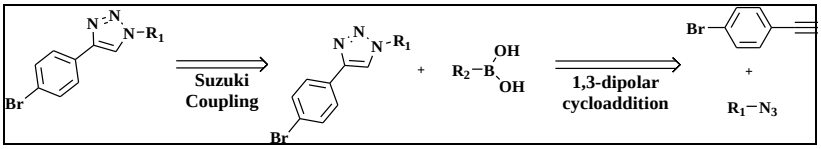

Scheme 5. *Retro-synthetic approach for the synthesis of the triazole derivatives **51-76**.*

Concerning the formation of triazole ring, we performed two different strategies on the basis of the availability of the starting reactants. In more details, when we started from the commercially available azide **77**, the traditional protocol for 1,3-dipolar cycloaddition at room temperature for 18 h in presence of $CuSO_4$ as catalyst and sodium ascorbate in a mixture of *t*-BuOH/H_2O 1:1 was used (Scheme 6a).[116] On the contrary, when the azides were generated *in situ* with sodium azide starting from the corresponding halides, the microwave irradiation technique provided a faster way to obtain the desired triazole intermediates **85-87** (Scheme 6b) in a one pot reaction.[154] Different reaction conditions have been tested to finally select the better ones. The best results were obtained setting the microwaves at 200 W and 250 psi and conducting the reaction at 125°C for 30 minutes.

The synthesis of intermediate **89** required a different procedure owing to the presence of the sulfonyl functionality which is a strong electron-withdrawing group that could negatively affect the reaction outcome. Indeed, the copper-catalyzed coupling reaction of azides with alkynes (Figure 17) was proved to firstly produce 5-cuprated N-substituted triazole intermediates (A) whose stability is governed by various factors including the type of azides and alkynes, the reaction medium and the temperature. In this frame particularly

crucial are the azide structural features: when R_1 is alkyl or aryl, the N^1-N^2 bond is stable, and the corresponding 1,2,3-triazoles are easily obtained. On the contrary, when R_1 is a strong electron-withdrawing group, such as sulfonyl group, the electron density on the N^1 atom of the intermediate (A) is low, and the N^1-N^2 bond is readily cleaved in favour of a variety of by-products rather than the desired cycloadduct.

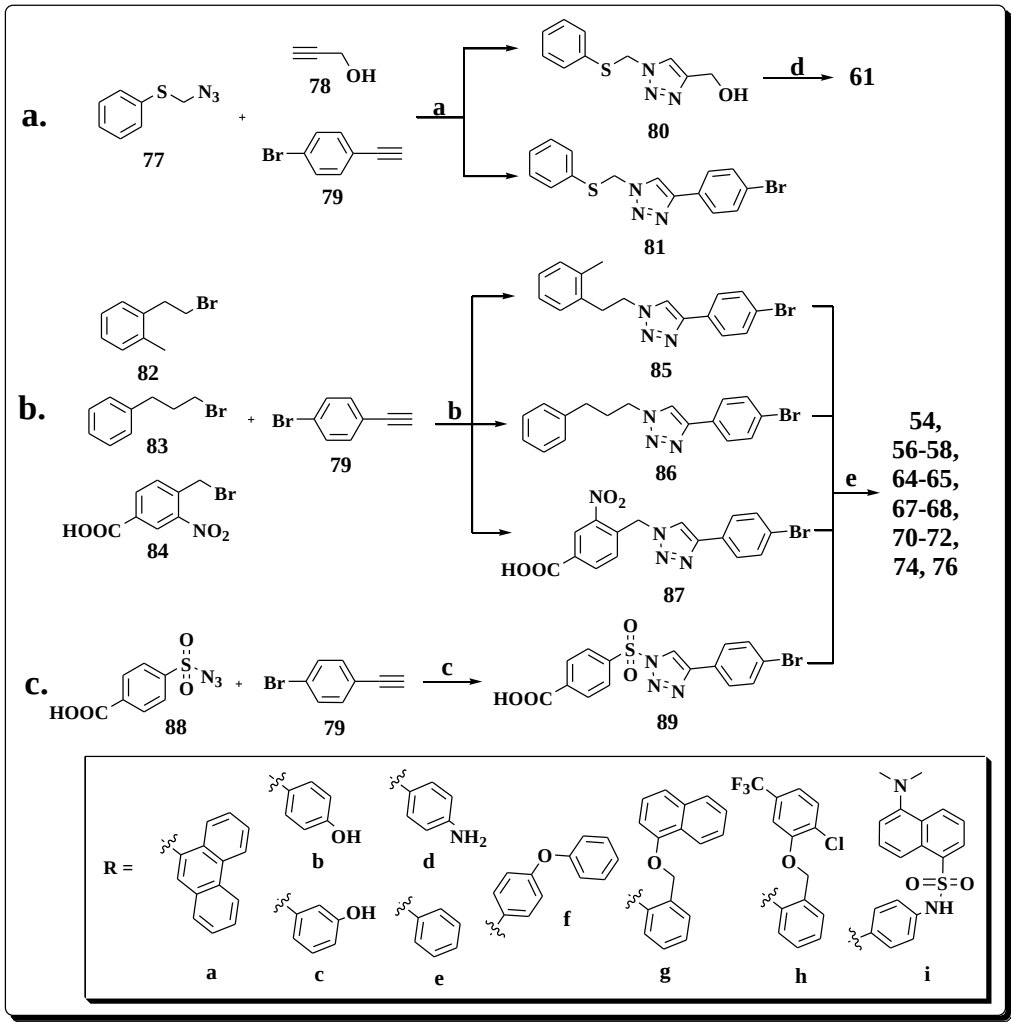

Reagents and conditions: (a) $CuSO_4$, sodium ascorbate, H_2O/*t*-BuOH 1:1, r.t., overnight; (b) $CuSO_4$, Cu(0), NaN_3, *t*-BuOH/H_2O 1:1, MW, 30 min; (c) CuI, 2,6 lutidine, $CHCl_3$ dry, 12h, 0°C (d) C_6H_5COCl, DMF dry, reflux, overnight; (e) $RB(OH)_2$ **a-i**, CsF, $Pd(dppf)Cl_2$, H_2O/THF, MW, 20-30 min.

Scheme 6. *Synthetic strategy for the synthesis of compounds* ***54***, ***56-58***, ***61***, ***64-65***, ***67-68***, ***70-72***, ***74*** *and* ***76****.*

However, we were able to obtain the desired sulfonyl triazole intermediate **89**, carrying out the cycloaddition between 1-bromo-4-ethynylbenzene **79** and 4-carboxybenzenesulfonazide **88** in dry chloroform at 0° C in presence of 2,6-lutidine as base (Scheme 6c).[155-157]

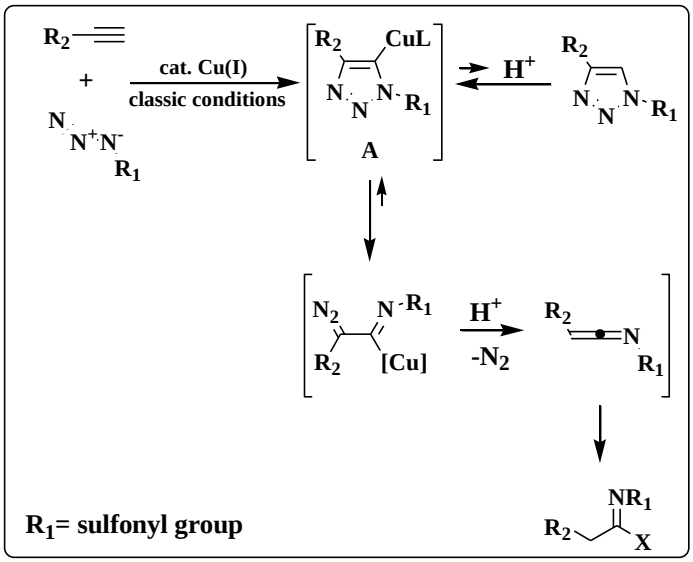

Figure 17. *Copper-catalyzed cycloaddition of sulfonyl azides with alkynes and opening process of triazoles.*

As we can easily note, all the strategies employed to obtain the triazole ring need of the presence of copper as catalyst which seems to be essential for the regioselective formation of the desired 1,4-disubstitued triazoles.

The triazole adducts **81**, **85-87** and **89**, obtained in the first step, were finally subjected to the Suzuki cross-coupling reaction with the appropriate boronic acids **a-i** following the experimental conditions previously optimized by us,[141] implying for the use of $Pd(dppf)Cl_2$ as catalyst and CsF as base in a mixture of THF/H_2O 1:1, under microwaves irradiation; the desired final compounds **54**, **56-58**, **64-65**, **67-68**, **70-72**, **74** and **76** (Chart 9) were obtained in satisfactory yields.

On the contrary, compound **61** was obtained submitting the triazole **80** to direct acylation with benzoyl chloride in DMF as solvent (Scheme 6).

Finally, in order to synthesize compound **73**, we took advantages of a multicomponent one-pot reaction between phenyl-1-propyne **90** and azidomethyl phenyl sulfide **77** in presence of CuI-N-bromosuccinimide (NBS); this step provided the desired 1,4,5-trisubstitued-1,2,3-triazole **91** bearing a iodine atom at C-5 position.[158] In the last step, the triazole intermediate **91** was subjected to the Suzuki cross-coupling reaction with 4-formyl-phenyl-boronic acid **92** affording compound **73** in good yield (Scheme 7).

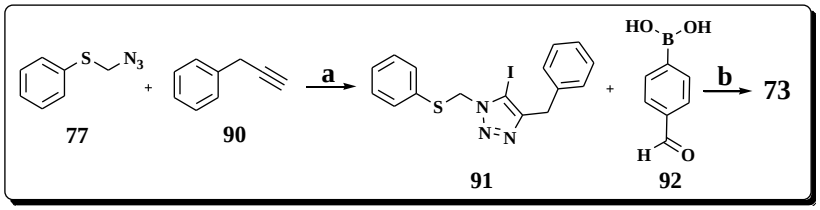

[b]Reagents and conditions: (a) CuI, DIPEA, NBS, THF, r.t., 4h; (b) CsF, Pd(dppf)Cl_2, H_2O/THF, MW, 30 min.

Scheme 7. *Synthetic strategy for the synthesis of compound **73**.*

Concerning the mechanism involved in the formation of the 5-iodo-1,2,3-triazole scaffold, it has been demonstrated that the oxidation–reduction reaction between NBS and CuI is the crucial step. Indeed, it is responsible for the *in situ* generation of I^+, which is trapped by the carbon anion intermediate from the click reaction (Figure 18).

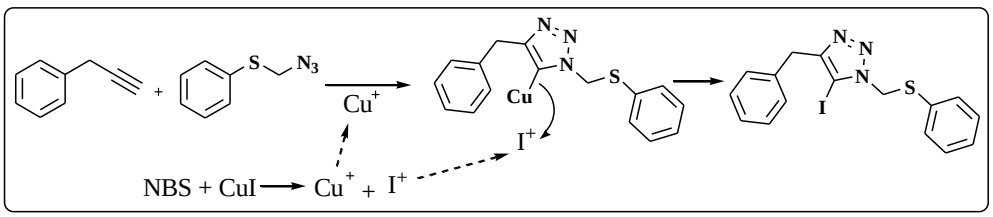

Figure 18. *Mechanism involved in the formation of 5-iodo-1,2,3-triazole scaffold.*

During these processes, the Cu^+ do not suffer oxidation; instead, it acts as catalyst for the click reaction. Consequently, catalytic amount of CuI plays

double fundamental roles. As first it provides Cu^+ which is the catalyst, necessary in the Huisgen's cycloaddition between azide and terminal alkynes for the regioselective production of the 1,2,3-triazole 1,4-disubstitued. Furthermore it provides I^- that NBS provides to oxidize to I^+.

4.3. Bioactivity

The biological screening of the synthesized molecules was made in collaboration with Professor Oliver Werz of the University of Tuebingen (Germany).

In more details, to assess the ability of the selected compounds **54**, **56-58**, **61**, **64-65**, **67-68**, **70-74** and **76** to interfere with the activity of mPGES-1, a cell-free assay using the microsomal fractions of IL-1β-stimulated A549 cells, as source for mPGES-1, was applied. In a first screening round all compounds, solubilised in dimethylsulfoxide (DMSO), were tested at a concentration of 10 μM. The mPGES-1 inhibitor compound MK-886 **8** (IC_{50} = 2.4 μM)[101] was used as reference control, and DMSO (0.3%, v/v) was used as vehicle control. Compounds **54**, **57**, **70** and **73** significantly inhibited mPGES-1 activity, whereas all other derivatives were essentially inactive (Table 3).

Interestingly, these data confirmed the results from the docking studies indicating **54** and **70** as mPGES-1 inhibitors. More detailed analysis of **54** in concentration-response studies (Figure 19) revealed an IC_{50} value of 3.2 μM and indicated an almost complete inhibition of mPGES-1 activity at 30 μM. In contrast to **54**, compound **70** failed to entirely suppress mPGES-1 activity and the concentration-response curve seemingly reached a plateau with maximum inhibition of approx. 40% at the highest concentration (Figure 19).

Compound	mPGES-1 activity	
	IC_{50} [µM]	Remaining activity at 30 µM
54	3.2	12.0% ± 3.7**
56	> 30	89.0% ± 2.9
57	> 30	60.1% ± 4.3**
58	> 30	78.2% ± 12.8
61	> 30	76.1% ± 7.9
64	> 30	73.6% ± 8.0
65	> 30	96.8% ± 0.5
67	> 30	91.9% ± 8.1
68	> 30	87.9% ± 8.4
70	> 30	59.8% ± 7.2**
71	> 30	85.0% ± 9.3
72	> 30	90.0% ± 6.8
73	> 30	72.1% ± 4.2*
74	> 30	98.2% ± 7.3
76	> 30	88.7% ± 2.7

Table 3. *Effect of test compounds **54**, **56-58**, **61**, **64-65**, **67-68**, **70-74** and **76** on the activity of mPGES-1. Data are given as mean +/- S.E., n=4-6. *p < 0.05, **p < 0.01.*

Previous studies on acidic mPGES-1 inhibitors showed that such compounds often interact also with other enzymes within the arachidonic acid cascade, such as 5-LO or FLAP.[89;93] On the other hand, interference with 5-LO or FLAP, the key enzymes in the formation of LTs from arachidonic acid, is considered a valuable characteristic of a given mPGES-1 inhibitor, because dual suppression of PGE_2 and LT formation might be superior over single interference in terms of higher anti-inflammatory efficacy as well as in terms of reduced side effects.[47] Thus, the test compounds were further analysed for

inhibition of 5-LO activity, in a cell-free assay using isolated human recombinant 5-LO as enzyme source. The well-recognized 5-LO inhibitor (*E*)-*N*-hydroxy-*N*-(3-(3-phenoxyphenyl)-allyl)acetamide (BWA4C)[159] was used as positive control, DMSO (0.3%, v/v) was used as vehicle control. Intriguingly, among the test compounds, **70** was the most active derivative with IC_{50} = 0.8 µM, followed by **71**, **54** and **67** (Table 4, IC_{50} = 3.3 µM, 7.2 µM, and 8.3 µM, respectively) that all inhibited 5-LO activity in a concentration-dependent manner. Also **56**, **64**, **73** and **76** significantly inhibited 5-LO at a concentration of 30 µM but the magnitude of inhibition did not exceed 50% (Table 4) and thus IC_{50} values could not be determined.

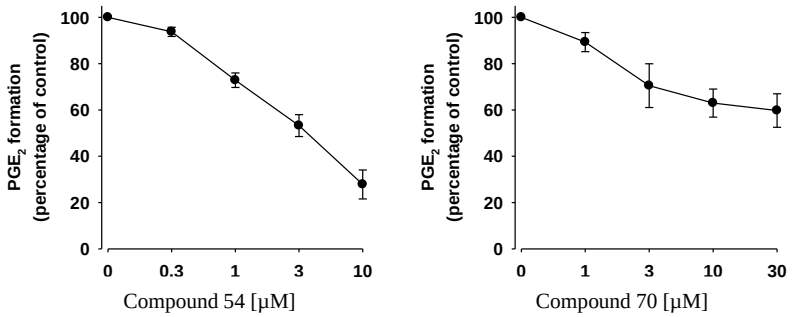

Figure 19. *Inhibition of mPGES-1. Concentration-response curves of compounds **54** and **70** for inhibition of mPGES-1 activity in microsomal preparations of IL-1β-stimulated A549 cells.*

Finally, the potential inhibitory effect of the test compounds **54**, **56-58**, **61**, **64-65**, **67-68**, **70-74** and **76** on FLAP in human neutrophils activated by ionophore A23187 was tested using compound MK-886 **8** (IC_{50} for FLAP in neutrophils approx. 70 nM)[102] as control and DMSO (0.3%, v/v) as vehicle control. As shown in Table 4, compound **70** revealed the best inhibitory activity (IC_{50} = 0.6 µM) followed by compound **71** (IC_{50} = 2.8 µM). A remarkable and concentration-dependent suppression of cellular 5-LO products synthesis was found for **57** with IC_{50} = 0.4 µM and also for **56** and **74** (IC_{50} = 0.9 and 1.7 µM respectively) although the compounds hardly inhibited 5-LO in cell-free assay. This suggests that, to suppress 5-LO products

formation, **56**, **57** and **74**, in intact cells, may primarily act on other targets different from 5-LO enzyme, presumably on FLAP. Such mechanism may also be attributed to compounds **61** and **73**, though with lower potencies (IC_{50} = 8.9 and 6.1 µM, respectively).

Comp.	5-LO activity; cell-free		5-LO activity; intact neutrophils	
	IC $_{50}$ [µM]	**Remaining activity at 30 µM**	**IC $_{50}$ [µM]**	**Remaining activity at 30 µM**
54	6.7	20.0% ± 0.9**	9.2	20.1% ± 11.0**
56	> 30	62.3% ± 1.4**	0.9	34.8% ± 7.0** a)
57	27	48.8% ± 0.4**	0.4	1.1% ± 0.3** a)
58	> 30	82.9% ± 0.9	> 30	85.7% ± 3.5
61	> 30	80.8% ± 5.3	9.3	14.6% ± 5.2**
64	> 30	58.4% ± 12.7*	> 30	70.2% ± 8.5
65	> 30	77.4% ± 0.9	> 30	79.9% ± 10.7
67	8.8	10.1% ± 4.6**	> 30	52.7% ± 15.0*
68	> 30	82.5% ± 4.4	> 30	92.1% ± 8.1
70	0.8	13.6% ± 2.8** a)	0.6	3.5% ± 2.5** a)
71	4.1	5.1% ± 0.8**	2.8	21.2% ± 4.3** a)
72	> 30	78.4% ± 10.3	> 30	84.5% ± 3.4
73	> 30	57.3% ± 1.2**	6.0	17.3% ± 2.5** a)
74	> 30	60.7% ± 10.0	1.7	22.0% ± 2.6** a)
76	> 30	59.2% ± 6.4*	> 30	70.1% ± 9.0

a) remaining activity at 10 µM

Table 4. *Effect of test compounds on the activity of 5-LO in cell-free and cell-based (intact neutrophils) assays. Data given as mean +/- S.E., n=4-6. *p < 0.05, **p < 0.01.*

All in all, based on the outcomes of the biological activity data, **54** is the most efficient inhibitor of mPGES-1, **57** might act as a FLAP inhibitor, while **70**

could be a potent direct 5-LO inhibitor, besides moderate inhibition of mPGES-1. Hence, we aimed to rationalize the results through molecular modeling studies. As preliminary remarked, it should be put in evidence that compounds **54** and **57**, inhibiting the two MAPEG family members, showed quite similar chemical features; on the contrary, the more encumbering ligand **70** seems to target no structurally related MAPEG enzymes.

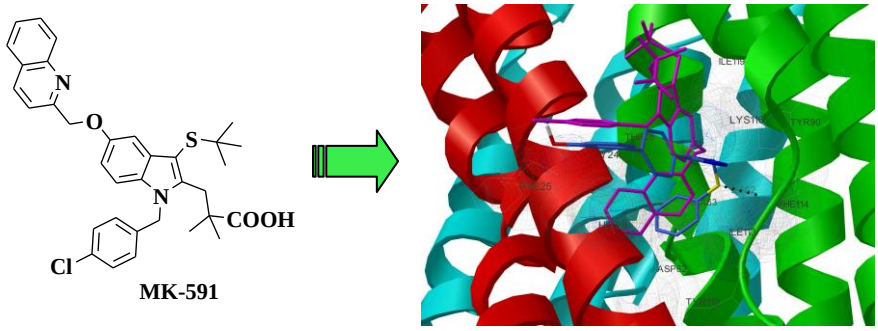

Figure 20. *Chemical structure of MK-591 and 3D model of interactions of **57** with FLAP. The figure highlights similar interactions for both **57** and MK-591 with arachidonic acid-binding site.*

For our calculations we used the three dimensional structure of FLAP in complex with the inhibitor MK591 solved by Ferguson *et al.*[160] in 2007 (PDB ID code 2Q7M). Owing to the lack of crystal structure information on 5-LO, we used a 15-LO[161] (PDB ID code 1lox) enzyme, presenting the highest sequence similarity (38% identity with human 5-LO) among the dioxygenase family (8-, 9-, 11-, 12-LO).

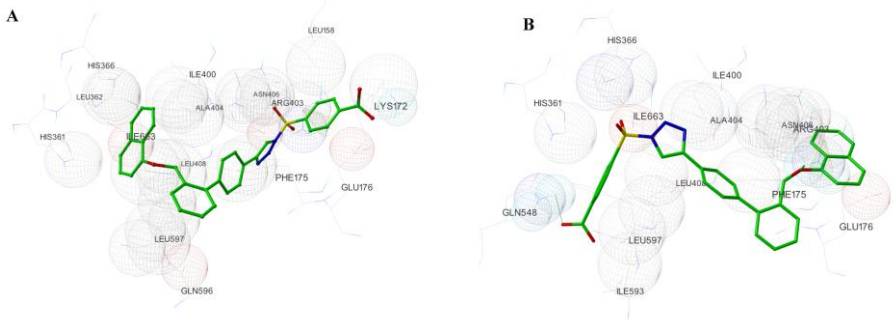

Figure 21. *3D model of interaction of **70** and 15-LO enzyme active site.*

Taking into account the considerations reported above for the MGST-1 enzyme, also in the case of FLAP, the binding specificity was conferred by the H-bond with the Lys116. In our proposed pose, **57** (Figure 20) interacts not only with the fundamental amino acids, but also adopts the equivalent spatial disposition of the co-crystallized inhibitor,[161] maintaining the same interactions network. Moreover, the phenyl group in R_1 forms a π-π stacking with Phe25.

Three different classes of inhibitors can be generally considered for 5-LO: (1) antioxidant agents interfering with the redox catalytic cycle of the enzyme, (2) iron-chelating agents and (3) nonredox-type inhibitors, which compete with arachidonic acid for the binding to the enzyme.[162] In our docking studies, we supposed that **70** acts as nonredox-type LO inhibitor.

As described for mPGES-1, the rationalization of the 5-LO binding mode was obtained considering the fundamental amino acids in the active site of the enzyme as reported by Wouters *et al.*,[163] taking in consideration the specific polar interaction of the carboxylate moiety of arachidonic acid with $Lys409_{5\text{-}L0}$ ($Arg403_{15\text{-}LO}$).

For compound **70**, we obtained two different conformation families, accounting for two independent high affinity binding modes (Figure 21A-B). In both the conformations, the specific interaction with Arg403 was maintained. In more details, in the first conformation type (Figure 21A) the phenyl group in R_1 shows a cation-π interaction, while in the second conformation type (Figure 21B), the same cation-π interaction with Arg403 was exerted by the naphtyl group in R_2 present in the alternative conformation. In the latter case, the oxygen atom in R_2 forms an additional H-bond with the positively charged (Arg403) residue. Even if R_1 and R_2 are located on the opposite sites of the target pocket, the other interactions with the receptor counterpart remain unmodified and are in accordance with the structural

requirements indicated by Wouters *et al.*,[163] that is two hydrophobic groups, an aromatic ring and two hydrogen bond acceptors.

~Chapter 5~

Optimization Processes on Compound 54, the New Hit Emerged as Promising mPGES-1 Inhibitor

Encouraged by the interesting biological results obtained from the triazole derivatives **54**, **56-58**, **61**, **64-65**, **67-68**, **70-74** and **76** that allowed us to identify some potential inhibitors of mPGES-1 enzyme, in the last part of this project we directed our attention to a new hit, compound **54**, that emerged as a selective inhibitor of the target enzyme (IC_{50} = 3.2 μM). In order to improve its biological activity, we decided to rely on some well-reasoned structural changes of the basic molecule (Chart 10). In more details, taking into consideration the model of interaction between compound **54** and its target enzyme (Figure 16A), we decided to keep unchanged the basic scaffold of compound **54** bearing an aromatic moiety with a carboxylic function in 1-position of the triazole ring and a biphenylic system linked on C-4 of the scaffold. In fact, the carboxylic group seems to be responsible for the mPGES-1-binding specificity as it was considered crucial for the interaction with Arg113, the key residue involved in PGH_2 binding. On the other hand, the biphenyl system seems to project the appropriate substituent at the right distance to interact with polar amino acids present in the upper side of the catalytic pocket where GSH is located, such as Thr33, Arg37, Lys67 and Arg129.

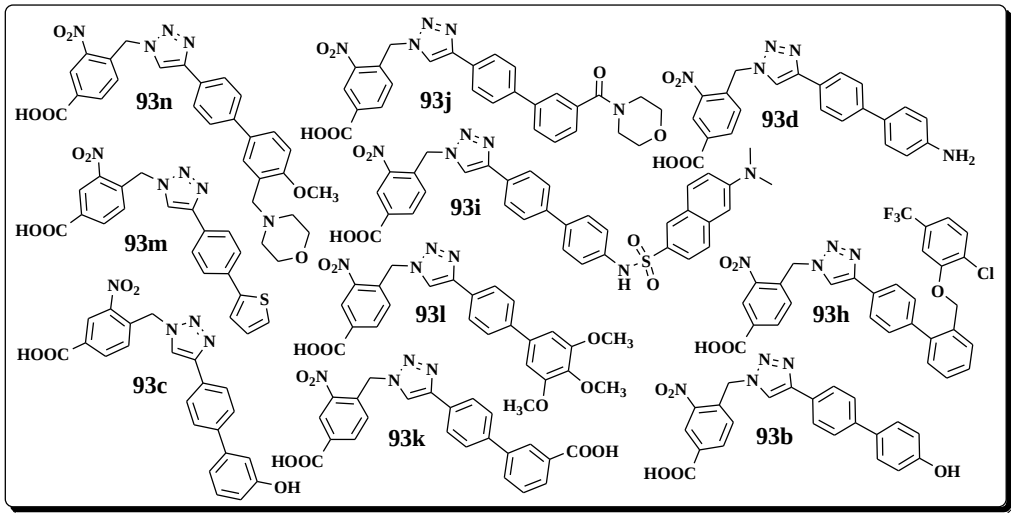

Chart 10. *Collection of compound **54**-derivatives.*

On the basis of these preliminary considerations, as start we decided to vary the type and the position of the substituents on the second ring of the biphenyl system in order to explore more chemical space. Moreover, we also proved to replace one phenyl group of the biphenyl with an aromatic eterocycle, like tiophene (compound **93m**) in order to definitively establish the crucial role played by the biphenyl system in the interaction with enzyme active site.

5.1. Chemistry

Concerning the synthesis of analogues **93b-d** and **93h-n**, as already reported for the synthesis of the first generation of triazole derivatives **54**, **56-58**, **61**, **64-65**, **67-68**, **70-74** and **76**, the retro-synthetic approach suggested us to obtain the triazole ring through the above described 1,3 dipolar cycloaddition among the appropriate terminal alkynes and azides, while to generate the decorated biphenyl system we could rely on the versatile Suzuki coupling reaction, that afforded us the desired compounds (Scheme 8).

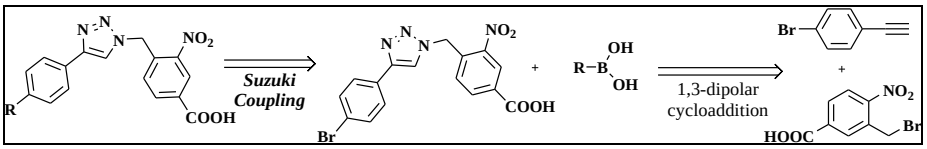

Scheme 8. *Retro-synthetic approach for the synthesis of derivatives **93b-d** and **93h-n**.*

In more details, the triazole ring was generated as usual in a one pot reaction, taking advantages on the microwaves technology that allowed us to obtain *in situ* the azide starting from the corresponding halide and sodium azide (Scheme 9). Also in this case the 1,3-dipolar cycloaddition required the presence of Cu(I) as catalyst for the reaction regiocontrol.[116] The triazole intermediate **87**, obtained from the first step, was further subjected to the Suzuki cross-coupling reaction with the appropriate boronic acid **b-d**, **h-n** following the experimental conditions previously optimized by us,[141] requiring the use of Pd(dppf)Cl_2 as catalyst and CsF as base in a mixture

THF/H_2O 1:1, under microwaves irradiation; the desired compounds **93b-d** and **93h-n** (Chart 10) were obtained in satisfactory yields.

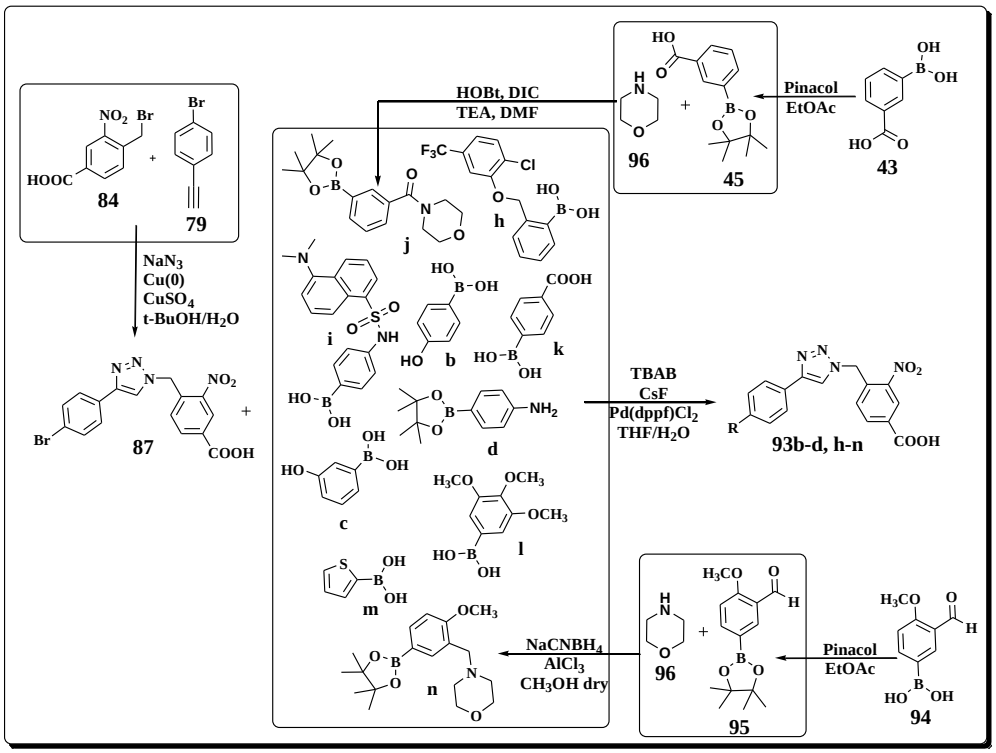

Scheme 9. *Synthetic protocol employed to generate derivatives **93b-d** and **93h-n**.*

The boronic acids employed in the last step, are all commercially available except for pinacol esters **j** and **n**. These last were obtained, as shown in Scheme 9, starting from the appropriate boronic acids **43** and **94** which were first protected as pinacol esters **45** and **95** to reduce the polarity of the intermediates and make easier the purification step on silica column. Finally, to obtain the advanced intermediate **n**, the pinacol ester **95** was subjected to a reductive amination reaction with morpholin **96**, while to generate the amidic derivate **j**, the pinacol ester **45** was subjected to the reaction of amidation with morpholin **96** using TEA as base, HOBt and DIC as carboxylate activators and DMF as solvent.

The synthesized compounds **93b-d** and **93h-n** are currently under biological investigation in the laboratories of Professor Oliver Werz of the University of Tuebingen (Germany) and, in our opinion, the results could be very useful to trace clearer guidelines for further structural optimization which could lead to discover new potent mPGES-1 inhibitors as promising drug candidates.

Conclusions

In conclusion, in the course of the present project an efficient approach toward the discovery of new agents able to target mPGES-1 enzyme has been outlined. In more details, starting from compound **6**, emerged as promising inhibitor of mPGES-1 expression, and basing on the experience gained in handling the densely functionalized γ-hydroxybutenolide scaffold, we were able to discover new hits possessing a better biological profile compared to the lead molecule **6**.

Furthermore, in order to explore more chemical space useful to discover new and more effective inhibitors of mPGES-1 expression as promising anti-inflammatory candidates, a new collection of γ-hydroxy-butenolides bearing amido-aromatic appendages has been developed and their biological evaluation is still in progress.

Concerning the discovery of new agents able to directly interfere with the target enzyme, taking advantages of molecular modelling studies and basing either on the highly efficient and reliable 'click chemistry' approach as well as the versatile Suzuki cross-coupling reaction, a collection of triazole based compounds was successfully realized. Biological studies, performed on these molecules in collaboration with professor Oliver Werz' group, allowed us to identify three interesting molecules as promising candidates for the discovery of potent and safer anti-inflammatory drugs: compound **54** displaying a selective inhibitory activity towards mPGES-1 (IC_{50} = 3.2 μM), compound **70** that dually inhibits 5-LO and mPGES-1 and compound **57** acting as FLAP inhibitor (IC_{50} = 0.4 μM).

Finally, as last task of this project we focused our efforts to amplify chemical diversity of the triazole scaffold in order to gain a clear structure-activity profile useful for further lead optimization process.

In the course of this project, in addition to mastering the main spectroscopic and spectrometric techniques of the structural elucidation, I had the opportunity to gain experience on some of the most advanced methods of

organic synthesis, such us Suzuki cross-coupling reaction, a versatile process for carbon-carbon bond formation, 1,3-dipolar cycloaddition reaction (click reaction), a powerful tool in the hands of chemists for rapid and easy generation of large library of compounds, and finally photooxydation reaction that is potentially able to furnish a lot of interesting compounds of heterocycle nature.

Furthermore, as some of the synthesis presented here were carried out with microwaves heating, I became skilful in the use of this technology. Finally, I also experienced the most recent and advanced computer aided methods applied for drug design processes that allowed to rapidly direct the synthetic efforts towards those molecules showing, at least in theory, the best affinity for the selected target.

Experimental Section

~Chapter 6~

Inhibitors of mPGES-1 Expression

6.1. LUDI design

The Ludi module of Insight II (Accelrys, San Diego, CA) was used for the in silico design of compounds **41a-f** and **42a-e**. Computation was performed on a Silicon Graphics Indigo 2 workstation equipped with a R10000 processor. The 3D complex structure bee venom PLA_2 (1POC)-PM[4] was imported into the graphic modeling program Insight II; the tetracyclic portion of PM **5** was deleted from the active site of the above-mentioned adduct, whereas the tridimensional coordinates of the γ-hydroxybutenolide ring were kept unaltered. On this data set, LUDI performed a database screening on the User_link_library (provided by Accelerys version 1998 and 2000.2) to select appropriate aromatic and heteroaromatic fragments to replace the sesterterpene skeleton of PM **5** by linking the γ-hydroxybutenolide ring. The value of the maximum RMS deviation was fixed at 0.4 Å, the lipo weight was set at 10, the H bond weight was set at 1 and the value of the minimum separation was definitively 3.00. The other parameters were used as standard default. For each fragment, the LUDI score was calculated by means of the scoring function mentioned as *energy estimate_3*.

6.2. Methods and materials

All water and air sensitive reactions were carried out under an inert atmosphere (N_2 or Ar) in oven- or flame-dried glassware. DCM and THF were distilled from CaH_2 immediately prior to use. Water was degassed under vacuum (10 mbar). All reagents were used from commercial sources without any further purification.

Microwave reactions were performed on a CEM Discover® single mode platform using 10 mL pressurized vials.

Reactions were monitored on silica gel 60 F254 (Merck) plates and visualized with potassium permanganate or ninhydrin and under UV (λ = 254 nm, 365 nm). Flash column chromatography was performed using Merck 60/230–400

mesh silica gel. Analytical and semi-preparative reverse-phase HPLC purifications were performed on a Waters instrument using Jupiter C-18 column (250 · 4.60 mm, 5 µm, 300 Å; 250 · 10.00 mm, 10 µm, 300 Å, respectively). Purity grade of final products was determined on a Agilent 1100 HPLC using analytical reverse-phase columns (Method: Jupiter C-18, 250 · 4.60 mm, 5 µm, 300 Å). Reaction yields refer to chromatographically and spectroscopically pure products. Proton-detected (^{1}H, HMBC, HSQC) and carbon-detected NMR spectra were recorded on Bruker instruments of Avance series operating at 300, 500 and 600 MHz and 75, 125 and 150 MHz, respectively. Chemical shifts are expressed in parts per million (ppm) on the delta (δ) scale. The solvent peak was used as internal reference: for ^{1}H NMR $CDCl_3$ = 7.26 ppm and CD_3OD = 3.34 ppm; for ^{13}C NMR: $CDCl_3$ = 77.0 ppm and CD_3OD = 47.7 ppm. Multiplicities are reported as follows: s, singlet; d, doublet; t, triplet; m, multiplet; dd, doublet of doublets.

Electrospray mass spectrometry (ES-MS) was performed on a LCQ DECA ThermoQuest (San Josè, California, USA) mass spectrometer.

[5,6,8,11,12,14,15(n)-3H] PGE_2 and [9,10-3H]oleic acid were purchased from Amersham Biosciences (Barcelona, Spain). The rest of reagents were from Sigma (St. Louis, MO, USA). Escherichia coli strain CECT 101 was a gift from Professor Uruburu, Department of Microbiology, University of Valencia, Spain.

6.2.1. Photooxidation of 3-bromofuran 36

A two neck flask with 150 mL of dry DCM was cooled to -78 °C. Under stirring, 3-bromofuran **36** (612 µL, 6.8 mmol) and finely powdered polystyrene-bound rose bengal catalyst (150 mg) were added. Then the base (2 equiv.) was introduced and the oxygen bubbled for 15 min. After the 300 W lamp was turned on, the solution was stirred at -78 °C in a continuous flow of oxygen for 9 h until the reaction appeared complete by TLC. The mixture was

allowed to warm to 0 °C, the catalyst was filtered off and the solution rapidly washed with an aqueous solution of HCl 1M (150 mL). The aqueous layer was extracted with DCM (3 x 100 mL). The organics were finally dried with Na_2SO_4, filtered and concentrated *in vacuo*. The residue was purified on a semipreparative C-18 reverse-phase-HPLC column, leaving the desired product (**37** or **39**) as an oil.

4-Bromo-5-hydroxy-5*H*-furan-2-one 37. ^{1}H-NMR (300 MHz, $CDCl_3$): δ

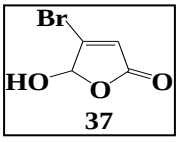

37

6.42 (1H, s), 6.04 (1H, s). ^{13}C-NMR (75 MHz, $CDCl_3$): δ 169.4, 148.1, 124.0, 99.6. ES-MS calcd. for $C_4H_2BrO_3$: $[M-H]^-$ 176.93 and 178.92 (1:1); found 176.9 and 178.9 (1:1).

3-Bromo-5-hydroxy-5*H*-furan-2-one 39. ^{1}H-NMR (300 MHz, $CDCl_3$): δ

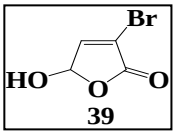

39

7.34 (1H, d, *J*=1.5 Hz), 6.24 (1H, d, *J*=1.5 Hz). ^{13}C-NMR (75 MHz, $CDCl_3$): δ 167.7, 149.3, 117.8, 98.7. ES-MS calcd. for $C_4H_2BrO_3$: $[M-H]^-$ 176.93 and 178.92 (1:1); found 176.8 and 178.8 (1:1).

6.2.2. Protection of 37 and 39 as THP ethers

A solution of **37** or **39** (40 mg, 0.22 mmol) and DHP (51 μL, 0.56 mmol) in 4 ml of dry DCM was cooled to 0 °C in ice-bath. Upon stirring *p*-toluensulfonic acid monohydrate (192 mg, 1.12 mmol) was slowly added keeping the temperature at 0 °C for 10 min. The mixture was allowed to warm to room temperature and the reaction was stopped after 4 h. The solution was diluted with 20 mL of DCM and then washed with a 1:1:2 mixture of saturated NaCl, saturated $NaHCO_3$ and water (20 mL). The organic layer was dried, filtered and concentrated in *vacuo.* The crude brown oil obtained was purified by flash chromatography (100% *n*-hexane to 30% diethyl ether/*n*-hexane) to give, depending on the starting material, intermediates **38** or **40**.

4-Bromo-5-(tetrahydropyran-2-yloxy)-5*H*-furan-2-one 38. Yield: 95%; ^{1}H-NMR (300 MHz, $CDCl_3$): δ 6.38 (1H, s), 6.10 (1H, s), 5.16 (1H, s), 3.96-3.90 (1H, m), 3.81-3.75 (1H, m), 1.78-1.54 (6H, m). ^{13}C-NMR (75 MHz, $CDCl_3$): δ 168.7, 148.6, 124.3, 98.8, 98.4, 64.3, 30.2, 25.4, 19.0. ES-MS calcd. for $C_9H_{12}BrO_4$: $[M+H]^+$ 262.98 and 264.98 (1:1); found 262.9 and 264.9 (1:1).

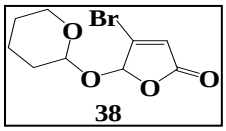

38

3-Bromo-5-(tetrahydropyran-2-yloxy)-5*H*-furan-2-one 40. Yield: 87%; ^{1}H-NMR (300 MHz, $CDCl_3$): δ 7.32 (1H, d, *J*=1.5 Hz), 6.21 (1H, d, *J*=1.5 Hz), 5.12-5.10 (1H, m), 3.87-3.80 (1H, m), 3.66-3.61 (1H, m), 1.80-1.64 (6H, m). ^{13}C-NMR (75 MHz, $CDCl_3$): δ 166.5, 147.8, 118.1, 98.2, 95.0, 63.2, 30.1, 25.4, 19.0. ES-MS calcd. for $C_9H_{12}BrO_4$: $[M+H]^+$ 262.98 and 264.98 (1:1); found 262.9 and 264.9 (1:1).

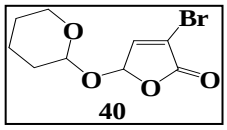

40

6.2.3. Synthesis of 3,4-dibromo-5-(2-methoxy-ethoxymethoxy)-5H-furan-2-one 34

Mucobromic acid **33** (100 mg, 0.387 mmol) was dissolved in 10 mL of dry DCM and MEM-Cl (66 µL, 0.581 mmol) was added to the solution. DIPEA (101 µL, 0.581 mmol) was added dropwise over a period of 15 min. After 4 h, the reaction mixture was quenched with 20 mL of HCl 1 M. The aqueous layer was extracted with DCM (3 x 30 mL) and the organics were dried with Na_2SO_4, filtered and concentrated *in vacuo*. The crude dark oil obtained was purified by flash chromatography (5% diethyl ether/*n*-hexane to 20% diethyl ether/*n*-hexane) to give **34** (115 mg, 85% yield): ^{1}H NMR δ (300 MHz; $CDCl_3$): δ 6.10 (1H, s), 5.20 (1H, d, *J* = 7.2 Hz), 4.87 (1H, d), 3.79 (1H, m), 3.40 (3H, s), 3.60 (1H, m), 3.54 (2H, dd); ES-MS calcd. for $C_8H_{11}Br_2O_5$: [M+H]+ 344.89, 346.89 and 348.89 (1:2:1); found $[M+H]^+$ 344.8, 346.8 and 348.8 (1:2:1).

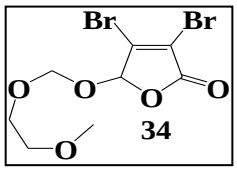

34

6.2.4. Esterification of boronic acids 43 and 44

The boronic acids **43** and **44** (0.667 mmol) were dissolved in 6 mL of ethyl acetate and, stirring the solution, pinacol (0.667 mmol) was added. After 4h the reaction was stopped adding anhydrous Na_2SO_4 (1 g) and $CaCl_2$ (1 g). The mixture was filtered and concentrated in *vacuo* (Yield: 91% of **45** and 90% of **46**).

6.2.5. Synthesis of amides: general procedure

The pinacol ester **45** or **46** (1 equiv.) and the appropriate ammine **a-f** (2 equiv.) were dissolved in DMF. TEA, HOBt and DIC (2 equiv. of each) were added. The mixture was leaved at r.t. for 48 hours under stirring. When TLC showed the consumption of the pinacol ester, the reaction was stopped adding HCl 1N (10 mL). The aqueous phase was extracted with ethyl acetate (3 x 10 mL) and the organic phase was washed firstly with a saturate solution of $NaHCO_3$ and then with brine. Afterward the organics were dried over Na_2SO_4, filtered and concentrated in *vacuo*. The crude was purified by flash chromatography (10% diethyl ether/*n*-hexane to 70% diethyl ether/*n*-hexane).

Pyrrolidin-1-yl-[4-(4,4,5,5-tetramethyl-[1,3,2]dioxaborolan-2-yl)-phenyl]-methanone 47a. Yield: 87%; ^{1}H NMR δ (300 MHz; $CDCl_3$): 7.98 (2H, d), 7.38 (2H, d), 3.59 (2H, t), 3.34 (2H, t), 1.94 (2H, quint), 1.84 (2H, quint), 1.31 (12H, s). ES-MS calcd. For $C_{17}H_{25}BNO_3$: $[M+H]^+$ 302.18; found 302.1.

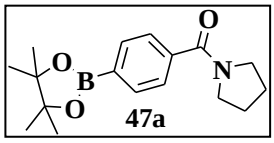

47a

Morpholin-4-yl-[4-(4,4,5,5-tetramethyl-[1,3,2]dioxaborolan-2-yl)-phenyl]-methanone 47b. Yield: 83%; ^{1}H NMR δ (300 MHz; $CDCl_3$): 7.89 (2H, d), 7.35 (2H, d), 4.20 (2H, t), 3.87 (2H, t), 3.79 (4H, m), 1.32 (12H, s). ES-MS calcd. for $C_{17}H_{25}BNO_4$: $[M+H]^+$ 318.18; found 318.2.

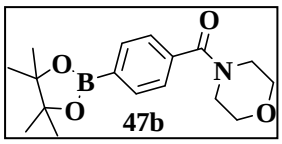

47b

N-Phenyl-4-(4,4,5,5-tetramethyl-[1,3,2]dioxaborolan-2-yl)-benzamide 47c.

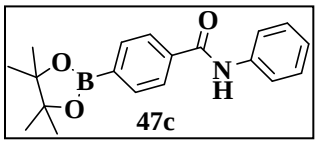

47c

Yield: 71%; NMR δ (300 MHz; $CDCl_3$): 7.88 (2H, d), 7.42 (2H, d), 7.42-7.36 (5H, m), 1.32 (12H, s). ES-MS calcd. for $C_{19}H_{22}BNO_3$: $[M+H]^+$ 324.17; found 324.1.

N-Benzyl-4-(4,4,5,5-tetramethyl-[1,3,2]dioxaborolan-2-yl)-benzamide 47d.

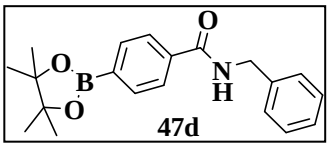

47d

Yield: 88%; NMR δ (300 MHz; $CDCl_3$): 7.97 (2H, d), 7.33 (2H, d), 7.34-7.28 (5H, m), 4.62 (2H, d), 1.34 (12H, s). ES-MS calcd. for $C_{20}H_{25}BNO_3$: $[M+H]^+$ 338.18; found 338.1.

Piperidin-1-yl-[4-(4,4,5,5-tetramethyl-[1,3,2]dioxaborolan-2-yl)-phenyl]-methanone 47e. Yield: 90%; NMR δ (300 MHz; $CDCl_3$): 7.93 (2H, d), 7.38 (2H, d), 3.80 (2H, t), 3.32 (2H, t), 1.66 (4H, quint), 1.48 (2H, quint), 1.33 (12H, s). ES-MS calcd. for $C_{18}H_{27}BNO_3$: $[M+H]^+$ 316.20; found 316.2.

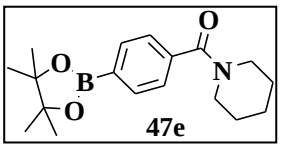

47e

Piperazin-1-yl-[4-(4,4,5,5-tetramethyl-[1,3,2]dioxaborolan-2-yl)-phenyl]-methanone 47f. Yield: 72%; ^{1}H NMR δ (300 MHz; $CDCl_3$): 7.81 (2H, d), 7.32 (2H, d), 3.79 (2H, t), 3.72 (2H, t), 3.24 (2H, t), 3.12 (2H, t), 1.47 (9H, s), 1.31 (12H, s). ES-MS calcd. for $C_{22}H_{34}BN_2O_5$: $[M+H]^+$ 4178.25; found 417.2.

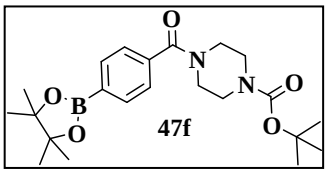

47f

Pyrrolidin-1-yl-[3-(4,4,5,5-tetramethyl-[1,3,2]dioxaborolan-2-yl)-phenyl]-methanone 48a. Yield: 89%; ^{1}H NMR δ (300 MHz; $CDCl_3$): 8.06 (1H, s), 7.87 (1H, d), 7.48 (1H, d), 7.39 (1H, t), 3.63 (2H, t), 3.47 (2H, t), 2.01 (2H, quint), 1.92 (2H, quint), 1.36 (12H, s). ES-MS calcd. for $C_{17}H_{25}BNO_3$: $[M+H]^+$

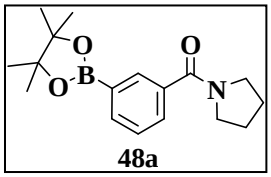

48a

302.18; found 302.2.

Morpholin-4-yl-[3-(4,4,5,5-tetramethyl-[1,3,2]dioxaborolan-2-yl)-phenyl]-methanone 48b. Yield: 85%; ^{1}H NMR δ (300 MHz; $CDCl_3$): 7.99 (1H, s), 7.83 (1H, d), 7.45 (1H, d), 7.37 (1H, t), 3.85 (2H, t), 3.70 (4H, m), 3.52 (2H, t), 1.34 (12H, s). ES-MS calcd. for $C_{17}H_{25}BNO_4$: $[M+H]^+$ 318.18; found 318.1.

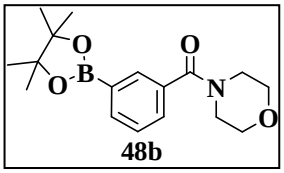

48b

N-Phenyl-3-(4,4,5,5-tetramethyl-[1,3,2]dioxaborolan-2-yl)-benzamide 48c. Yield: 75%; ^{1}H NMR δ (300 MHz; $CDCl_3$): 8.23 (1H, s), 8.02 (1H, d), 7.92 (1H, d), 7.65 (2H, d), 7.45 (1H, t), 7.33 (2H, t), 7.11 (1H, t), 1.33 (12H, s). ES-MS calcd. for $C_{19}H_{23}BNO_3$: $[M+H]^+$ 324.17; found 324.1.

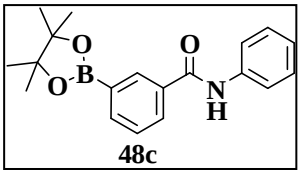

48c

N-Benzyl-3-(4,4,5,5-tetramethyl-[1,3,2]dioxaborolan-2-yl)-benzamide 48d. Yield: 89%; NMR δ (300 MHz; $CDCl_3$): 8.31 (1H, s), 8.12 (1H, d), 7.83 (1H, d), 7.52 (1H, t), 7.40-7.35 (3H, m), 7.58 (2H, d), 4.63 (2H, d), 1.33 (12H, s). ES-MS calcd. for $C_{20}H_{25}BNO_3$: $[M+H]^+$ 338.18; found 338.1.

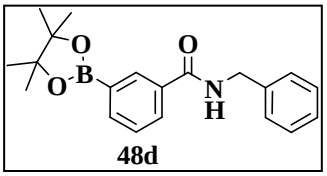

48d

Piperidin-1-yl-[3-(4,4,5,5-tetramethyl-[1,3,2]dioxaborolan-2-yl)-phenyl]-methanone 48e. Yield: 91%; NMR δ (300 MHz; $CDCl_3$): 7.98 (1H, s), 7.89 (1H, d), 7.44 (1H, d), 7.37 (1H, t), 3.80 (2H, t), 3.31 (2H, t), 1.64 (4H, quint), 1.48 (2H, quint), 1.31 (12H, s). ES-MS calcd. for $C_{18}H_{27}BNO_3$: $[M+H]^+$ 316.20; found 316.3.

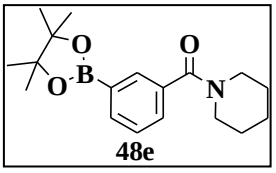

48e

6.2.6. Microwave-assisted Suzuki coupling: general procedure

In a CEM Discover vial intermediates **34** or **38** or **40** (1 equiv), the appropriate boronic acid **a-i** or **47a-f** or **48a-e** (1.5 equiv), $Pd(dppf)Cl_2$ (0.03 equiv), TBAB (0.5 equiv) and CsF (4 equiv) were placed. Under argon, water (500 µL) and THF (500 µL) were added. The mixture was irradiated for 3-6 minutes, setting the power at 200 W, the temperature at 120 °C, the pressure at 250 psi and the Power Max ON. At the end of the reaction, the vial was cooled to 50 °C by gas jet cooling before it was opened. After diluting (10 mL) with DCM, 10 mL of an aqueous solution of HCl 1 N was added. The aqueous layer was extracted with DCM (3 x 10 mL). The organics were then dried over Na_2SO_4, filtered and concentrated in *vacuo*. The crude products were purified by flash chromatography (10% diethyl ether/*n*-hexane to 40% diethyl ether/*n*-hexane) to furnish compounds **35a-d**, **31e-i**, **32e-i**, **49a-f** or **50a-e**.

3-Bromo-5-(2-methoxy-ethoxymethoxy)-4-[4-(pyrrolidine-1-carbonyl)-phenyl]-5H-furan-2-one 49a. Yield: 74%; ^{1}H-NMR δ (300 MHz; $CDCl_3$):

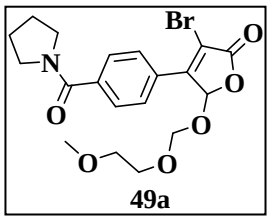

49a

7.93 (2H, d), 7.52 (2H, d), 6.58 (1H, s), 5.18 (1H, d), 4.87 (1H, d), 3.83-3.76 (1H, m), 3.69-3.63 (1H, m), 3.58 (2H, t), 3.41 (3H, s), 3.55-3.40 (4H, m), 1.90-2.05 (4H, m); ES-MS calcd. for $C_{19}H_{23}BrNO_6$: $[M+H]^+$ 440.06 and 442.06 (1:1); found 440.0 and 442.0 (1:1).

3-Bromo-5-(2-methoxy-ethoxymethoxy)-4-[4-(morpholine-4-carbonyl)-phenyl]-5H-furan-2-one 49b. Yield: 63%; ^{1}H-NMR δ (300 MHz; $CDCl_3$):

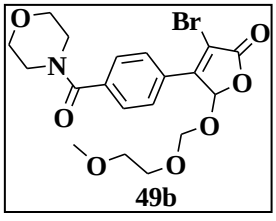

49b

7.97 (2H, d), 7.48 (2H, d), 6.57 (1H, s), 5.17 (1H, d), 4.88 (1H, d), 3.97 (4H, m), 3.78-3.73 (3H, m), 3.68-3.60 (1H, m), 3.56 (2H, t), 3.41 (3H, s), 3.40 (2H, t); ES-MS calcd. for $C_{19}H_{23}BrNO_7$: $[M+H]^+$ 456.06 and 458.06 (1:1); found 456.3 and 458.3 (1:1).

4-[4-Bromo-2-(2-methoxy-ethoxymethoxy)-5-oxo-2,5-dihydro-furan-3-yl]-N-phenyl-benzamide 49c. Yield: 65%; ^{1}H-NMR δ (300 MHz; $CDCl_3$): 8.05 (2H, d), 7.49 (2H, d), 7.18 (2H, t), 6.91 (1H, t), 6.79 (2H, d), 6.59 (1H, s), 5.19 (1H, d), 4.88 (1H, d), 3.75-3.72 (1H, m), 3.66-3.63 (1H, m), 3.53 (2H, t), 3.38 (3H, s). ES-MS calcd. for $C_{21}H_{21}BrNO_6$: $[M+H]^+$ 462.05 and 464.05 (1:1); found 462.6 and 464.6 (1:1).

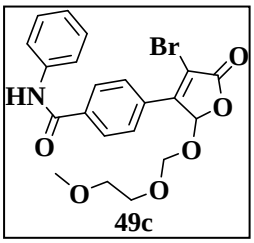

49c

N-Benzyl-4-[4-bromo-2-(2-methoxy-ethoxymethoxy)-5-oxo-2,5-dihydro-furan-3-yl]-benzamide 49d. Yield: 61%; ^{1}H-NMR δ (300 MHz; $CDCl_3$): 7.86 (2H, d), 7.47 (2H, d), 7.18 (2H, t), 6.91 (1H, t), 6.79 (2H, d), 6.57 (1H, s), 5.15 (1H, d), 4.85 (1H, d), 4.65 (2H, d), 3.75-3.72 (1H, m), 3.66-3.63 (1H, m), 3.53 (2H, t), 3.38 (3H, s); ES-MS calcd. for $C_{22}H_{23}BrNO_6$: $[M+H]^+$ 476.06 and 478.06 (1:1); found 476.4 and 478.4 (1:1).

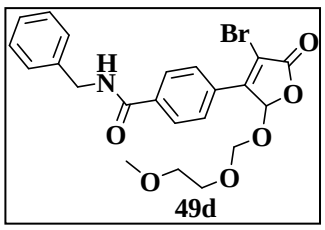

49d

3-Bromo-5-(2-methoxy-ethoxymethoxy)-4-[4-(piperidine-1-carbonyl)-phenyl]-5H-furan-2-one 49e. Yield: 75%; ^{1}H-NMR δ (300 MHz; $CDCl_3$): 7.99 (2H, d), 7.57 (2H, d), 6.58 (1H, s), 5.18 (1H, d), 4.87 (1H, d), 3.79-3.73 (2H, m), 3.68-3.58 (4H, m), 3.41 (3H, s), 3.35 (2H, t), 1.76 (4H, m), 1.55 (2H, quint); ES-MS calcd. for $C_{20}H_{25}BrNO_6$: $[M+H]^+$ 454.08 and 456.08 (1:1); found 454.2 and 456.2 (1:1).

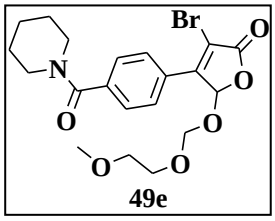

49e

4-{4-[4-Bromo-2-(2-methoxy-ethoxymethoxy)-5-oxo-2,5-dihydro-furan-3-yl]-benzoyl}-piperazine-1-carboxylic acid tert-butyl ester 49f. Yield: 59%; ^{1}H-NMR δ (300 MHz; $CDCl_3$): 7.99 (2H, d), 7.52 (2H, d), 6.58 (1H, s), 5.17 (1H, d), 4.87 (1H, d), 3.81 (4H, m), 3.79-3.74 (1H, m), 3.67-

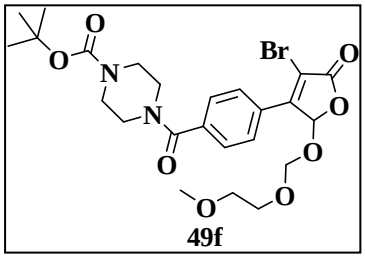

49f

3.62 (5H, m), 3.57 (2H, t), 3.41 (3H, s), 1.48 (9H, s); ES-MS calcd. for $C_{24}H_{32}BrN_2O_8$: $[M+H]^+$ 555.13 and 557.12 (1:1); found 555.1 and 557.1 (1:1).

3-Bromo-5-(2-methoxy-ethoxymethoxy)-4-[3-(pyrrolidine-1-carbonyl)-phenyl]-dihydro-furan-2-one 50a. Yield: 71%; ^{1}H-NMR δ (300 MHz; $CDCl_3$): 8.05 (1H, d), 8.01 (1H, s), 7.63 (1H, d), 7.55 (1H, t), 5.18 (1H, d), 4.87 (1H, d), 3.63 (2H, t), 3.49 (2H, t), 3.69-3.63 (1H, m), 3.58 (2H, t), 3.41 (3H, s), 2.19-2.14 (4H, m), 2.03-1.90 (2H, m); ES-MS calcd. for $C_{19}H_{23}BrNO_6$: $[M+H]^+$ 440.06 and 442.06 (1:1); found 440.1 and 442.1 (1:1).

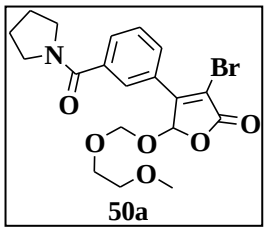

50a

3-Bromo-5-(2-methoxy-ethoxymethoxy)-4-[3-(morpholine-4-carbonyl)-phenyl]-dihydro-furan-2-one 50b. Yield: 64%; ^{1}H-NMR δ (300 MHz; $CDCl_3$): 7.95 (1H, s), 7.90 (1H, d), 7.55 (1H, d), 7.44 (1H, t), 6.56 (1H, s), 5.18 (1H, d), 4.92 (1H, d), 3.99 (4H, m), 3.81 (2H, t), 3.79-3.74 (1H, m), 3.67-3.62 (1H, m), 3.57 (2H, t), 3.41 (3H, s), 3.36 (2H, m); ES-MS calcd. for $C_{19}H_{23}BrNO_7$: $[M+H]^+$ 456.06 and 458.06 (1:1); found 456.1 and 458.1 (1:1).

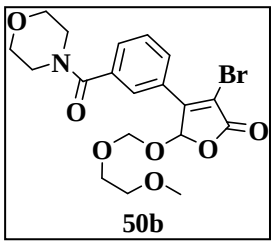

50b

3-[4-Bromo-2-(2-methoxy-ethoxymethoxy)-5-oxo-2,5-dihydro-furan-3-yl]-N-phenyl-benzamide 50c. Yield: 66%; ^{1}H-NMR δ (300 MHz; $CDCl_3$): 8.36 (1H, s), 8.12 (1H, d), 7.88 (1H, d), 7.61 (2H, d), 7.41 (1H, t), 7.21-7.14 (3H, m), 6.57 (1H, s), 5.15 (1H, d), 4.85 (1H, d), 3.75-3.72 (1H, m), 3.66-3.63 (1H, m), 3.53 (2H, t), 3.38 (3H, s); ES-MS calcd. for $C_{21}H_{21}BrNO_5$: $[M+H]^+$ 462.05 and 464.05 (1:1); found 462.2 and 464.2 (1:1).

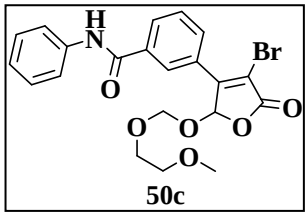

50c

N-Benzyl-3-[4-bromo-2-(2-methoxy-ethoxymethoxy)-5-oxo-2,5-dihydro-furan-3-yl]-benzamide 50d. Yield: 63%; ^{1}H-NMR δ (300 MHz; $CDCl_3$): 8.21 (1H, s), 8.06 (1H, d), 7.81 (1H, d), 7.45 (1H, t), 7.52-7.32 (5H, m), 6.54 (1H, s), 5.15 (1H, d), 4.85 (1H, d), 4.58 (2H, d), 3.75-3.72 (1H, m), 3.66-3.63 (1H, m), 3.53 (2H, t), 3.38 (3H, s); ES-MS calcd. for $C_{22}H_{23}BrNO_6$: $[M+H]^+$ 476.06 and 478.06 (1:1); found 476.1 and 478.1 (1:1).

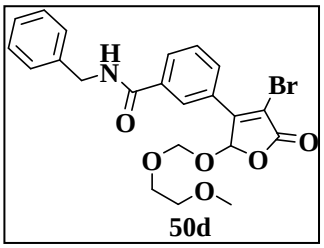

50d

3-Bromo-5-(2-methoxy-ethoxymethoxy)-4-[3-(piperidine-1-carbonyl)-phenyl]-5H-furan-2-one 50e. Yield: 72%; ^{1}H-NMR δ (300 MHz; $CDCl_3$): 8.05 (1H, d), 7.87 (1H, s), 7.55 (1H, d), 7.48 (1H, t), 6.58 (1H, s), 5.18 (1H, d), 4.87 (1H, d), 3.79-3.73 (1H, m), 3.68-3.58 (5H, m), 3.41 (3H, s), 3.36 (2H, t), 1.71 (4H, quint), 1.55 (2H, quint); ES-MS calcd. for $C_{20}H_{25}BrNO_6$: [M+H]+ 454.08 and 456.08 (1:1); found 454.0 and 456.0 (1:1).

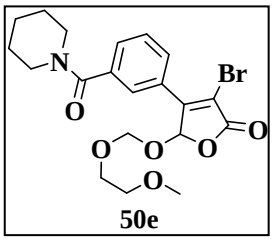

50e

6.2.7. MEM-cleavage: general procedure

The MEM-protected intermediates **49a-f**, **50a-e** and **35a-d** were dissolved in a solution of TFA/TIS/H_2O 95:2.5:2.5. The mixture was stirred at room temperature for 1.5 h and concentrated in *vacuo* to leave dark oil purified by flash chromatography (100% *n*-hexane to 30% diethyl ether/*n*-hexane). All the products **27a-d**, **41a-f** and **42a-e** were obtained as white solids.

3-Bromo-5-hydroxy-4-(1H-indol-2-yl)-5H-furan-2-one 27a. Yield: 90%; ^{1}H-NMR δ (300 MHz; $CDCl_3$): 9.25 (1H, s), 7.72 (1H, d, *J*=7.0 Hz), 7.46 (2H, m), 7.38 (1H, t), 7.20 (1H, d, *J*=8.3 Hz), 6.48 (1H, s); ^{13}C-NMR δ (75 MHz; $CDCl_3$): 166.7, 149.1,

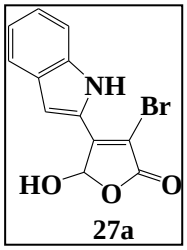

27a

139.6, 135.5, 134.8, 129.1, 124.0, 124.4, 124.3, 122.9, 112.0, 98.1; ES-MS calcd. for $C_{12}H_7BrNO_3$: $[M-H]^-$ 293.97 and 291.97 (1:1); found 293.8 and 291.8 (1:1).

4-Benzofuran-2-yl-3-bromo-5-hydroxy-5H-furan-2-one 27b. Yield: 88%;

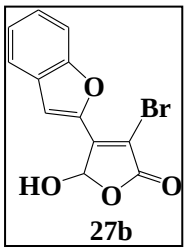

27b

^{1}H-NMR δ (300 MHz; $CDCl_3$): 7.74 (1H, s), 7.73 (1H, d, *J*=7.8 Hz), 7.59 (1H, d, *J*=8.2 Hz), 7.47 (1H, t), 7.35 (1H, t), 6.55 (1H, s); ^{13}C-NMR δ (75 MHz; $CDCl_3$): 166.8, 151.1, 141.2, 137.0, 135.8, 130.8, 126.2, 125.8, 124.6, 124.1, 113.2, 99.1; ES-MS calcd. for $C_{12}H_6BrO_4$: $[M-H]^-$ 294.95 and 292.95 (1:1); found 294.9 and 292.9 (1:1).

3-Bromo-5-hydroxy-4-styryl-5H-furan-2-one 27c. Yield: 89%; ^{1}H-NMR δ

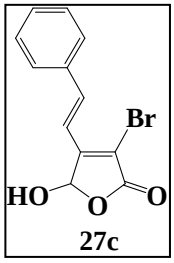

27c

(300 MHz; $CDCl_3$): 7.59 (3H, m), 7.42 (2H, d, *J*=8.3 Hz), 7.38 (1H, d, *J*=16.4 Hz), 6.98 (1H, d, *J*=16.4 Hz), 6.34 (1H, s); ^{13}C-NMR δ (75 MHz; $CDCl_3$): 166.3, 156.3, 136.2, 130.5, 130.4, 130.2, 129.7, 128.2, 128.1, 127.1, 107.1, 103.8; ES-MS calcd. for $C_{12}H_8BrO_3$: $[M-H]^-$ 280.97 and 278.97 (1:1); found 280.8 and 278.8 (1:1).

3-Bromo-4-[2-(4-fluoro-phenyl)-vinyl]-5-hydroxy-5H-furan-2-one 27d.

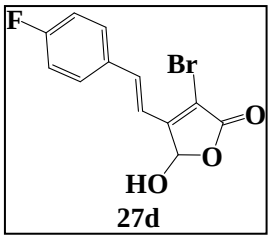

27d

Yield: 88%; ^{1}H-NMR δ (300 MHz; $CDCl_3$): 7.58 (2H, d, *J*=8.2 Hz), 7.36 (1H, d, *J*=16.2 Hz), 7.11 (2H, d, *J*=8.2 Hz), 6.90 (1H, d, *J*=16.2 Hz), 6.34 (1H, s); ^{13}C-NMR δ (75 MHz; $CDCl_3$): 166.5, 163.5, 103.8, 156.7, 107.6, 127.9, 130.8, 132.5, 130.1, 117.1; ES-MS calcd. for $C_{12}H_7BrFO_3$: $[M-H]^-$ 298.96 and 296.96 (1:1); found 298.9 and 296.9 (1:1).

3-Bromo-5-hydroxy-4-[4-(pyrrolidine-1-carbonyl)-phenyl]-5H-furan-2-one 41a. Yield: 92%; ^{1}H-NMR δ (500 MHz; $CDCl_3$): 7.88 (2H, d, *J*=7.8 Hz),

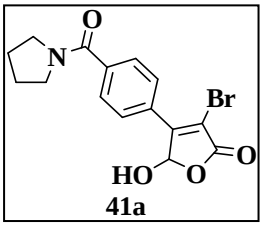

41a

7.49 (2H, d, *J*=8.2), 6.32 (1H, s), 3.60 (2H, t), 3.35 (2H, t), 1.95 (2H, quint), 1.85 (2H, quint); ^{13}C-NMR δ (125 MHz; $CDCl_3$): 168.2, 165.1, 154.0, 140.4, 134.8, 129.1, 128.6, 110.0, 99.6, 45.2, 28.3. ES-MS calcd. for $C_{15}H_{15}BrNO_4$: $[M+H]^+$ 352.01 and 354.01 (1:1); found 352.2 and 354.2 (1:1).

3-Bromo-5-hydroxy-4-[4-(morpholine-4-carbonyl)-phenyl]-5H-furan-2-one 41b. Yield: 90%; ^{1}H-NMR δ (500 MHz; $CDCl_3$): 8.02 (2H, d, *J*=7.8 Hz),

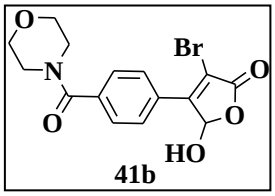

41b

7.49 (2H, d, *J*=8.2 Hz), 6.40 (1H, s), 3.79 (4H, m), 3.63 (4H, m); ^{13}C-NMR δ (125 MHz; $CDCl_3$): 168.7, 166.1, 154.1, 139.2, 135.3, 129.5, 128.9, 111.2, 99.1, 67.5, 66.9. ES-MS calcd. for $C_{15}H_{15}BrNO_5$: $[M+H]^+$ 368.01 and 370.00 (1:1); found 368.2 and 470.2 (1:1).

4-(4-Bromo-2-hydroxy-5-oxo-2,5-dihydro-furan-3-yl)-N-phenyl-benzamide 41c. Yield: 89%; ^{1}H-NMR δ (500 MHz; CD_3OD): 7.99 (2H, d,

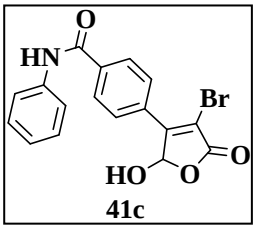

41c

J=7.8 Hz), 7.54 (2H, d, *J*=8.2 Hz), 7.22 (2H, t), 6.92-6.85 (3H, m), 6.57 (1H, s); ^{13}C-NMR δ (125 MHz; $CDCl_3$): 166.5, 164.2, 154.5, 139.8, 138.8, 137.8, 134.2, 129.8, 128.5, 124.6, 121.1, 110.5, 98.9. ES-MS calcd. for $C_{17}H_{13}BrNO_4$: $[M+H]^+$ 373.99 and 375.99 (1:1); found 373.9 and 375.9 (1:1).

N-Benzyl-4-(4-bromo-2-hydroxy-5-oxo-2,5-dihydro-furan-3-yl)-benzamide 41d. Yield: 82%; ^{1}H-NMR δ (500 MHz; $CDCl_3$): 8.01 (2H, d,

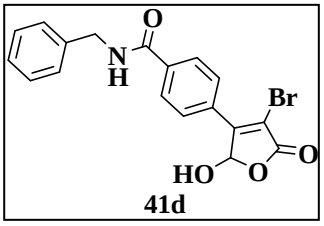

41d

J=7.8 Hz), 7.67 (1H, t), 7.88-7.77 (4H, m), 7.45 (2H, d, *J*=8.2 Hz), 6.46 (1H, s), 4.67 (2H, d, *J*=7.2 Hz); ^{13}C-NMR δ (125 MHz; $CDCl_3$): 168.4, 165.8, 153.9, 141.8, 139.6, 134.6, 129.1, 128.9, 128.3,

127.5, 126.2, 111.4, 99.7, 50.6. ES-MS calcd. for $C_{18}H_{15}BrNO_4$: $[M+H]^+$ 388.01 and 390.01 (1:1); found 388.1 and 390.1 (1:1).

3-Bromo-5-hydroxy-4-[4-(piperidine-1-carbonyl)-phenyl]-5H-furan-2-one 41e. Yield: 91%; ^{1}H-NMR δ (500 MHz; $CDCl_3$): 7.89 (2H, d, *J*=7.8 Hz), 7.31 (2H, d, *J*=8.2 Hz), 6.24 (1H, s), 3.71 (2H, t), 3.31 (2H, t), 1.70 (4H, quint), 1.52 (2H, quint); NMR δ (125 MHz; $CDCl_3$): 168.5, 164.8, 153.7, 139.8, 134.5, 129.4, 128.1, 111.1, 99.1, 45.4, 28.6, 26.7. ES-MS calcd. for $C_{16}H_{17}BrNO_4$: $[M+H]^+$ 366.03 and 368.02 (1:1); found 366.0 and 368.0 (1:1).

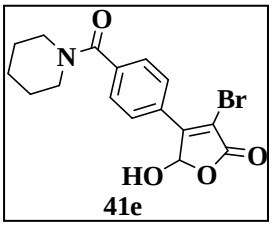

41e

3-Bromo-5-hydroxy-4-[4-(piperazine-1-carbonyl)-phenyl]-5H-furan-2-one 41f. Yield: 80%; ^{1}H-NMR δ (500 MHz; $CDCl_3$): 7.95 (2H, d, *J*=7.8 Hz), 7.44 (2H, d, *J*=8.2 Hz), 6.39 (1H, s), 3.81 (4H, m), 3.24 (2H, t), 3.13 (2H, t); ^{13}C-NMR δ (125 MHz; $CDCl_3$): 168.2, 165.8, 154.5, 139.6, 134.9, 129.1, 128.3, 110.6, 99.7, 67.1, 66.2. ES-MS calcd. for $C_{15}H_{16}BrN_2O_4$: $[M + H]^+$ 367.02 and 369.02 (1:1); found 367.8 and 369.8 (1:1).

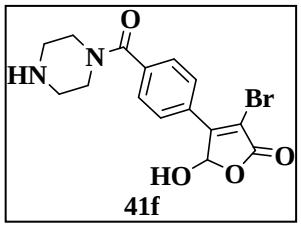

41f

3-Bromo-5-hydroxy-4-[3-(pyrrolidine-1-carbonyl)-phenyl]-5H-furan-2-one 42a. Yield: 90%; ^{1}H-NMR δ (500 MHz; $CDCl_3$): 8.07 (1H, d, *J*=7.8 Hz), 8.04 (1H, s), 7.61 (1H, d, *J*=8.2 Hz), 7.49 (1H, t), 6.37 (1H, s), 3.61 (2H, t), 3.47 (2H, t), 2.01 (2H, quint), 1.95 (2H, quint); NMR δ (125 MHz; $CDCl_3$): 167.6, 165.2, 153.0, 134.7, 129.7, 129.1, 128.4, 127.7, 126.9, 109.0, 98.9, 49.9, 46.7, 26.0, 23.9. ES-MS calcd. for $C_{15}H_{15}BrNO_4$: $[M+H]^+$ 352.01 and 354.01 (1:1); found 352.6 and 354.6 (1:1).

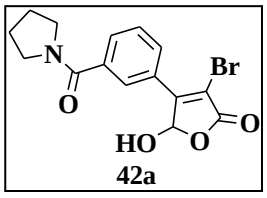

42a

3-Bromo-5-hydroxy-4-[3-(morpholine-4-carbonyl)-phenyl]-dihydro-furan-2-one 42b. Yield: 87%; ^{1}H-NMR δ (500 MHz; $CDCl_3$): 8.06 (1H, d, *J*=7.8 Hz), 7.96 (1H, s), 7.57 (1H, t), 7.39 (1H, d, *J*=8.2 Hz), 6.37 (1H, s), 3.83 (4H, m), 3.62 (4H, m); ^{13}C-NMR δ (125 MHz; $CDCl_3$): 169.2, 166.3, 154.2, 135.0, 130.7, 130.0, 129.6, 129.3, 127.9, 111.0, 99.5, 67.7, 67.4. ES-MS calcd. for $C_{15}H_{15}BrNO_5$: $[M+H]^+$ 368.01 and 370.00 (1:1); found 368.2 and 370.2 (1:1).

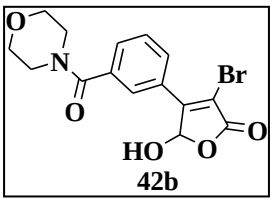

42b

3-(4-Bromo-2-hydroxy-5-oxo-2,5-dihydro-furan-3-yl)-N-phenyl-benzamide 42c. Yield: 86%; ^{1}H-NMR δ (500 MHz; $CDCl_3$): 8.41 (1H, s), 8.17 (1H, d, *J*=7.8 Hz), 7.92 (1H, d, *J*=8.2 Hz), 7.61 (2H, d, *J*=8.2 Hz), 7.41 (1H, t), 7.23-7.16 (3H, m), 6.56 (1H, s). ^{13}C-NMR δ (125 MHz; $CDCl_3$): 166.9, 164.7, 154.3, 138.5, 134.8, 130.5, 129.6, 129.1, 128.8, 128.2, 127.7, 124.5, 121.5, 109.9, 99.6. ES-MS calcd. for $C_{17}H_{13}BrNO_4$: $[M+H]^+$ 373.99 and 375.99 (1:1); found 374.3 and 376.3 (1:1).

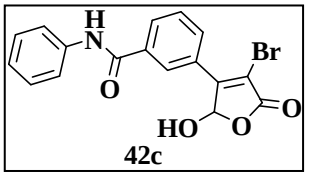

42c

N-Benzyl-3-(4-bromo-2-hydroxy-5-oxo-2,5-dihydro-furan-3-yl)-benzamide 42d. Yield: 84%; ^{1}H-NMR δ (500 MHz; $CDCl_3$): 8.33 (1H, s), 8.13 (1H, d, *J*=7.8 Hz), 7.77 (1H, d, *J*=8.2 Hz), 7.53 (1H, t), 7.42-7.27 (5H, m), 6.50 (1H, s), 4.58 (2H, d, *J*=8.3 Hz); ^{13}C-NMR δ (125 MHz; $CDCl_3$): 168.2, 165.0, 154.3, 141.4, 139.3, 134.8, 129.5, 128.8, 128.2, 127.6, 127.3, 126.3, 125.4, 110.5, 99.5, 50.4. ES-MS calcd. for $C_{18}H_{15}BrNO_4$: $[M+H]^+$ 388.01 and 390.01 (1:1); found 388.2 and 390.2 (1:1).

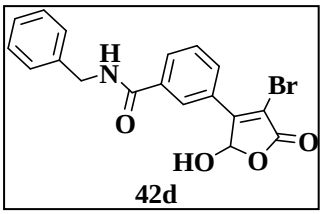

42d

3-Bromo-5-hydroxy-4-[3-(piperidine-1-carbonyl)-phenyl]-5H-furan-2-one 42e. Yield: 92%; ^{1}H-NMR δ (500 MHz; $CDCl_3$): 8.01 (1H, d, *J*=7.8 Hz), 7.87 (1H, s), 7.52 (1H, d, *J*=8.2 Hz), 7.44 (1H, t), 6.27 (1H, s), 3.69 (2H, t), 3.35

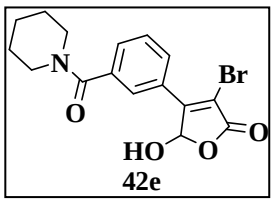

42e

(2H, t), 1.70 (4H, quint), 1.55 (2H, quint); ^{13}C-NMR δ (125 MHz; $CDCl_3$): 168.7, 164.3, 153.3, 134.5, 130.2, 129.6, 129.2, 128.8, 127.4, 110.6, 99.5, 45.7, 29.1, 26.2. ES-MS calcd. for $C_{16}H_{17}BrNO_4$: $[M+H]^+$ 366.03 and 368.02 (1:1); found 366.0 and 368.0 (1:1).

6.2.8. THP-cleavage: general procedure

The THP-protected intermediates **31e-i** and **32e-i** were dissolved in a solution of TFA/TIS/H_2O 95:2.5:2.5. The mixture was stirred at room temperature for 1.5 h and concentrated in *vacuo* to leave white precipitate that was purified by flash chromatography (100% *n*-hexane to 30% diethyl ether/*n*-hexane). All the products **28e-i** and **29e-i** were obtained as white solids.

4-Benzo[*b*]tiophen-2-yl-5-hydroxy-5*H*-furan-2-one 28e. Yield: 90%. ^{1}H-NMR δ (600 MHz, $CDCl_3$): 7.87 (2H, d, *J*=7.7 Hz) 7.83 (1H, s), 7.48-7.42 (2H, m), 6.52 (1H, s), 6.29 (1H, s); ^{13}C-NMR δ (150 MHz, $CDCl_3$): 169.6, 156.4, 141.1, 139.3, 131.8, 128.0, 127.6, 125.5, 125.2, 122.3, 114.9, 97.3; ES-MS calcd. for $C_{12}H_7O_3S$: $[M-H]^-$ 231.01; found 231.0.

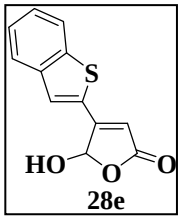

28e

5-Hydroxy-4-phenyl-5*H*-furan-2-one 28f. Yield: 89%. ^{1}H-NMR δ (600 MHz, $CDCl_3$): 7.73-7.71 (2H, dd, *J*=2.5, 8.2 Hz), 7.52-7.48 (3H, m), 6.55 (1H, s), 6.43 (1H, s); ^{13}C-NMR δ (150 MHz, $CDCl_3$): 171.1, 162.3, 131.9, 129.5, 129.4, 128.2, 116.0, 98.6; ES-MS calcd. for $C_{10}H_7O_3$: $[M-H]^-$ 175.03; found 175.1.

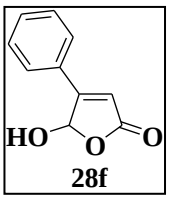

28f

4-(2-Hydroxy-5-oxo-2,5-dihydro-furan-3-yl)-benzaldehyde 28g. Yield: 93%.^{1}H-NMR δ (600 MHz, CD_3OD): 10.08 (1H, s), 7.99 (2H, d, *J*=8.3 Hz), 7.88 (2H, d, *J*=8.3 Hz), 6.61 (1H, s), 6.54 (1H, s); ^{13}C-NMR δ (150 MHz, CD_3OD): 191.6, 170.4,

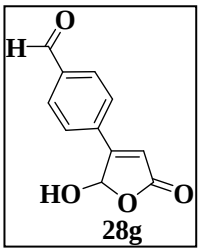

28g

162.2, 137.3, 135.9, 129.4, 128.5, 114.5, 97.8; ES-MS calcd. for $C_{11}H_7O_4$: [M-H]$^-$ 203.03; found 203.1.

5-Hydroxy-4-(4-methoxy-phenyl)-5*H*-furan-2-one 28h. Yield: 91%. ^{1}H-NMR δ (600 MHz, CD_3OD): 7.75 (2H, d, *J*=9.0 Hz), 7.02 (2H, d, *J*=9.0 Hz), 6.52 (1H, s), 6.37 (1H, s), 3.86 (3H, s); ^{13}C-NMR δ (150 MHz, CD_3OD): 172.2, 163.8, 162.4, 129.3, 121.9, 113.5, 111.0, 98.0, 54.4; ES-MS calcd. for $C_{11}H_9O_4$: [M-H]$^-$ 205.05; found 205.0.

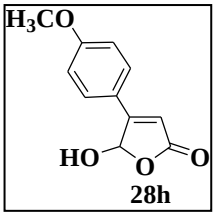

28h

5-Hydroxy-4-naphthalen-1-yl-5*H*-furan-2-one 28i. Yield: 88%. ^{1}H-NMR δ (600 MHz, CD_3OD): 8.18 (1H, d), 8.00-7.95 (2H, m), 7.70 (1H, d), 7.63-7.54 (3H, m), 6.75 (1H, s), 6.48 (1H, s); ^{13}C-NMR δ (150 MHz, CD_3OD): 169.8, 163.8, 133.5, 130.8, 130.4, 128.9, 128.2, 127.6, 127.2, 126.9, 126.5, 124.4, 119.8, 99.8; ES-MS calcd. for $C_{14}H_9O_3$: [M-H]$^-$ 225.05; found 225.2.

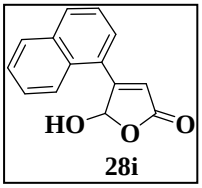

28i

3-Benzo[*b*]thiophen-2-yl-5-hydroxy-5*H*-furan-2-one 29e. Yield: 91%. ^{1}H-NMR δ (600 MHz, $CDCl_3$): 8.02 (1H, s), 7.86-7.81 (2H, m), 7.41-7.38 (2H, m), 7.24 (1H, s), 6.28 (1H, s); ^{13}C-NMR δ (150 MHz, $CDCl_3$): 168.4, 142.5, 142.3, 139.9, 132.9, 130.1, 127.8, 127.5, 126.7, 126.4, 122.7, 96.7; ES-MS calcd. For $C_{12}H_7O_3S$: [M-H]$^-$ 231.01; found 231.0.

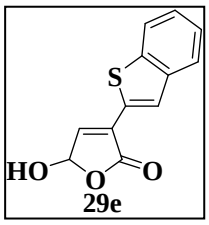

29e

5-Hydroxy-4-phenyl-5*H*-furan-2-one 29f. Yield: 89%. ^{1}H-NMR δ (600 MHz, CD_3OD): 7.71-7.68 (2H, m), 7.48-7.44 (3H, m), 7.35 (1H, s), 6.72 (1H, s); ^{13}C-NMR δ (150 MHz, CD_3OD): 168.6, 139.5, 131.5, 131.3, 129.3, 128.1, 128.0, 97.0; ES-MS calcd. for $C_{10}H_7O_3$: [M-H]$^-$ 175.03; found 175.3.

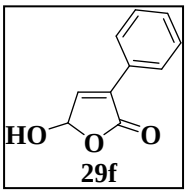

29f

3-(5-Hydroxy-2-oxo-2,5-dihydro-furan-3-yl)-benzaldehyde 29g. Yield: 91%. ^{1}H-NMR δ (600 MHz, CD_3OD): 10.02 (1H, s), 8.12 (2H, d, *J*=8.3 Hz), 7.97 (2H, d, *J*=8.3 Hz), 7.76 (1H, s), 6.22 (1H, s); ^{13}C-NMR δ (150 MHz, CD_3OD): 191.9, 169.9, 142.7, 136.8, 135.1, 132.4, 129.3, 127.7, 96.7; ES-MS calcd. for $C_{11}H_7O_4$: $[M-H]^-$ 203.03; found 203.1.

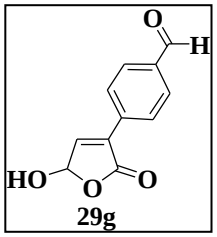

29g

5-Hydroxy-3-(4-methoxy-phenyl)-5*H*-furan-2-one 29h. Yield: 90%. ^{1}H-NMR δ (600 MHz, CD_3OD): 7.86 (2H, d, *J*=9.0 Hz), 7.42 (1H, s), 6.97 (2H, d, *J*=9.0 Hz), 6.15 (1H, s), 3.82 (1H, s); ^{13}C-NMR δ (150 MHz, CD_3OD): 170.5, 160.6, 142.0, 132.5, 128.3, 121.2, 113.5, 96.3, 54.1; ES-MS calcd. for $C_{11}H_9O_4$: $[M-H]^-$ 205.05; found 205.0.

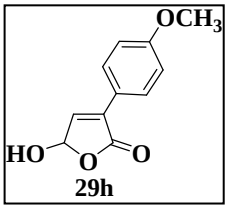

29h

5-Hydroxy-3-naphthalen-1-yl-5*H*-furan-2-one 29i. Yield: 88%. ^{1}H-NMR δ (600 MHz, CD_3OD): 7.98-7.91 (3H, m), 7.59-7.52 (4H, m), 7.49 (1H, s), 6.36 (1H, s); ^{13}C-NMR δ (150 MHz, CD_3OD): 171.2, 149.2, 134.2, 132.4, 133.3, 131.1, 127.7, 127.2, 126.3, 125.8, 125.4, 124.7, 124.4, 97.3; ES-MS calcd. for $C_{14}H_9O_3$: $[M-H]^-$ 225.05; found 225.2.

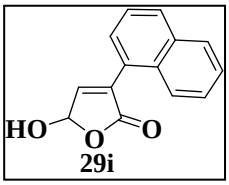

29i

6.2.9. Synthesis of acetic acid 3-benzo[b]thiophen-2-yl-5-oxo-2,5-dihydro-furan-2-yl ester 30

Compound **28e** was dissolved in dry DMF and, stirring the mixture at room temperature, acetic anhydride (5 equiv.) and DIPEA (5 equiv.) were added. After 2 h, the mixture was diluted with 10 mL of HCl 1 N and the aqueous phase was extracted with DCM (3 x 10 mL). The organics were dried over Na_2SO_4, filtered and concentrated *in vacuo*. Yield: 81%; ^{1}H-NMR δ (300 MHz, $CDCl_3$): 7.86 (1H, d, *J*=7.8 Hz), 7.50 (1H, s), 7.44 (3H, m), 6.52 (1H, s), 6.35 (1H, s), 2.23 (3H, s); ^{13}C-NMR δ (75 MHz, $CDCl_3$): 170.5, 170.1, 157.1,

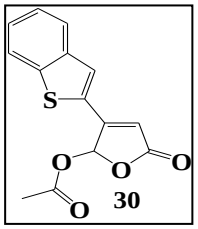

30

141.1, 139.3, 132.8, 128.6, 127.7, 125.4, 125.2, 122.3, 115.2, 108.5, 22.1; ES-MS calcd. for $C_{14}H_9O_4S$: $[M-H]^-$ 273.03; found 273.3.

~Chapter 7~

Selective Inhibitors of mPGES-1

7.1. General methods

All water and air sensitive reactions were carried out under an inert atmosphere (Ar or N_2) in oven- or flame-dried glassware. All the chemicals, commercially available, were used as received. DCM and THF were distilled from CaH_2 immediately prior to use. Water was degassed under *vacuum* (10 mbar).

Microwave reactions were performed on a CEM Discover® single mode platform using 10 mL pressurized vials.

Reactions were monitored on silica gel 60 F254 (Merck) plates and visualized with potassium permanganate or cerium sulfate and under UV (λ=254 nm, 365 nm). Flash column chromatography was performed using Merck 60/230-400 mesh silica gel. Analytical and semipreparative reverse-phase HPLC purifications were performed on a Waters instrument using Jupiter C-18 column (250 x 4.60 mm, 5 µm, 300 Å; 250 x 10.00 mm, 10 µm, 300 Å, respectively).

Reaction yields refer to chromatographically and spectroscopically pure products.

Proton detected (^{1}H, HMBC, HSQC) and carbon detected NMR spectra were recorded on Bruker instruments of Avance series operating at 300, 500 and 600 MHz and 75, 125 and 150 MHz, respectively. Chemical shifts are expressed in parts per million (ppm) on the delta (δ) scale. The solvent peak was used as internal reference: for ^{1}H NMR $CDCl_3$ = 7.26 ppm, CD_3OD = 3.34 ppm; for ^{13}C NMR: $CDCl_3$ = 77.0 ppm, CD_3OD = 47.7 ppm. Multiplicities are reported as follows: s, singlet; d, doublet; t, triplet; quint, quintuplet; m, multiplet; dd, doublet of doublets.

Electrospray mass spectrometry (ES-MS) was performed on a LCQ DECA ThermoQuest (San Josè, California, USA) mass spectrometer.

7.2. Methods and materials

7.2.1. Esterification of boronic acids 43 and 94

The boronic acids **43** and **94** (0.667 mmol) were dissolved in 6 mL of ethyl acetate and, stirring the solution, pinacol (0.667 mmol) was added. After 4h the reaction was stopped adding anhydrous Na_2SO_4 (1 g) and $CaCl_2$ (1 g). The mixture was filtered and concentrated in *vacuo* (Yield: 91% of **45** and 89% of **95**).

7.2.2. Synthesis of 4-[2-methoxy-5-(4,4,5,5-tetramethyl-[1,3,2]dioxaborolan-2-yl)-benzyl]-morpholine n

Under inert atmosphere (N_2), 1 equiv. of boronic ester **95** was dissolved in anhydrous CH_3OH (1 mL/0.18 mmol of ester). The mixture was kept under stirring at room temperature; anhydrous amine **96** (4 equiv.), $ZnCl_2$ (0.5 equiv.) and $NaCNBH_3$ (1 equiv.) were added. After 4 h, when the reagents disappeared, the reaction was stopped and 10 mL of an aqueous solution of NaOH 0.1 M was added. After concentration of CH_3OH *in vacuo*, the aqueous phase was extracted with ethyl acetate (3 x 10 mL) and the organics were dried over Na_2SO_4, filtered and concentrated *in vacuo*. The obtained oil was purified on silica gel by flash chromatography (100% *n*-hexane to 50% ethyl acetate/*n*-hexane). Yield: 75%: ^{1}H NMR δ (300 MHz; $CDCl_3$): 7.98 (1H, d), 7.78 (1H, s), 7.24 (1H, d), 4.53 (2H, s), 4.10 (2H, t), 3.93 (3H, s), 3.76 (2H, t), 3.47 (4H, m), 1.35 (12H, s); ES-MS calcd. for $C_{18}H_{29}BNO_4$: $[M+H]^+$ 334.21; found 334.1.

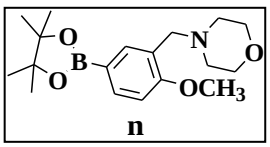

n

7.2.3. Synthesis of morpholin-4-yl-[3-(4,4,5,5-tetramethyl-[1,3,2]dioxaborolan-2-yl)-phenyl]-methanone j

The pinacol ester **45** (1 equiv.) and morpholine **96** (2 equiv.) were dissolved in DMF. TEA, HOBt and DIC (2 equiv. of each one) were added. The mixture was leaved at room temperature for 48 hours under stirring. When TLC showed the consumption of the pinacol ester **45**, the reaction was stopped adding HCl 1N (10 mL). The aqueous phase was extracted with ethyl acetate (3 x 10 mL) and the organic phase was washed firstly with a saturate solution of $NaHCO_3$ and then with brine. The organics were dried over Na_2SO_4, filtered and concentrated in *vacuo*. The crude was purified by flash chromatography (10% diethyl ether/*n*-hexane to 50% diethyl ether/*n*-hexane) with yield: 85%. ^{1}H NMR δ (300 MHz; $CDCl_3$): 7.99 (1H, s), 7.83 (1H, d), 7.45 (1H, d), 7.37 (1H, t), 3.85 (2H, t), 3.70 (4H, m), 3.52 (2H, t), 1.34 (12H, s). ES-MS calcd. for $C_{17}H_{25}BNO_4$: $[M+H]^+$ 318.18; found 318.3.

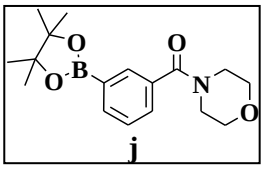

j

7.2.4. Synthesis of 1,4-disubstituted 1,2,3-triazoles 80-81: general procedure

Propargyl alcohol **78** or 1-bromo-4-ethynylbenzene **79** (1 mmol) and azidomethyl phenyl sulfide **77** (1.2 mmol) were suspended in a 1:1 mixture of water and *t*-BuOH (1.5 mL each). Sodium ascorbate (100 µL of freshly prepared 1 M solution in water) was added, followed by Cu(II) sulfate pentahydrate (100 µL of a 0.1 M solution in water). The heterogeneous mixture was vigorously stirred overnight at room temperature. When TLC analysis indicated complete consumption of the reactants, the reaction mixture was diluted with 50 mL of water and cooled in ice; the white precipitate was collected by filtration. After being washed with cold water (20 mL), the precipitate was dried under *vacuum* to afford the pure product as a white powder.

(1-phenylsulfanylmethyl-1H-[1,2,3]triazol-4-yl)-methanol 80. Yield: 89%;

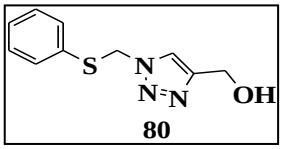

80

^{1}H-NMR δ (300 MHz; $CDCl_3$): 7.55 (1H, s), 7.28-7.22 (5H, m), 5.55 (2H, s), 4.63 (2H, s); ES-MS calcd. for $C_{10}H_{12}N_3OS$: $[M+H]^+$ 222.06; found 222.2.

4-(4-bromo-phenyl)-1-phenylsulfanylmethyl-1H-[1,2,3]triazole 81. Yield: 93%; ^{1}H-NMR δ (300 MHz; $CDCl_3$): 7.76 (1H, s), 7.64 (2H, d), 7.53 (2H, d), 7.40-7,28 (5H, m), 5.65 (2H, s); HRMS calcd. for $C_{15}H_{13}BrN_3S$: $[M+H]^+$ 345.99 and 347.99 (1:1); found 345.8 and 347.8 (1:1).

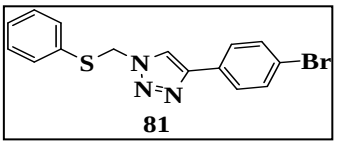

81

7.2.5. Synthesis of triazoles 85-87 from halides 82-84: general procedure

The appropriate halide **82-84** (1.1 mmol), 1-bromo-4-ethynylbenzene **79** (1.0 mmol) and sodium azide (1.3 mmol) were suspended in a 1:1 mixture of water and *t*-BuOH (1.5 mL each) in a 10 mL crimp-sealed thick-walled glass tube equipped with a small magnetic stirring bar. Copper wire (0.80 mmol) and copper sulphate solution (1N, 200 μL) were added to the mixture. Then the mixture was irradiated for 30 minutes setting the power at 200 W, the temperature at 120 °C, the pressure at 250 psi and the Power Max ON. After completion of the reaction, the vial was cooled to 50 °C by gas jet cooling before it was opened. The mixture was then diluted with water (20 mL) and filtered. The residue was washed with cold water (20 mL), 0.25 N HCl (20 mL) and finally with petroleum ether (20 mL) to furnish the desired triazoles **85-87**.

4-(4-Bromo-phenyl)-1-(2-o-tolyl-ethyl)-1H-[1,2,3]triazole 85. Yield: 77%;

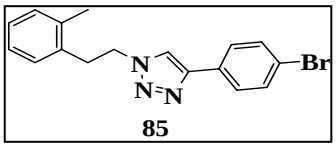

85

^{1}H-NMR δ (300 MHz; $CDCl_3$): 7.63 (2H, d), 7.52 (2H, d), 7.38 (1H, s), 7.17-7.12 (4H, m), 4.60 (2H, t), 3.23 (2H, t), 2.25 (3H, s); HRMS calcd. for $C_{17}H_{17}BrN_3$: $[M+H]^+$ 342.05 and 344.05 (1:1); found 342.0 and 344.0 (1:1).

4-(4-Bromo-phenyl)-1-(3-phenyl-propyl)-1H-[1,2,3]triazole 86. Yield: 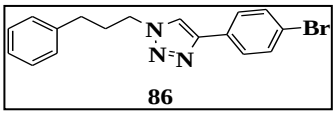

86
79%; ^{1}H-NMR δ (300 MHz; $CDCl_3$): 7.71-7.68 (3H, m), 7.55 (2H, d), 7.31-7.17 (5H, m), 4.40 (2H, t), 2.70 (2H, t), 2.30 (2H, quint); HRMS calcd. for $C_{17}H_{17}BrN_3$: $[M+H]^+$ 342.05 and 344.05 (1:1); found 342.0 and 344.0 (1:1).

4-[4-(4-Bromo-phenyl)-[1,2,3]triazol-1-ylmethyl]-3-nitro-benzoic acid 87. 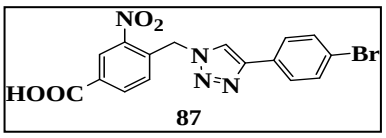

87
Yield: 73%; ^{1}H-NMR δ (300 MHz; CD_3OD): 8.72 (1H, s), 8.35 (1H, s), 8.24 (1H, d), 7.70 (2H, d), 7.56 (2H, d), 7.18 (1H, d), 6.08 (2H, s); HRMS calcd. for $C_{16}H_{12}BrN_4O_4$: $[M+H]^+$ 403.00 and 404.99 (1:1); found 403.3 and 405.3 (1:1).

7.2.6. Synthesis of 4-[4-(4-bromo-phenyl)-[1,2,3]triazole-1-sulfonyl]-benzoic acid 89

1-Bromo-4-ethynylbenzene **79** (0.60 mmol) and 4-carboxybenzene-sulfonazide **88** (0.50 mmol) were dissolved in 1.00 mL of dry chloroform. 2,6-lutidine (0.60 mmol) and CuI (0.05 mmol) were added and the solution was stirred for 12 h at 0°C under inert atmosphere of nitrogen. When TLC analysis indicated complete consumption of the reactants, the reaction mixture was diluted with 10 mL of water. The aqueous layer was extracted with ethyl acetate (3 x 10 mL). The organics were dried over Na_2SO_4, filtered and concentrated in *vacuo*. The crude was purified by flash chromatography (10% diethyl ether/*n*-hexane to 80% diethyl ether/n-hexane) and furnished 57% of pure desired triazole **89** as a white powder.^{1}H-NMR δ (300 MHz; CD_3OD): 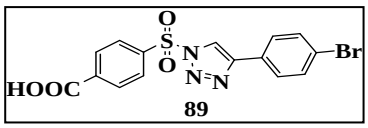

89
8.48 (1H, s), 8.23-8.16 (4H, m), 7.66 (2H, d), 7.53 (2H, d); HRMS calcd. for $C_{15}H_{11}BrN_3O_4S$: $[M+H]^+$ 407.96 and 409.96 (1:1); found 407.8 and 409.8 (1:1).

7.2.7. Synthesis of 4-benzyl-5-iodo-1-phenylsulfanylmethyl-1H-[1,2,3]triazole 91

3-Phenyl-1-propyne **90** (1.0 mmol) and azidomethyl phenyl sulfide **77** (1.1 mmol) were suspended in THF (30 mL). DIPEA (1.1 mmol), NBS (1.1 mmol) and CuI (1.1 mmol) were successively added. The mixture was stirred at room temperature for 4 h. After removal of the solvent, the crude product was dissolved in ethyl acetate (5 mL) and diluted with water (10 mL). The aqueous layer was extracted with ethyl acetate (3 x 10 mL). The organics were dried over Na_2SO_4, filtered and concentrated in *vacuo*. The crude was purified by flash chromatography (5% diethyl ether/*n*-hexane to 15% diethyl ether/*n*-hexane) to give compound **91**. Yield: 51%: ^{1}H NMR δ (300 MHz; $CDCl_3$): δ 7.32-7.21 (10H, m), 5.60 (2H, s), 4.03 (2H, s); HRMS calcd. for $C_{16}H_{15}IN_3S$: $[M+H]^+$ 408.00; found 408.2.

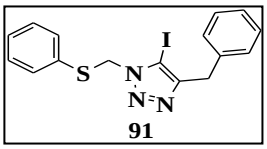

91

7.2.8. Suzuki coupling: general procedure

In a CEM Discover® vial, each of the intermediate **81**, **85-87**, **89** or **91** (1 equiv), the appropriate boronic acid **a-i** or **92** (1.5 equiv.), $Pd(dppf)Cl_2$ (0.05 equiv.) and CsF (4 equiv.) were placed. Water (500 µL) and THF (500 µL) were added under argon atmosphere. The mixture was irradiated for 20-30 minutes, setting the power at 200 W, the temperature at 120 °C, the pressure at 250 psi and the Power Max ON. At completion of the reaction, the vial was cooled to 50 °C by gas jet cooling before it was opened. After diluting with 10 mL of aqueous solution of HCl 1 N, the aqueous layer was extracted with ethyl acetate (3 x 10 mL). The organics were then dried over Na_2SO_4, filtered and concentrated in *vacuo*. The crude was purified by flash chromatography (10% diethyl ether/*n*-hexane to 40% diethyl ether/*n*-hexane).

4-(4-Biphenyl-4-yl-[1,2,3]triazol-1-ylmethyl)-3-nitro-benzoic acid 54.

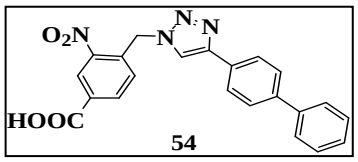

54

Yield: 84%; ^{1}H-NMR δ (500 MHz; CD_3OD): 8.77 (1H, s), 8.63 (1H, s), 8.04 (1H, d, *J*=8.11 Hz), 7.89 (1H, d, *J*=7.89 Hz), 7.73 (2H, d, *J*=7.89 Hz), 7.61 (2H, d, *J*=7.23 Hz), 7.38 (2H, d, *J*=8.11 Hz), 7.25 (2H, t), 7.05 (1H, t), 6.22 (2H, s); ^{13}C-NMR δ (125 MHz; CD_3OD): 165.5, 147.0, 146.1, 139.5, 138.4, 134.3, 133.0, 130.1, 129.4, 128.0, 126.9, 126.2, 125.7, 125.4, 125.1, 124.8, 121.9, 49.8. ES-MS calcd. for $C_{22}H_{17}N_4O_4$: $[M+H]^+$ 401.12; found 401.3.

4'-(1-Phenylsulfanylmethyl-1H-[1,2,3]triazol-4-yl)-biphenyl-4-ol 56. Yield: 52%; ^{1}H-NMR δ (300 MHz; $CDCl_3$): 7.84 (1H, s), 7.80 (2H, d, *J*=6.36 Hz), 7.58 (2H, d, *J*=7.89 Hz), 7.50 (2H, d, *J*=8.11 Hz), 7.35-7.29 (5H, m), 6.90 (2H, d, *J*=8.55 Hz), 5.67 (2H, s); ^{13}C-NMR δ (75 MHz; $CDCl_3$): 155.4, 155.1, 146.0, 140.1, 139.2, 130.4, 128.9, 127.5, 126.1, 124.4, 117.9, 116.8, 113.6, 112.8, 52.6. ES-MS calcd. for $C_{21}H_{18}N_3OS$: $[M+H]^+$ 360.11; found 360.4.

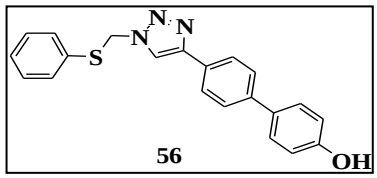

56

4'-(1-Phenylsulfanylmethyl-1H-[1,2,3]triazol-4-yl)-biphenyl-3-ol 57. Yield: 47%; ^{1}H-NMR δ (600 MHz; CD_3OD): 7.95 (1H, s), 7.79 (2H, d, *J*=8.77 Hz), 7.63 (2H, d, *J*=8.33 Hz), 7.39-7.35 (5H, m), 7.26 (1H, t), 7.10 (1H, d, *J*=7.89 Hz), 7.08 (1H, t), 6.81 (1H, dd, *J*=2.63, 8.33 Hz), 5.71 (2H, s); ^{13}C-NMR δ (150 MHz; CD_3OD): 155.9, 155.7, 146.4, 140.3, 139.6, 131.4, 130.7, 128.0, 127.9, 126.2, 124.7, 118.3, 117.2, 117.0, 113.3, 112.5, 52.9. ES-MS calcd. for $C_{21}H_{18}N_3OS$: $[M+H]^+$ 360.11; found 360.2.

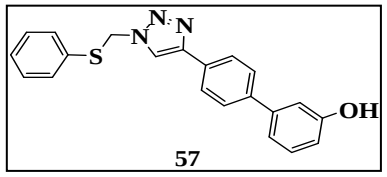

57

4-(4-Phenanthren-9-yl-phenyl)-1-(3-phenyl-propyl)-1H-[1,2,3]triazole 58.

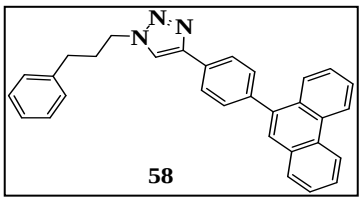

Yield: 78%; ^{1}H-NMR δ (300 MHz; $CDCl_3$): 8.26 (1H, dd, *J*=2.55, 8.11 Hz), 7.97-7.88 (7H, m), 7.78 (1H, s), 7.70-7.50 (8H, m), 7.31-7.28 (2H, d, *J*=6.80 Hz), 4.45 (2H, t), 2.92 (2H, t), 2.82 (2H, quint); ^{13}C-NMR δ (75 MHz; $CDCl_3$): 146.3, 137.4, 134.3, 134.0, 130.5, 130.1, 129.8, 129.5, 129.2, 129.0, 128.5, 127.9, 127.6, 126.8, 126.6, 126.4, 126.1, 125.9, 125.7, 125.4, 125.1, 124.1, 123.6, 121.5, 52.0, 30.3, 20.5. ES-MS calcd. for $C_{31}H_{26}N_3$: $[M+H]^+$ 440.20; found 440.4.

4'-[1-(3-Phenyl-propyl)-1H-[1,2,3]triazol-4-yl]-biphenyl-4-ol 64. Yield:

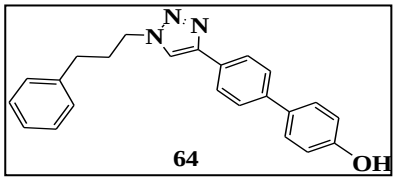

50%; ^{1}H-NMR δ (300 MHz; $CDCl_3$): 7.85 (2H, d, *J*=7.67 Hz), 7.73 (1H, s), 7.60 (2H, d, *J*=7.45 Hz), 7.51 (2H, d, *J*=8.11 Hz), 7.30-7.24 (5H, m), 6.90 (2H, d, *J*=8.33 z), 4.40 (2H, t), 2.69 (2H, t), 2.30 (2H, quint); ^{13}C-NMR δ (75 MHz; $CDCl_3$): 153.1, 148.5, 141.2, 139.6, 137.4, 128.9, 128.3, 127.8, 127.3, 126.5, 126.1, 125.5, 121.6, 120.4, 50.2, 33.6, 31.5. ES-MS calcd. for $C_{23}H_{22}N_3O$: $[M+H]^+$ 356.17; found 356.3.

4-[2'-(Naphthalen-1-yloxymethyl)-biphenyl-4-yl]-1-(3-phenyl-propyl)-1H-[1,2,3]triazole 65. Yield: 67%; ^{1}H-NMR δ (300 MHz; CD_3OD): 8.25 (1H, d,

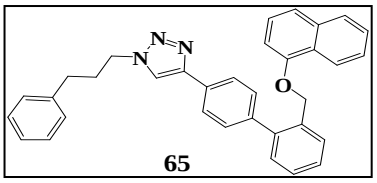

J=6.80 Hz), 7.73 (4H, m), 7.48-7.12 (12H, m), 7.21 (1H, s), 7.15 (2H, m), 6.68 (1H, d, *J*=7.67 Hz), 5.09 (2H, s), 4.35 (2H, t), 2.64 (2H, t), 2.25 (2H, quint); ^{13}C-NMR δ (75 MHz; CD_3OD): 155.3, 148.4, 141.4, 141.3, 134.3, 133.3, 131.3, 129.8, 129.7, 129.5, 129.1, 128.7, 128.3, 127.6, 127.0, 126.9, 126.5, 126.1, 125.9, 125.3, 125.1, 121.6, 121.1, 120.8, 119.5, 105.8, 71.1, 50.9, 33.1, 31.6. ES-MS calcd. for $C_{34}H_{30}N_3O$: $[M+H]^+$ 496.23; found 496.1.

4-[2'-(2-Chloro-5-trifluoromethyl-phenoxymethyl)-biphenyl-4-yl]-1-(3-phenyl-propyl)-1H-[1,2,3]triazole 67. Yield: 72%; ^{1}H-NMR δ (600 MHz; $CDCl_3$): 7.90 (2H, d, *J*=8.11 Hz), 7.77 (1H, s), 7.57 (1H, t), 7.49-7.44 (5H, m), 7.32 (1H, t), 7.28-7.18 (5H, m), 7.14 (1H, d, *J*=8.11 Hz), 6.96 (1H, s), 5.08 (2H, s), 4.43 (2H, t), 2.72 (2H, t), 2.33 (2H, quint); ^{13}C-NMR δ (150 MHz; $CDCl_3$): 155.6, 148.3, 141.5, 141.3, 134.0, 131.7, 129.8, 129.7, 129.2, 129.1, 128.9, 128.7, 128.4, 127.6, 127.2, 126.7, 126.4, 126.1, 125.6, 123.9, 121.1, 118.4, 110.6, 69.8, 50.6, 31.8, 33.9. ES-MS calcd. for $C_{31}H_{26}ClF_3N_3O$: $[M+H]^+$ 548.16; found 548.6.

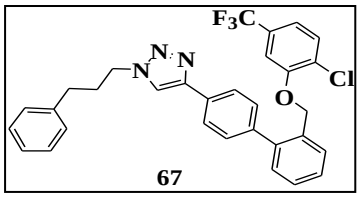

67

4-[2'-(2-Chloro-5-trifluoromethyl-phenoxymethyl)-biphenyl-4-yl]-1-(2-o-tolyl-ethyl)-1H-[1,2,3]triazole 68. Yield: 70%; ^{1}H-NMR δ (300 MHz; $CDCl_3$): 7.82 (2H, d, *J*=8.11 Hz), 7.57 (1H, d, *J*=5.48 Hz), 7.49-7.37 (6H, m), 7.18-7.12 (6H, m), 6.95 (1H, s), 5.07 (2H, s), 4.62 (2H, t), 3.27 (2H, t), 2.27 (3H, s); ^{13}C-NMR δ (75 MHz; $CDCl_3$): 155.9, 148.1, 141.7, 135.6, 135.5, 134.3, 131.5, 130.1, 129.8, 129.7, 129.5, 129.4, 129.3, 128.7, 128.2, 126.9, 126.5, 126.3, 126.1, 125.6, 125.5, 123.5, 121.0, 118.2, 110.5, 69.6, 50.3, 33.5, 18.0. ES-MS calcd. for $C_{31}H_{26}ClF_3N_3O$: $[M+H]^+$ 548.16; found 548.3.

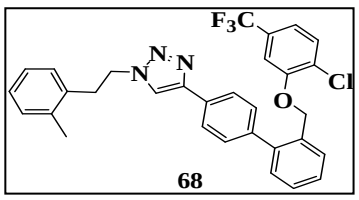

68

4-{4-[2'-(Naphthalen-1-yloxymethyl)-biphenyl-4-yl]-1,2,3]triazole-1-sulfonyl}-benzoic acid 70. Yield: 32%; ^{1}H-NMR δ (500 MHz; CD_3OD): 8.25 (1H, d, *J*=7.67 Hz), 7.96 (1H, s), 7.83-7.78 (4H, m), 7.55-7.40 (12H, m), 7.31 (1H, t), 6.72 (1H, d, *J*=7.67 Hz), 5.14 (2H, s); ^{13}C-NMR δ (125 MHz; CD_3OD): 172.4, 155.5, 149.1, 143.9, 142.0, 135.4, 134.9, 133.4, 132.1, 131.9, 130.3, 130.1, 129.9, 129.6, 129.3, 127.9, 127.4, 127.1, 126.7, 126.4, 125.8,

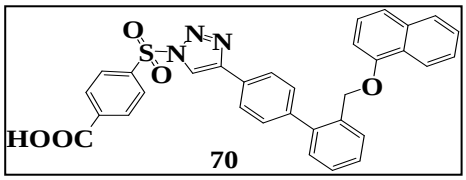

70

125.4, 125.0, 123.1, 121.3, 120.6, 105.9, 71.7. ES-MS calcd. for $C_{32}H_{24}N_3O_5S$: $[M+H]^+$ 562.14; found 562.5.

5-Dimethylamino-naphthalene-1-sulfonic acid {4'-[1-(3-phenyl-propyl)-1H-[1,2,3]triazol-4-yl]-biphenyl-4-yl}-amide 71. Yield: 38%; ^{1}H-NMR δ

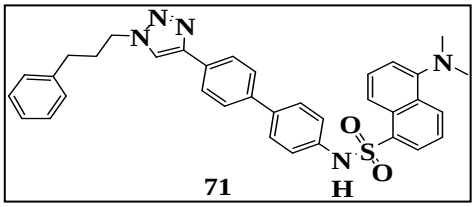

71

(300 MHz; CD_3OD): 8.50 (2H, dd, *J*=5.92, 8.77 Hz), 8.32 (1H, s), 8.25 (1H, d, *J*=7.23 Hz), 7.82 (2H, d, *J*=8.33 Hz), 7.65 (1H, t), 7.54 (1H, t), 7.43-7.37 (4H, m), 7.28-7.17 (7H, m), 7.02 (1H, d, *J*=8.33 Hz), 4.46 (2H, t), 2.88 (6H, s), 2.68 (2H, t), 2.29 (2H, quint); ^{13}C-NMR δ (75 MHz; CD_3OD): 148.3, 141.5, 140.1, 139.8, 137.9, 136.5, 134.2, 131.0, 130.1, 129.5, 129.3, 129.0, 128.5, 128.3, 127.2, 126.5, 126.3, 126.0, 125.6, 125.1, 124.6, 124.4, 123.2, 122.2, 121.6, 50.1, 46.2, 33.2, 31.6. ES-MS calcd. for $C_{35}H_{34}N_5O_2S$: $[M+H]^+$ 588.24; found 588.2.

4-[2'-(Naphthalen-1-yloxymethyl)-biphenyl-4-yl]-1-(2-o-tolyl-ethyl)-1H-[1,2,3]triazole 72. Yield: 52%; ^{1}H-NMR δ (300 MHz; CD_3OD): 8.21 (1H, d,

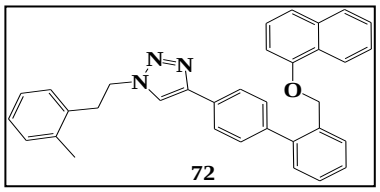

72

J=7.67 Hz), 7.80-7.75 (3H, m), 7.68 (2H, d, *J*=8.11 Hz), 7.51-7.40 (8H, m), 7.31 (1H, d, *J*=7.45 Hz), 7.16-7.09 (3H, m), 7.04 (1H, d, *J*=6.80 Hz), 6.71 (1H, d, *J*=7.67 Hz), 5.12 (2H, s), 4.61 (2H, t), 3.26 (2H, t), 2.25 (3H, s); ^{13}C-NMR δ (75 MHz; CD_3OD): 155.2, 148.6, 141.3, 135.2, 134.6, 133.9, 130.9, 130.7, 129.8, 129.6, 129.3, 129.2, 129.1, 128.9, 127.4, 126.9, 126.5, 126.3, 126.1, 125.9, 125.7, 125.5, 125.1, 125.0, 121.6, 121.1, 120.6, 105.6, 71.2, 50.9, 32.8, 18.1. ES-MS calcd. for $C_{34}H_{30}N_3O$: $[M+H]^+$ 496.23; found 496.1.

4-(5-Benzyl-3-phenylsulfanylmethyl-3H-[1,2,3]triazol-4-yl)-benzaldehyde 73. Yield: 94%; ^{1}H-NMR δ (300 MHz; $CDCl_3$): 10.05 (1H, s), 7.85 (2H, d,

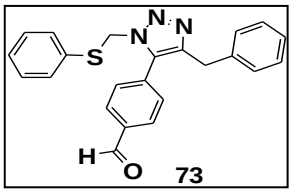

73

J=7.67 Hz), 7.26-7.17 (10H, m), 7.08 (2H, d, *J*=6.80 Hz), 5.52 (2H, s), 3.98 (2H, s); ^{13}C-NMR δ (75 MHz; $CDCl_3$): 190.5, 155.9, 142.6, 141.2, 138.0, 136.9, 133.6, 130.6, 129.5, 128.0, 127.0, 125.1, 117.5, 113.7, 112.8, 53.3, 29.7. ES-MS calcd. for $C_{23}H_{20}N_3OS$: $[M+H]^+$ 386.12; found 386.2.

4'-[1-(2-o-Tolyl-ethyl)-1H-[1,2,3]triazol-4-yl]-biphenyl-4-ylamine 74.

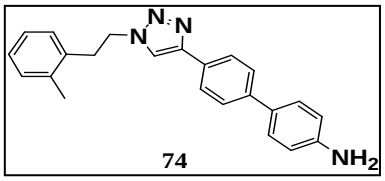

74

Yield: 52%; ^{1}H-NMR δ (500 MHz; CD_3OD): 8.13 (1H, s), 7.86 (2H, d, *J*=8.33 Hz), 7.75 (2H, d, *J*=8.33 Hz), 7.71 (2H, d, *J*=8.33 Hz), 7.28 (2H, d, *J*=8.33 Hz), 7.16-7.00 (4H, m), 4.71 (2H, t), 3.32 (2H, t), 2.33 (3H, s). ^{13}C-NMR δ (125 MHz; CD_3OD): 146.9, 139.9, 137.6, 135.9, 135.5, 130.3, 129.8, 129.4, 128.3, 127.6, 126.7, 126.1, 125.8, 125.5, 121.4, 120.2, 50.5, 33.6, 18.9; ES-MS calcd. for $C_{23}H_{23}N_4$: $[M+H]^+$ 355.18; found 355.4.

4-(4'-Phenoxy-biphenyl-4-yl)-1-(3-phenyl-propyl)-1H-[1,2,3]triazole 76.

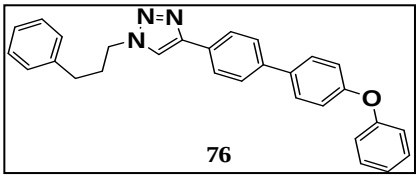

76

Yield: 68%; ^{1}H-NMR δ (300 MHz; $CDCl_3$): 8.87 (2H, d, *J*=8.11 Hz), 7.73 (1H, s), 7.65 (2H, d, *J*=8.11 Hz), 7.60 (2H, d, *J*=8.33 Hz), 7.35-7.27 (7H, m), 7.11-7.07 (5H, m), 4.41 (2H, t), 2.69 (2H, t), 2.31 (2H, quint); ^{13}C-NMR δ (75 MHz; $CDCl_3$): 155.8, 155.1, 148.5, 141.7, 141.4, 135.5, 129.5, 128.7, 128.6, 127.3, 126.9, 126.7, 126.5, 125.6, 121.4, 121.1, 120.4, 116.8, 50.5, 33.5, 31.4. ES-MS calcd. for $C_{29}H_{26}N_3O$: $[M+H]^+$ 432.20; found 432.4.

4-[4-(4'-Hydroxy-biphenyl-4-yl)-[1,2,3]triazol-1-ylmethyl]-3-nitro-benzoic acid 93b. Yield: 47%; ^{1}H-NMR δ (300 MHz; CD_3OD): 8.75 (1H, s), 8.53 (1H, s), 8.25 (1H, d, *J*=8.09 Hz), 7.89 (2H, d, *J*=7.89 Hz), 7.71 (2H, d, *J*=7.89 Hz),

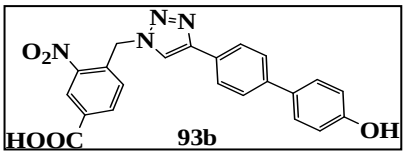

93b

7.49 (2H, d, *J*=7.23 Hz), 7.24 (1H, d, *J*=8.11 Hz), 6.81 (2H, d, *J*=8.35 Hz), 6.19 (2H, s); ^{13}C-NMR δ (75 MHz; CD_3OD): 165.1, 157.3, 148.1, 141.3, 135.0, 134.2, 133.2, 131.7, 130.2, 128.2, 127.8, 127.1, 126.6, 126.0, 125.9, 122.1, 115.5, 50.8. ES-MS calcd. for $C_{22}H_{17}N_4O_5$: $[M+H]^+$ 417.11; found 417.1.

4-[4-(3'-Hydroxy-biphenyl-4-yl)-[1,2,3]triazol-1-ylmethyl]-3-nitro-benzoic acid 93c. Yield: 42%; ^{1}H-NMR δ (300 MHz; CD_3OD): 8.76 (1H, s), 8.23 (1H, d, *J*=8.09 Hz) 8.12 (1H, s), 7.83 (2H, d, *J*=8.11 Hz), 7.62 (2H, d, *J*=7.89 Hz), 7.41 (1H, s), 7.23 (1H, t), 6.77-6.72 (3H, m), 6.05 (2H, s); ^{13}C-NMR δ (75 MHz; CD_3OD): 165.7, 155.5, 147.5, 142.2, 141.4, 135.1, 131.7, 130.5, 129.2, 128.6, 128.1, 127.1, 126.8, 125.6, 125.7, 122.6, 117.2, 115.1, 113.8, 50.7. ES-MS calcd. for $C_{22}H_{17}N_4O_5$: $[M+H]^+$ 417.11; found 417.1.

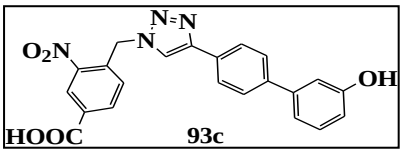

93c

4-[4-(4'-Amino-biphenyl-4-yl)-[1,2,3]triazol-1-ylmethyl]-3-nitro-benzoic acid 93d. Yield: 49%; ^{1}H-NMR δ (300 MHz; CD_3OD): 8.77 (1H, s), 8.53 (1H, s), 8.26 (1H, d, *J*=8.09 Hz), 7.88 (2H, d, *J*=7.89 Hz), 7.70 (2H, d, *J*=7.89 Hz), 7.49 (2H, d, *J*=7.23 Hz), 7.24 (1H, d, *J*=8.11 Hz), 6.81 (2H, d, *J*=8.35 Hz), 6.22 (2H, s); ^{13}C-NMR δ (75 MHz; CD_3OD): 165.4, 157.1, 147.9, 140.8, 134.8, 134.6, 133.5, 131.3, 129.7, 128.6, 127.3, 126.8, 126.1, 125.8, 125.4, 121.8, 115.8, 50.5. ES-MS calcd. for $C_{22}H_{18}N_5O_4$: $[M+H]^+$ 416.13; found 416.1.

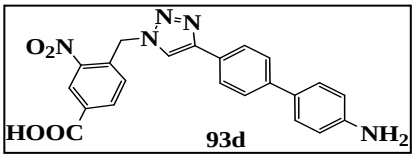

93d

4-{4-[2'-(2-Chloro-5-trifluoromethyl-phenoxymethyl)-biphenyl-4-yl]-[1,2,3]triazol-1-ylmethyl}-3-nitro-benzoic acid 93h. Yield: 62%; ^{1}H-NMR δ (300 MHz; $CDCl_3$): 8.78 (1H, s), 8.48 (1H,s), 8.29 (1H, d, *J*=8.11 Hz), 7.90

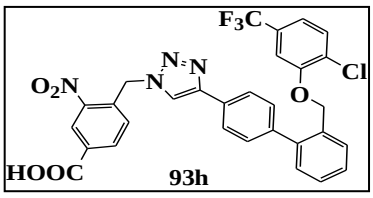

93h

(2H, d, *J*=8.09 Hz), 7.65 (1H, d, *J*=5.48 Hz), 7.50 (2H, d, *J*=8.11 Hz), 7.45-7.37 (6H, m), 7.18 (1H, d, *J*=5.48 Hz), 6.18 (2H, s), 5.15 (2H, s); ^{13}C-NMR δ (75 MHz; $CDCl_3$): 165.6, 155.6, 148.1, 141.2, 135.6, 135.2, 134.3, 131.7, 130.1, 129.9, 129.7, 129.5, 129.4, 129.1, 128.5, 128.2, 126.8, 126.5, 126.3, 126.1, 125.6, 125.5, 123.5, 121.0, 118.2, 110.5, 69.0, 50.3. ES-MS calcd. for $C_{30}H_{21}ClF_3N_4O_5$: $[M+H]^+$ 609.11; found 609.1.

4-{4-[4'-(6-Dimethylamino-naphthalene-2-sulfonylamino)-biphenyl-4-yl]-[1,2,3]triazol-1-ylmethyl}-3-nitro-benzoic acid 93i. Yield: 51%; ^{1}H-NMR δ

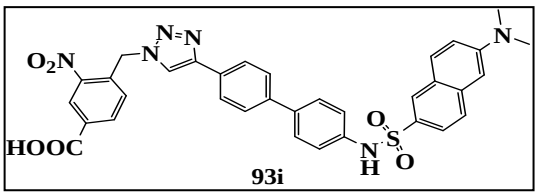

93i

(300 MHz; CD_3OD): 8.77 (1H, s), 8.55 (1H, s), 8.24 (2H, d, *J*=8.09 Hz), 7.89 (1H, d, *J*=7.89 Hz), 7.71 (2H, d, *J*=7.89 Hz), 7.55 (2H, d, *J*=7.23 Hz), 7.50-7.46 (3H, m), 7.32 (2H, d, *J*=8.11 Hz), 7.13-7.09 (8H, m), 6.95 (1H, d, *J*=8.09 Hz), 6.85 (1H, d, *J*=8.11 Hz), 6.19 (2H, s);^{13}C-NMR δ (75 MHz; CD_3OD): 165.7, 156.9, 149.5, 149.1, 145.5, 140.5, 138.1, 136.6, 136.1, 135.4, 134.2, 133.2, 131.5, 130.3, 129.8, 128.5, 128.2, 128.0, 127.8, 127.3, 126.4, 126.0, 125.2, 123.5, 118.0, 115.3, 107.2, 50.5, 43.8. ES-MS calcd. for $C_{34}H_{29}N_6O_6S$: $[M+H]^+$ 649.18; found 649.1.

4-{4-[3'-(Morpholine-4-carbonyl)-biphenyl-4-yl]-[1,2,3]triazol-1-ylmethyl}-3-nitro-benzoic acid 93j. Yield: 56%; ^{1}H-NMR δ (300 MHz;

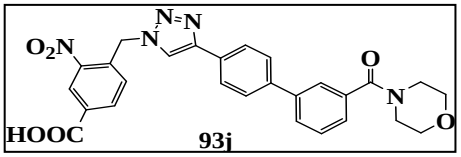

93j

CD_3OD): 8.79 (1H, s), 8.58 (1H, s), 8.35 (1H, d, *J*=8.09 Hz), 8.02 (2H, d, *J*=7.87 Hz), 7.88 (1H, d, *J*=7.23 Hz), 7.79 (2H, d, *J*=7.89 Hz), 7.75 (1H, s), 7.65 (1H,t), 7.45 (1H, d, *J*=8.09 Hz), 7.33 (1H, d, *J*=7.23 Hz), 6.23 (2H, s), 4.16 (2H, t), 3.88 (2H, t), 3.48 (4H, m); ^{13}C-NMR δ (75 MHz; CD_3OD): 165.9, 165.6, 157.2, 149.2, 140.5, 138.0, 136.6, 136.1,

135.4, 135.0, 134.2, 131.5, 130.2, 128.2, 127.8, 127.3, 126.3, 126.0, 125.8, 125.0, 70.9, 50.9, 50.2. ES-MS calcd. for $C_{27}H_{24}N_5O_6$: $[M+H]^+$ 514.16; found 514.2.

4'-[1-(4-Carboxy-2-nitro-benzyl)-1H-[1,2,3]triazol-4-yl]-biphenyl-3-carboxylic acid 93k. Yield: 45%; ^{1}H-NMR δ (300 MHz; CD_3OD): 8.77 (1H, s), 8.63 (1H, s), 8.38 (1H, s), 8.37 (1H, d, *J*=7.87 Hz), 8.08 (1H, d, *J*=7.23 Hz), 8.04 (1H, d, *J*=8.11 Hz), 8.09 (2H, d, *J*=7.23 Hz), 7.89 (2H, d, *J*=7.89 Hz), 7.35 (2H, d, *J*=8.11 Hz), 6.22 (2H, s); ^{13}C-NMR δ (75 MHz; CD_3OD): 165.9, 165.3, 157.8, 147.9, 142.9, 141.9, 135.5, 131.1, 130.2, 129.7, 129.2, 128.7, 127.5, 127.2, 126.0, 125.9, 122.2, 117.9, 114.3, 113.3, 50.8. ES-MS calcd. for $C_{23}H_{17}N_4O_6$: $[M+H]^+$ 445.11; found 445.1.

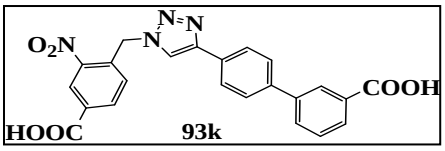

93k

4-[4-(3',4',5'-trimethoxy-biphenyl-4-yl)-[1,2,3]triazol-1-ylmethyl]-3-nitro-benzoic acid 93l. Yield: 71%; ^{1}H-NMR δ (300 MHz; CD_3OD): 8.79 (1H, s), 8.56 (1H, s), 8.34 (1H, d, *J*=8.11 Hz), 8.00 (2H, d, *J*=7.87 Hz), 7.81 (2H, d, *J*=7.89 Hz), 7.31 (1H, d, *J*=7.89 Hz), 7.01 (2H, s), 6.20 (2H, s), 4.01 (6H, s), 3.80 (3H, s); ^{13}C-NMR δ (75 MHz; CD_3OD): 165.7, 153.7, 147.9, 141.2, 137.7, 136.6, 134.5, 130.3, 129.2, 129.0, 128.7, 127.6, 127.3, 126.0, 125.9, 122.2, 104.5, 59.9, 55.5, 50.5. ES-MS calcd. for $C_{25}H_{23}N_4O_7$: $[M+H]^+$ 491.15; found 491.2.

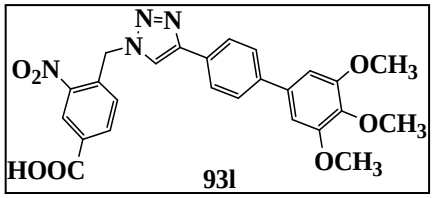

93l

3-Nitro-4-[4-(4-thiophen-2-yl-phenyl)-[1,2,3]triazol-1-ylmethyl]-benzoic acid 93m. Yield: 54%; ^{1}H-NMR δ (300 MHz; CD_3OD): 8.75 (1H, s), 8.55 (1H, s), 8.34 (1H, d, *J*=8.11 Hz), 7.92 (2H, d, *J*=7.87 Hz), 7.75 (2H, d, *J*=7.89 Hz), 7.51 (1H, d, *J*=7.89 Hz), 7.45 (1H, d, *J*=8.09 Hz), 7.27 (1H, , *J*=7.23 Hz), 7.12 (1H, d, *J*=8.11 Hz), 6.18 (2H, s); ^{13}C-NMR δ (75 MHz;

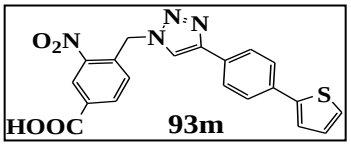

93m

CD_3OD): 165.6, 157.1, 148.1, 141.5, 135.0, 134.2, 133.2, 131.7, 130.2, 128.2, 127.8, 127.1, 126.6, 126.0, 125.6, 125.2, 122.2, 50.8. ES-MS calcd. for $C_{20}H_{15}N_4O_4S$: $[M+H]^+$ 407.07; found 407.0.

4-[4-(4'-Methoxy-3'-morpholin-4-ylmethyl-biphenyl-4-yl)-[1,2,3]triazol-1-ylmethyl]-3-nitro-benzoic acid 93n. Yield: 54%; ^{1}H-NMR δ (300 MHz; CD_3OD): 8.79 (1H, s), 8.56 (1H, s), 8.35 (1H, d, *J*=8.09 Hz), 8.02 (2H, d, *J*=7.87 Hz), 7.88 (1H, d, *J*=7.23 Hz), 7.79 (2H, d, *J*=7.89 Hz), 7.75 (1H, d, *J*=7.87 Hz), 7.33 (1H, d, *J*=7.23 Hz), 6.23 (2H, s), 4.12 (2H, t), 4.5 (2H, s), 4.01 (3H, s), 3.82 (2H, t), 3.45 (4H, m); ^{13}C-NMR δ (75 MHz; CD_3OD): 165.5, 158.8, 156.2, 149.2, 138.1, 136.5, 136.1, 135.4, 134.2, 131.4, 130.2, 128.9, 128.5, 127.6, 127.4, 126.7, 125.4, 122.5, 114.9, 71.1, 56.5, 56.1, 50.4, 49.8. ES-MS calcd. for $C_{28}H_{28}N_5O_6$: $[M+H]^+$ 530.20; found 530.2.

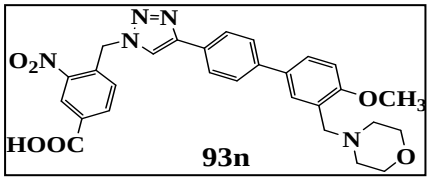

93n

7.2.9. Synthesis of benzoic acid 1-phenylsulfanylmethyl-1H-[1,2,3]triazol-4-ylmethyl ester 61

A mixture of compound **80** (0.3 equiv.) and 200 µL of benzoyl chloride in 2 mL of dry DMF were refluxed overnight under nitrogen atmosphere. When TLC analysis indicated complete consumption of limiting reactant **80**, the mixture was diluted with aqueous solution of HCl 1 N and extracted with ethyl acetate (3 x 10 mL). The organics were dried over Na_2SO_4, filtered and concentrated in *vacuo*. The crude was purified by flash chromatography (10% diethyl ether/*n*-hexane to 40% diethyl ether/*n*-hexane). Yield: 78%; ^{1}H-NMR δ (600 MHz; CD_3OD): 8.02 (2H, dd, *J*=1.32, 8.33 Hz), 7.96 (1H, s), 7.64 (1H, t), 5.50 (1H, t), 7.36 (2H, dd, *J*=2.19, 7.89 Hz), 7.28-7.25 (4H, m), 5.80 (2H, s), 5.40 (2H, s); ^{13}C-NMR δ (150 MHz; CD_3OD): 165.6, 142.4, 132.8,

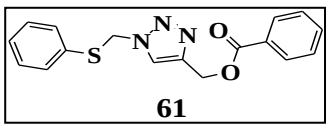

61

132.5, 131.8, 130.8, 128.9, 128.5, 128.1, 127.8, 123.6, 57.0, 53.3. ES-MS calcd. for $C_{17}H_{16}N_3O_2S$: $[M+H]^+$ 326.09; found 326.2.

Bibliography

[1] N. J. Talley, J. M. Evans, K. C. Fleming, W. S. Harmsen, A. R. Zinsmeister, L. J. Melton, III. *Dig. Dis. Sci.* **1995**, *40*(6), 1345-1350.

[2] H. F. Cheng, R. C. Harris. *Curr. Pharm. Des* **2005**, *11*(14), 1795-1804.

[3] J. C. O'Laughlin, J. W. Hoftiezer, K. J. Ivey. *Scand. J. Gastroenterol. Suppl* **1981**, *67*, 211-214.

[4] D. Y. Graham, J. L. Smith, S. M. Dobbs. *Dig. Dis. Sci.* **1983**, *28*(1), 1-6.

[5] J. W. Hoftiezer, J. C. O'Laughlin, K. J. Ivey. *Gut* **1982**, *23*(8), 692-697.

[6] L. Laine, S. Harper, T. Simon, R. Bath, J. Johanson, H. Schwartz, S. Stern, H. Quan, J. Bolognese. *Gastroenterology* **1999**, *117*(4), 776-783.

[7] W. L. Smith. *Biochem. J.* **1989**, *259*(2), 315-324.

[8] P. McGettigan, D. Henry. *JAMA* **2006**, *296*(13), 1633-1644.

[9] L. W. Hardy, N. P. Peet. *Drug Discov. Today* **2004**, *9*(3), 117-126.

[10] R. Macarron. *Drug Discov. Today* **2006**, *11*(7-8), 277-279.

[11] T. I. Oprea, H. Matter. *Curr. Opin. Chem. Biol.* **2004**, *8*(4), 349-358.

[12] G. Scapin. *Curr. Pharm. Des* **2006**, *12*(17), 2087-2097.

[13] P. J. Hajduk, J. Greer. *Nat. Rev Drug Discov.* **2007**, *6*(3), 211-219.

[14] A. Randazzo, C. Debitus, L. Minale, P. P. Garcia, M. J. Alcaraz, M. Paya, L. Gomez-Paloma. *J. Nat. Prod.* **1998**, *61*(5), 571-575.

[15] R. Lucas, C. Giannini, M. V. D'auria, M. Paya. *J. Pharmacol. Exp. Ther.* **2003**, *304*(3), 1172-1180.

[16] P. J. Proteau, W. H. Gerwick, F. Garcia-Pichel, R. Castenholz. *Experientia* **1993**, *49*(9), 825-829.

[17] K. Bartik, J. Braekman, D. Dalkoze, C. Stoller, J. Huysecom, G. Vandevyver, P. Ottingen. *Canadian Journal of Chemistry* **1987**, *65*, 2118-2121.

[18] Sharma G.V., Buyer J.S., Pomeranz G. *Journal Chemical Society* **1980**, 435-456.

[19] P. Garcia-Pastor, A. Randazzo, L. Gomez-Paloma, M. J. Alcaraz, M. Paya. *J. Pharmacol. Exp. Ther.* **1999**, *289*(1), 166-172.

[20] I. Posadas, M. C. Terencio, A. Randazzo, L. Gomez-Paloma, M. Paya, M. J. Alcaraz. *Biochem. Pharmacol.* **2003**, *65*(5), 887-895.

[21] M. D. Guerrero, M. Aquino, I. Bruno, M. C. Terencio, M. Paya, R. Riccio, L. Gomez-Paloma. *J. Med. Chem.* **2007**, *50*(9), 2176-2184.

[22] M. D. Guerrero, M. Aquino, I. Bruno, R. Riccio, M. C. Terencio, M. Paya. *Eur. J. Pharmacol.* **2009**, *620*(1-3), 112-119.

[23] H. Araki, H. Ukawa, Y. Sugawa, K. Yagi, K. Suzuki, K. Takeuchi. *Aliment. Pharmacol. Ther.* **2000**, *14 Suppl 1*, 116-124.

[24] G. Majno, Joris I. *Cells, tissues, and disease*, Blackwell Science, **1996**.

[25] W. E. Lands. *Annu. Rev. Physiol* **1979**, *41*, 633-652.

[26] R. A. Lewis, K. F. Austen, R. J. Soberman. *N. Engl. J. Med.* **1990**, *323*(10), 645-655.

[27] P. J. Barnes. *Br. J. Pharmacol.* **2010**.

[28] M. C. Monti, A. Casapullo, R. Riccio, L. Gomez-Paloma. *Bioorg. Med. Chem.* **2004**, *12*(6), 1467-1474.

[29] G. A. FitzGerald, C. Patrono. *N. Engl. J. Med.* **2001**, *345*(6), 433-442.

[30] L. Boulet, M. Ouellet, K. P. Bateman, D. Ethier, M. D. Percival, D. Riendeau, J. A. Mancini, N. Methot. *J. Biol. Chem.* **2004**, *279*(22), 23229-23237.

[31] B. Samuelsson, R. Morgenstern, P. J. Jakobsson. *Pharmacol. Rev.* **2007**, *59*(3), 207-224.

[32] K. Watanabe, K. Kurihara, T. Suzuki. *Biochim. Biophys. Acta* **1999**, *1439*(3), 406-414.

[33] T. Tanioka, Y. Nakatani, N. Semmyo, M. Murakami, I. Kudo. *J. Biol. Chem.* **2000**, *275*(42), 32775-32782.

[34] N. Tanikawa, Y. Ohmiya, H. Ohkubo, K. Hashimoto, K. Kangawa, M. Kojima, S. Ito, K. Watanabe. *Biochem. Biophys. Res. Commun.* **2002**, *291*(4), 884-889.

[35] M. Murakami, H. Naraba, T. Tanioka, N. Semmyo, Y. Nakatani, F. Kojima, T. Ikeda, M. Fueki, A. Ueno, S. Oh, I. Kudo. *J. Biol. Chem.* **2000**, *275*(42), 32783-32792.

[36] M. Murakami, K. Nakashima, D. Kamei, S. Masuda, Y. Ishikawa, T. Ishii, Y. Ohmiya, K. Watanabe, I. Kudo. *J. Biol. Chem.* **2003**, *278*(39), 37937-37947.

[37] P. J. Jakobsson, S. Thoren, R. Morgenstern, B. Samuelsson. *Proc. Natl. Acad. Sci. U. S. A* **1999**, *96*(13), 7220-7225.

[38] P. J. Jakobsson, R. Morgenstern, J. Mancini, A. Ford-Hutchinson, B. Persson. *Am. J. Respir. Crit Care Med.* **2000**, *161*(2 Pt 2), S20-S24.

[39] S. Thoren, R. Weinander, S. Saha, C. Jegerschold, P. L. Pettersson, B. Samuelsson, H. Hebert, M. Hamberg, R. Morgenstern, P. J. Jakobsson. *J. Biol. Chem.* **2003**, *278*(25), 22199-22209.

[40] C. Jegerschold, S. C. Pawelzik, P. Purhonen, P. Bhakat, K. R. Gheorghe, N. Gyobu, K. Mitsuoka, R. Morgenstern, P. J. Jakobsson, H. Hebert. *Proc. Natl. Acad. Sci. U. S. A* **2008**, *105*(32), 11110-11115.

[41] T. Yamada, J. Komoto, K. Watanabe, Y. Ohmiya, F. Takusagawa. *J. Mol. Biol.* **2005**, *348*(5), 1163-1176.

[42] T. Hammarberg, M. Hamberg, A. Wetterholm, H. Hansson, B. Samuelsson, J. Z. Haeggstrom. *J. Biol. Chem.* **2009**, *284*(1), 301-305.

[43] M. D. Martinez, A. Wetterholm, A. Kohl, A. A. McCarthy, D. Niegowski, E. Ohlson, T. Hammarberg, S. Eshaghi, J. Z. Haeggstrom, P. Nordlund. *Nature* **2007**, *448*(7153), 613-616.

[44] H. Ago, Y. Kanaoka, D. Irikura, B. K. Lam, T. Shimamura, K. F. Austen, M. Miyano. *Nature* **2007**, *448*(7153), 609-612.

[45] M. Nakanishi, V. Gokhale, E. J. Meuillet, D. W. Rosenberg. *Biochimie* **2010**, *92*(6), 660-664.

[46] R. W. Friesen, J. A. Mancini. *J. Med. Chem.* **2008**, *51*(14), 4059-4067.

[47] A. Koeberle, O. Werz. *Curr. Med. Chem.* **2009**, *16*(32), 4274-4296.

[48] Y. Guan, Y. Zhang, A. Schneider, D. Riendeau, J. A. Mancini, L. Davis, M. Komhoff, R. M. Breyer, M. D. Breyer. *Am. J. Physiol Renal Physiol* **2001**, *281*(6), F1173-F1177.

[49] A. L. Fuson, P. Komlosi, T. M. Unlap, P. D. Bell, J. Peti-Peterdi. *Am. J. Physiol Renal Physiol* **2003**, *285*(3), F558-F564.

[50] M. Lazarus, C. J. Munday, N. Eguchi, S. Matsumoto, G. J. Killian, B. K. Kubata, Y. Urade. *Endocrinology* **2002**, *143*(6), 2410-2419.

[51] N. Alfaidy, M. Sun, J. R. Challis, W. Gibb. *Endocrine.* **2003**, *20*(3), 219-225.

[52] M. Westman, M. Korotkova, K. E. af, A. Stark, L. P. Audoly, L. Klareskog, A. K. Ulfgren, P. J. Jakobsson. *Arthritis Rheum.* **2004**, *50*(6), 1774-1780.

[53] F. Kojima, H. Naraba, S. Miyamoto, M. Beppu, H. Aoki, S. Kawai. *Arthritis Res. Ther.* **2004**, *6*(4), R355-R365.

[54] K. Masuko-Hongo, F. Berenbaum, L. Humbert, C. Salvat, M. B. Goldring, S. Thirion. *Arthritis Rheum.* **2004**, *50*(9), 2829-2838.

[55] X. Li, H. Afif, S. Cheng, J. Martel-Pelletier, J. P. Pelletier, P. Ranger, H. Fahmi. *J. Rheumatol.* **2005**, *32*(5), 887-895.

[56] K. Subbaramaiah, K. Yoshimatsu, E. Scherl, K. M. Das, K. D. Glazier, D. Golijanin, R. A. Soslow, T. Tanabe, H. Naraba, A. J. Dannenberg. *J. Biol. Chem.* **2004**, *279*(13), 12647-12658.

[57] F. Cipollone, A. Iezzi, M. Fazia, M. Zucchelli, B. Pini, C. Cuccurullo, C. D. De, B. G. De, R. Muraro, R. Bei, F. Chiarelli, A. M. Schmidt, F. Cuccurullo, A. Mezzetti. *Circulation* **2003**, *108*(9), 1070-1077.

[58] U. A. Chaudhry, H. Zhuang, B. J. Crain, S. Dore. *Alzheimers. Dement.* **2008**, *4*(1), 6-13.

[59] M. Korotkova, S. B. Helmers, I. Loell, H. Alexanderson, C. Grundtman, C. Dorph, I. E. Lundberg, P. J. Jakobsson. *Ann. Rheum. Dis.* **2008**, *67*(11), 1596-1602.

[60] M. Nakanishi, D. C. Montrose, P. Clark, P. R. Nambiar, G. S. Belinsky, K. P. Claffey, D. Xu, D. W. Rosenberg. *Cancer Res.* **2008**, *68*(9), 3251-3259.

[61] D. Kamei, M. Murakami, Y. Nakatani, Y. Ishikawa, T. Ishii, I. Kudo. *J. Biol. Chem.* **2003**, *278*(21), 19396-19405.

[62] K. Yoshimatsu, N. K. Altorki, D. Golijanin, F. Zhang, P. J. Jakobsson, A. J. Dannenberg, K. Subbaramaiah. *Clin. Cancer Res.* **2001**, *7*(9), 2669-2674.

[63] K. Gudis, A. Tatsuguchi, K. Wada, T. Hiratsuka, S. Futagami, Y. Fukuda, T. Kiyama, T. Tajiri, K. Miyake, C. Sakamoto. *Hum. Pathol.* **2007**, *38*(12), 1826-1835.

[64] S. Hasan, M. Satake, D. W. Dawson, H. Funahashi, E. Angst, V. L. Go, H. A. Reber, O. J. Hines, G. Eibl. *Pancreas* **2008**, *37*(2), 121-127.

[65] M. Herfs, L. Herman, P. Hubert, F. Minner, M. Arafa, P. Roncarati, Y. Henrotin, J. Boniver, P. Delvenne. *Cancer Immunol. Immunother.* **2009**, *58*(4), 603-614.

[66] H. Hanaka, S. C. Pawelzik, J. I. Johnsen, M. Rakonjac, K. Terawaki, A. Rasmuson, B. Sveinbjornsson, M. C. Schumacher, M. Hamberg, B. Samuelsson, P. J. Jakobsson, P. Kogner, O. Radmark. *Proc. Natl. Acad. Sci. U. S. A* **2009**, *106*(44), 18757-18762.

[67] Y. Omi, N. Shibata, T. Okamoto, T. Obara, M. Kobayashi. *Acta Histochem. Cytochem.* **2009**, *42*(4), 105-109.

[68] M. Camacho, X. Leon, M. T. Fernandez-Figueras, M. Quer, L. Vila. *Head Neck* **2008**, *30*(9), 1175-1181.

[69] N. Baryawno, B. Sveinbjornsson, S. Eksborg, A. Orrego, L. Segerstrom, C. O. Oqvist, S. Holm, B. Gustavsson, B. Kagedal, P. Kogner, J. I. Johnsen. *Neuro. Oncol.* **2008**, *10*(5), 661-674.

[70] S. Mattila, H. Tuominen, J. Koivukangas, F. Stenback. *Neuropathology.* **2009**, *29*(2), 156-165.

[71] T. Seo, A. Tatsuguchi, S. Shinji, M. Yonezawa, K. Mitsui, S. Tanaka, S. Fujimori, K. Gudis, Y. Fukuda, C. Sakamoto. *Virchows Arch.* **2009**, *454*(6), 667-676.

[72] D. Kamei, K. Yamakawa, Y. Takegoshi, M. Mikami-Nakanishi, Y. Nakatani, S. Oh-Ishi, H. Yasui, Y. Azuma, N. Hirasawa, K. Ohuchi, H. Kawaguchi, Y. Ishikawa, T. Ishii, S. Uematsu, S. Akira, M. Murakami, I. Kudo. *J. Biol. Chem.* **2004**, *279*(32), 33684-33695.

[73] M. Lazarus, B. K. Kubata, N. Eguchi, Y. Fujitani, Y. Urade, O. Hayaishi. *Arch. Biochem. Biophys.* **2002**, *397*(2), 336-341.

[74] S. Thoren, P. J. Jakobsson. *Eur. J. Biochem.* **2000**, *267*(21), 6428-6434.

[75] C. E. Trebino, J. D. Eskra, T. S. Wachtmann, J. R. Perez, T. J. Carty, L. P. Audoly. *J. Biol. Chem.* **2005**, *280*(17), 16579-16585.

[76] A. N. Hata, R. M. Breyer. *Pharmacol. Ther.* **2004**, *103*(2), 147-166.

[77] C. Yokoyama, T. Yabuki, M. Shimonishi, M. Wada, T. Hatae, S. Ohkawara, J. Takeda, T. Kinoshita, M. Okabe, T. Tanabe. *Circulation* **2002**, *106*(18), 2397-2403.

[78] F. Celotti, S. Laufer. *Pharmacol. Res.* **2001**, *43*(5), 429-436.

[79] M. Peters-Golden, W. R. Henderson, Jr. *N. Engl. J. Med.* **2007**, *357*(18), 1841-1854.

[80] K. Subbaramaiah, W. J. Chung, P. Michaluart, N. Telang, T. Tanabe, H. Inoue, M. Jang, J. M. Pezzuto, A. J. Dannenberg. *J. Biol. Chem.* **1998**, *273*(34), 21875-21882.

[81] L. M. Szewczuk, L. Forti, L. A. Stivala, T. M. Penning. *J. Biol. Chem.* **2004**, *279*(21), 22727-22737.

[82] E. Candelario-Jalil, A. C. de Oliveira, S. Graf, H. S. Bhatia, M. Hull, E. Munoz, B. L. Fiebich. *J. Neuroinflammation.* **2007**, *4*, 25.

[83] T. Bage, T. Modeer, T. Kawakami, H. C. Quezada, T. Yucel-Lindberg. *Biochim. Biophys. Acta* **2007**, *1773*(10), 1589-1598.

[84] I. Wobst, S. Schiffmann, K. Birod, T. J. Maier, R. Schmidt, C. Angioni, G. Geisslinger, S. Grosch. *Biochem. Pharmacol.* **2008**, *76*(1), 62-69.

[85] V. Ulivi, R. Cancedda, F. D. Cancedda. *J. Cell Physiol* **2008**, *217*(2), 433-441.

[86] X. Song, H. P. Lin, A. J. Johnson, P. H. Tseng, Y. T. Yang, S. K. Kulp, C. S. Chen. *J. Natl. Cancer Inst.* **2002**, *94*(8), 585-591.

[87] O. Quraishi, J. A. Mancini, D. Riendeau. *Biochem. Pharmacol.* **2002**, *63*(6), 1183-1189.

[88] G. Bannenberg, S. E. Dahlen, M. Luijerink, G. Lundqvist, R. Morgenstern. *J. Biol. Chem.* **1999**, *274*(4), 1994-1999.

[89] D. Riendeau, R. Aspiotis, D. Ethier, Y. Gareau, E. L. Grimm, J. Guay, S. Guiral, H. Juteau, J. A. Mancini, N. Methot, J. Rubin, R. W. Friesen. *Bioorg. Med. Chem. Lett.* **2005**, *15*(14), 3352-3355.

[90] J. E. Thompson, R. M. Cubbon, R. T. Cummings, L. S. Wicker, R. Frankshun, B. R. Cunningham, P. M. Cameron, P. T. Meinke, N. Liverton, Y. Weng, J. A. DeMartino. *Bioorg. Med. Chem. Lett.* **2002**, *12*(8), 1219-1223.

[91] B. Cote, L. Boulet, C. Brideau, D. Claveau, D. Ethier, R. Frenette, M. Gagnon, A. Giroux, J. Guay, S. Guiral, J. Mancini, E. Martins, F. Masse, N. Methot, D. Riendeau, J. Rubin, D. Xu, H. Yu, Y. Ducharme, R. W. Friesen. *Bioorg. Med. Chem. Lett.* **2007**, *17*(24), 6816-6820.

[92] J. Wang, D. Limburg, J. Carter, G. Mbalaviele, J. Gierse, M. Vazquez. *Bioorg. Med. Chem. Lett.* **2010**, *20*(5), 1604-1609.

[93] A. Koeberle, H. Zettl, C. Greiner, M. Wurglics, M. Schubert-Zsilavecz, O. Werz. *J. Med. Chem.* **2008**, *51*(24), 8068-8076.

[94] A. Koeberle, F. Pollastro, H. Northoff, O. Werz. *Br. J. Pharmacol.* **2009**, *156*(6), 952-961.

[95] D. Claveau, M. Sirinyan, J. Guay, R. Gordon, C. C. Chan, Y. Bureau, D. Riendeau, J. A. Mancini. *J. Immunol.* **2003**, *170*(9), 4738-4744.

[96] J. A. Mancini, M. Abramovitz, M. E. Cox, E. Wong, S. Charleson, H. Perrier, Z. Wang, P. Prasit, P. J. Vickers. *FEBS Lett.* **1993**, *318*(3), 277-281.

[97] J. A. Mancini, K. Blood, J. Guay, R. Gordon, D. Claveau, C. C. Chan, D. Riendeau. *J. Biol. Chem.* **2001**, *276*(6), 4469-4475.

[98] B. P. van Rees, A. Sivula, S. Thoren, H. Yokozaki, P. J. Jakobsson, G. J. Offerhaus, A. Ristimaki. *Int. J. Cancer* **2003**, *107*(4), 551-556.

[99] S. K. Kulkarni, V. P. Singh. *Curr. Top. Med. Chem.* **2007**, *7*(3), 251-263.

[100] S. Tries, W. Neupert, S. Laufer. *Inflamm. Res.* **2002**, *51*(3), 135-143.

[101] A. Koeberle, U. Siemoneit, U. Buhring, H. Northoff, S. Laufer, W. Albrecht, O. Werz. *J. Pharmacol. Exp. Ther.* **2008**, *326*(3), 975-982.

[102] L. Fischer, M. Hornig, C. Pergola, N. Meindl, L. Franke, Y. Tanrikulu, G. Dodt, G. Schneider, D. Steinhilber, O. Werz. *Br. J. Pharmacol.* **2007**, *152*(4), 471-480.

[103] A. Koeberle, H. Northoff, O. Werz. *Biochem. Pharmacol.* **2009**, *77*(9), 1513-1521.

[104] M. Hendlich. *Acta Crystallogr. D. Biol. Crystallogr.* **1998**, *54*(Pt 6 Pt 1), 1178-1182.

[105] L. Hu, M. L. Benson, R. D. Smith, M. G. Lerner, H. A. Carlson. *Proteins* **2005**, *60*(3), 333-340.

[106] J. J. Irwin, B. K. Shoichet. *J. Chem. Inf. Model.* **2005**, *45*(1), 177-182.

[107] H. M. Berman, J. Westbrook, Z. Feng, G. Gilliland, T. N. Bhat, H. Weissig, I. N. Shindyalov, P. E. Bourne. *Nucleic Acids Res.* **2000**, *28*(1), 235-242.

[108] D. S. Goodsell, A. J. Olson. *Proteins* **1990**, *8*(3), 195-202.

[109] H. J. Bohm. *J. Comput. Aided Mol. Des* **1992**, *6*(1), 61-78.

[110] N. Miyaura, K. Yamada, A. Suzuki. *Tetrahedron Letters* **1979**, *20*(36), 3437-3440.

[111] K. Matos, J. A. Soderquist. *J. Org. Chem.* **1998**, *63*(3), 461-470.

[112] A. S. J. K. Gillie. *Journal of American Chemical Society* **1980**, *102*, 4933-4941.

[113] R. F. Heck. *Palladium Reagents in Organic Syntheses,* **1985**.

[114] R. Huisgen. *1,3-Dipolar cycloaddition – introduction, survey, mechanism. In 1,3-Dipolar Cycloaddition Chemistry ,* **1984**, pp. 1-176.

[115] H. C. Kolb, M. G. Finn, K. B. Sharpless. *Angew. Chem. Int. Ed Engl.* **2001**, *40*(11), 2004-2021.

[116] V. V. Rostovtsev, L. G. Green, V. V. Fokin, K. B. Sharpless. *Angew. Chem. Int. Ed Engl.* **2002**, *41*(14), 2596-2599.

[117] C. W. Tornoe, C. Christensen, M. Meldal. *J. Org. Chem.* **2002**, *67*(9), 3057-3064.

[118] E. Bokor, T. Docsa, P. Gergely, L. Somsak. *Bioorg. Med. Chem.* **2010**, *18*(3), 1171-1180.

[119] S. B. Ferreira, A. C. Sodero, M. F. Cardoso, E. S. Lima, C. R. Kaiser, F. P. Silva, V. F. Ferreira. *J. Med. Chem.* **2010**, *53*(6), 2364-2375.

[120] A. J. McCarroll, C. S. Matthews, G. Wells, T. D. Bradshaw, M. F. Stevens. *Org. Biomol. Chem.* **2010**, *8*(9), 2078-2084.

[121] A. K. Jordao, P. P. Afonso, V. F. Ferreira, M. C. de Souza, M. C. Almeida, C. O. Beltrame, D. P. Paiva, S. M. Wardell, J. L. Wardell, E. R. Tiekink, C. R. Damaso, A. C. Cunha. *Eur. J. Med. Chem.* **2009**, *44*(9), 3777-3783.

[122] R. L. Vijaya Raghava, R. P. Venkat, N. N. Mishra, P. K. Shukla, G. Yadav, R. Srivastava, A. K. Shaw. *Carbohydr. Res.* **2010**, *345*(11), 1515-1521.

[123] K. Gollnick. *Adv. Photochem.* **1968**, 1-90.

[124] C. S. Foote. *Photochem. Photobiol.* **1991**, *54*(5), 659.

[125] M. Aquino, I. Bruno, R. Riccio, L. Gomez-Paloma. *Org. Lett.* **2006**, *8*(21), 4831-4834.

[126] N. Elander, J. R. Jones, S. Y. Lu, S. Stone-Elander. *Chem. Soc. Rev* **2000**, *29*, 239-243.

[127] C. O. Kappe. *Curr. Opin. Chem. Biol.* **2002**, *6*(3), 314-320.

[128] N. F. Kaiser, U. Bremberg, M. Larhed, C. Moberg, A. Hallberg. *Angew. Chem. Int. Ed Engl.* **2000**, *39*(20), 3595-3598.

[129] A. Dìaz-Ortis, F. Langa, A. de la Hoz, A. Moreno. *Eur. J. Org. Chem.* **2000**, *4*, 3659-3665.

[130] L. Zong, S. Zhou, N. Sgricca, M. C. Hawley, L. C. Kempel. *J. Microwave Power Electromagn. Energy* **2003**, *38*, 49-54.

[131] F. Langa, P. de la Cruz, E. Espìldora, J. J. Garcìa, M. C. Pèrez, A. de la Hoz. *Carbon* **2000**, *38*, 1641-1646.

[132] S. K. Das. *Synlett* **2004**, 915-920.

[133] Y. Xu, Q. X. Guo. *Heterocycles* **2004**, *63*, 903-908.

[134] R. S. Varma. *Clean Products and Processes* **1999**, 132-137.

[135] A. de la Hoz, A. Diaz-Ortiz, A. Moreno. *Chem. Soc. Rev.* **2005**, *34*(2), 164-178.

[136] F. Dal Piaz, A. Casapullo, A. Randazzo, R. Riccio, P. Pucci, G. Marino, L. Gomez-Paloma. *Chembiochem.* **2002**, *3*(7), 664-671.

[137] B. C. M. Potts, D. J. Faulkner, M. S. De Carvalho, R. S. Jacobs. *J. Am. Chem. Soc.* **1992**, *114*, 5093-5100.

[138] J. Zhang, P. G. Blazecka, D. Belmont, J. G. Davidson. *Org. Lett.* **2002**, *4*(25), 4559-4561.

[139] L. Kronberg, R. F. Christman. *Science of the Total Environment* **1989**, *81/82*, 219-230.

[140] G. Springsteen, B. A. Wang. *Tetrahedron Letters* **2002**, *58*, 5291-5300.

[141] M. Aquino, M. D. Guerrero, I. Bruno, M. C. Terencio, M. Paya, R. Riccio. *Bioorg. Med. Chem.* **2008**, *16*(19), 9056-9064.

[142] M. Larhed, G. Lindeberg, A. Hallberg. *Tetrahedron Letters* **1996**, *37*, 8219-8222.

[143] De Simone R., R. M. Andres, M. Aquino, I. Bruno, M. D. Guerrero, M. C. Terencio, M. Paya, R. Riccio. *Chem. Biol. Drug Des* **2010**, *76*(1), 17-24.

[144] F. A. Pasha, M. Muddassan, H. Jung, B. S. Yang, C. Lee, J. Soo Oh, S. Joo Cho, H. Cho. *Bull. Korean Chem.* **2008**, *29*, 647-655.

[145] A. Giroux, L. Boulet, C. Brideau, A. Chau, D. Claveau, B. Cote, D. Ethier, R. Frenette, M. Gagnon, J. Guay, S. Guiral, J. Mancini, E. Martins, F. Masse, N. Methot, D. Riendeau, J. Rubin, D. Xu, H. Yu, Y. Ducharme, R. W. Friesen. *Bioorg. Med. Chem. Lett.* **2009**, *19*(20), 5837-5841.

[146] A. A. San Juan, S. J. Cho. *J. Mol. Model.* **2007**, *13*(5), 601-610.

[147] M. D. AbdulHameed, A. Hamza, J. Liu, X. Huang, C. G. Zhan. *J. Chem. Inf. Model.* **2008**, *48*(1), 179-185.

[148] F. Rorsch, I. Wobst, H. Zettl, M. Schubert-Zsilavecz, S. Grosch, G. Geisslinger, G. Schneider, E. Proschak. *J. Med. Chem.* **2010**, *53*(2), 911-915.

[149] A. Hamza, M. D. AbdulHameed, C. G. Zhan. *J. Phys. Chem. B* **2008**, *112*(24), 7320-7329.

[150] P. J. Holm, P. Bhakat, C. Jegerschold, N. Gyobu, K. Mitsuoka, Y. Fujiyoshi, R. Morgenstern, H. Hebert. *J. Mol. Biol.* **2006**, *360*(5), 934-945.

[151] I. D. Kuntz, K. Chen, K. A. Sharp, P. A. Kollman. *Proc. Natl. Acad. Sci. U. S. A* **1999**, *96*(18), 9997-10002.

[152] A. L. Hopkins, C. R. Groom, A. Alex. *Drug Discov. Today* **2004**, *9*(10), 430-431.

[153] C. bad-Zapatero, J. T. Metz. *Drug Discov. Today* **2005**, *10*(7), 464-469.

[154] P. Appukkuttan, W. Dehaen, V. V. Fokin, E. E. Van der. *Org. Lett.* **2004**, *6*(23), 4223-4225.

[155] M. Whiting, V. V. Fokin. *Angew. Chem. Int. Ed Engl.* **2006**, *45*(19), 3157-3161.

[156] M. P. Cassidy, J. Raushel, V. V. Fokin. *Angew. Chem. Int. Ed Engl.* **2006**, *45*(19), 3154-3157.

[157] E. J. Yoo, M. Ahlquist, S. H. Kim, I. Bae, V. V. Fokin, K. B. Sharpless, S. Chang. *Angew. Chem. Int. Ed Engl.* **2007**, *46*(10), 1730-1733.

[158] L. Li, G. Zhang, A. Zhu, L. Zhang. *J. Org. Chem.* **2008**, *73*(9), 3630-3633.

[159] J. E. Tateson, R. W. Randall, C. H. Reynolds, W. P. Jackson, P. Bhattacherjee, J. A. Salmon, L. G. Garland. *Br. J. Pharmacol.* **1988**, *94*(2), 528-539.

[160] A. D. Ferguson, B. M. McKeever, S. Xu, D. Wisniewski, D. K. Miller, T. T. Yamin, R. H. Spencer, L. Chu, F. Ujjainwalla, B. R. Cunningham, J. F. Evans, J. W. Becker. *Science* **2007**, *317*(5837), 510-512.

[161] S. A. Gillmor, A. Villasenor, R. Fletterick, E. Sigal, M. F. Browner. *Nat. Struct. Biol.* **1997**, *4*(12), 1003-1009.

[162] O. Werz. *Curr. Drug Targets. Inflamm. Allergy* **2002**, *1*(1), 23-44.

[163] C. Charlier, J. P. Henichart, F. Durant, J. Wouters. *J. Med. Chem.* **2006**, *49*(1), 186-195.

List of Abbreviations

5-HETE	5-hydroxyeicosatetraenoic acid
5-HPETE	5-hydroperoxyeicosatetraenoic acid
CAP	chemical available for purchase
COX	cyclooxygenase
cPGES-2	cytosolic prostaglandin E_2 synthase
DBU	1,8-diazabicyclo[5.4.0]undec-7-ene
DCM	dichlorometane
DHP	dihydropyran
DIC	N,N'-dicyclohexylcarbodiimide
DIPEA	N,N-diisopropylethylamine
DMF	N,N-dimethylformamide
DMSO	dimethylsulfoxide
ES-MS	electrospray mass spectrometry
FLAP	5-lipoxygenase-activating protein
GSH	tripeptide glutathione
HMBC	heteronuclear multiple bond coherence
HOBt	N-hydroxybenzotriazole
HPLC	high-performance liquid chromatography
HSQC	heteronuclear single quantum coherence
HTS	high-throughput screening
IL-1β	interleukin 1β
LO	lipoxygenase
LPS	lipo-polysaccharide
LT	leukotriene
MAPEG	membrane associated proteins involved in eicosanoid and glutathione metabolism
MEM	metoxy-ethoxy-methyl-ether
MGST	microsomal glutathione transferase
mPGES-1	microsomal prostaglandin E_2 synthase-1
mPGES-2	microsomal prostaglandin E_2 synthase-2
MTT	3-(4,5-dimethylthiazol-2-yl)-2,5-diphenyltetrazolium bromide

MW	microwaves
NBS	N-bromosuccinimide
NMR	nuclear magnetic resonance
NSAID	non steroidal anti-inflammatory drug
PAF	platelet activating factor
PDB	protein data bank
PG	prostaglandin
PGES	prostaglandin E_2 synthase
PL	phospholipase
PM	petrosaspongiolide M
QM	quantum mechanic
QSAR	quantitative structure activity relationship
r.t.	room temperature
SAID	steroidal anti-inflammatory drug
SAR	structure activity relationship
TBAB	tetrabutil-ammonium-bromide
TEA	triethylamine
TFA	trifluoroacetic
THF	tetrahydrofuran
THP	tetrahydropyran
TIS	triisopropylsilane
TLC	thin layer chromatography
TNF-α	tumor necrosis factor-α
Tx	thromboxane
VEGF	vascular endothelial cell growth factor

Acknowledgements

I would like to thank all the people who contributed to the realization of this PhD project.

First of all, I want to acknowledge my supervisor, professor Ines Bruno, for giving me the opportunity to pursue this project and for scientifically supporting me during these last three years with extreme professionalism. My gratitude is also for professors Oliver Werz and Migual Paya for their crucial collaboration in biological assays.

Moreover I want to thank every component of the laboratory of Organic Chemistry that shared with me this fantastic period. Specifically, I want to thank the student, Martino Iacenda, Elvira Trucillo and Maria Stella Donisi, that worked with me to the realization of this project, and my colleagues Maria Chiara Monti, Stefania Terracciano, Anna Falcone, Maria Anna Euterpio, Maria Giovanna Chini and Annalisa Vilasi. But above all my gratitude is for Luigi Margarucci who is a good friend and companion of adventures rather than a colleague. Indeed, having always the right advice, he has been always prone to sustain and encourage me during the different hard times that featured my PhD course.

Last but not least my thanks go to Matteo and my brother Luca, who have been always present and ready to help me when it has been possible, and to my parents that, also in this case, believed in my capacity and supported my choices making every kind of sacrifices to allow me to become what I am today.

Rosa De Simone